UNIVERSITA' DEGLI STUDI DI PAVIA

Dipartimento di Biologia e Biotecnologie "L. Spallanzani"

Molecular signatures linked to stemness and tumorigenesis in tumorspheres from *in vitro* transformed cells

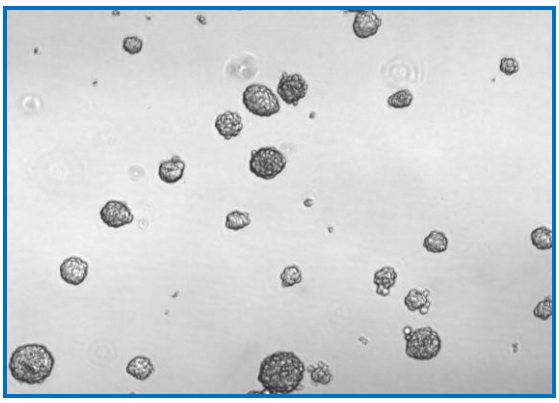

Bartolo Bono

Dottorato di Ricerca in

Genetica, Biologia Molecolare e Cellulare

XXIX Ciclo – A.A. 2013-2016

UNIVERSITA' DEGLI STUDI DI PAVIA

Dipartimento di Biologia e Biotecnologie "L. Spallanzani"

Molecular signatures linked to stemness and tumorigenesis in tumorspheres from *in vitro* transformed cells

Bartolo Bono

Supervised by Dr. Chiara Mondello

Dottorato di Ricerca in

Genetica, Biologia Molecolare e Cellulare

XXIX Ciclo – A.A. 2013-2016

Abstract

Tumors are characterized by an extensive heterogeneity, due to genetic and epigenetic changes occurring during tumor development. Moreover, a large body of evidence indicates that a layer of intra-tumoral heterogeneity is given by the presence of cells endowed with high tumorigenic potential and stemness features, named cancer stem cells (CSCs), which appear to be responsible for tumor initiation and maintenance in several tumors. CSC origin is still controversial, nevertheless, recent evidence has shown that they can originate form de-differentiation of bulk tumor cells and from differentiated cells that have undergone neoplastic transformation *in vitro*. *In vitro*-originated CSCs can constitute a useful and easy to handle tool to define and study genes and pathways involved in their generation and maintenance.

The goal of this PhD thesis consisted in the isolation of cells with CSC features from *in vitro* transformed cells in order to exploit them for the possible identification of molecular signatures associated with the CSC phenotype. To this scope, we used a cellular model developed in our laboratory from telomerase immortalized human fibroblasts, named cen3tel, which, during propagation in culture, spontaneously and gradually acquired oncogenic mutations determining the switch toward a neoplastic phenotype. According to *in vivo* tumorigenicity assays, we identified three phases of neoplastic transformation and, in this work, we focused our studies on cen3tel cells around population doubling 600 (cen3tel 600 cells) and 1000 (cen3tel 1000 cells), which represent advanced stages of transformation.

Using the sphere formation assay, a well-known tool to isolate and enrich CSCs from tumor cell populations, we demonstrated that both cen3tel cell populations contain a subset of cells able to form tumorspheres in serum free medium and in the presence of growth factors. Sphere cells were capable to form spheres with increasing frequency after disaggregation and replating, indicating that they are endowed with self renewal properties. Moreover, they showed an increased expression of the stemness gene *SOX2*, but displayed the same ability to differentiate into adipocytes and osteoblasts of their adherently growing counterpart. Compared to cen3tel cells grown in adhesion, sphere cells showed a modest increase in tumorigenic potential when injected in immunodeficient mice.

The analysis of the expression of a panel of genes involved in stemness and tumorigensis, such as c-*MYC*, *GNL3* (encoding for nucleostemin), and *NOTCH1* revealed that these genes were surprisingly down-regulated in sphere cells, while the tumor suppressor miR-34a was up-regulated. The deregulation of these genes in sphere cells was concerted and reversible when cells were plated in adherent culture conditions, suggesting that they are connected in a circuitry and probably act in the same functional process during sphere formation. Given that c-*MYC* is also a pro-apoptotic gene, we investigated whether decreased c-Myc levels in sphere cells could be functional to protect them from death. Analyzing the expression of several apoptotic markers, we demonstrated that there was not activation of apoptosis in sphere cells. Thus, deregulation of the expression of c-

MYC, *GNL3*, *NOTCH1* and miR-34a in sphere cells might play a role as a pro-survival mechanism allowing cells to escape apoptosis and grow in suspension. This mechanism might also contribute to tumor cell survival *in vivo*, once cells detach from the extracellular matrix.

To get further insights into the molecular features of cen3tel spheres, we compared genome wide gene expression profiles of cen3tel 600 and 1000 sphere cells with those of their corresponding adherent counterparts. We found ~650 genes up-regulated and ~150 down-regulated in both sphere cell populations. By functional enrichment analysis of the genes up-regulated in spheres, we found that the most overrepresented biological processes were related to chromatin organization, negative regulation of apoptosis, mevalonate and cholesterol metabolism, innate immunity and inflammation. Genes belonging to the first process were mainly histone variant genes, their deregulation might lead to a chromatin reorganization in sphere cells, which could in turn have consequences on gene expression. The up-regulation of genes related to the negative regulation of apoptosis, among which the anti-apoptotic gene *BCL2A1*, is in agreement with the lack of apoptosis activation in sphere cells.

By inhibiting the HMG-CoA reductase enzyme of the mevalonate/cholesterol biosynthetic pathway, whose gene was up-regulated in sphere cells, we demonstrated that the mevalonate pathway plays a crucial role in the regulation of sphere formation, both in cen3tel 600 and 1000 cells. Among the genes falling within the biological processes related to innate immunity and inflammation, we focused our attention on *IL1B*, *IL6* and *ISG15*. *IL1B* and *IL6* encode the pro-inflammatory cytokines IL-1β and IL-6, respectively, while *ISG15* is an interferon inducible gene encoding a small protein that can be free in the cytosol, conjugated to several protein or secreted in the intracellular space. Plating cen3tel 600 or 1000 cells in sphere forming medium in the presence of IL-1β, IL-6 or ISG15 we found that IL-1β has an inhibitory effect on sphere formation, while IL-6 and ISG15 enhance sphere formation.

Taken together, our results show that *in vitro* transformed cells, as cen3tel 600 and 1000 cells, are heterogeneous and plastic populations containing a subset of cells able to form tumorspheres, as observed in several tumors. Spheres derived from these cells displayed distinctive molecular features compared to the bulk of the populations and their characterization allowed highlighting pathways relevant to sphere formation and sphere cell survival. However, sphere cells were only slightly more tumorigenic than adherent cells. This could be due to an intrinsic weakness of the tumorigenic assay in mice, but could also indicate that different subpopulations can support tumorigenicity in transformed cells, highlighting a further level of complexity in tumor heterogeneity.

Acknowledgements

Firstly, I wish to thank my Supervisor Dr. Chiara Mondello for teaching and providing me all constructive knowledges and suggestions for the development of this research work.

Great appreciations go to Dr. Ilaria Chiodi for constantly giving me support and attention during my PhD.

I would like to express my special thanks for Martina Peritore who helped me realize some of experiments described in this thesis.

My grateful thanks are also extended to Dr. Cristina Belgiovine, Dr. Paola Ostano and Dr. Giovanna Chiorino for the proficient and competent collaboration, providing us resources to perform important experiments.

Special thanks to all my friends, especially those who I met in Pavia, without whom I would not have had encouragement and assistance during these years.

Finally, I must acknowledge my parents and my beautiful sister Tina, because without their love and support I would not have had the determination to reach this finish line.

Abbreviations

ABC	ATP-Binding Cassette
ALDH	Aldehyde Dehydrogenase
AML	Acute Myeloid Leukemia
ccRCCs	Clear Cell Renal Cell Carcinomas
CML	Chronic Myeloid Leukemia
Cen3tel	Centenarian 3 telomerase
CSC	Cancer Stem Cell
ECM	Extracellular Matrix
EGF	Epidermal Growth Factor
EGFR	Epidermal Growth Factor Receptor
EMT	Epithelial-Mesenchymal Transition
ESC	Embryonic Stem Cell
FACS	Fluorescence Activated Cell Sorting
FGF	Fibroblast Growth Factor
bFGF	Basic-Fibroblast Growth Factor
GBM	Glioblastoma Multiforme
GFP	Green Fluorescent Protein
GMP	Granulocyte-Macrophage Progenitor
GO	Gene Ontology
HMEC	Human Mammary Epithelial Cell
HSC	Hematopoietic Stem Cell
IFN	Interferon
IL	Interleukin
IRES	Internal Ribosome Entry Site
LMPP	Lymphoid Multipotent Primed Progenitor
LSC	Leukemia Stem Cell
MMP	Matrix Metalloproteinase
MMTV	Mouse Mammary Tumor Virus
NSG	NOD SCID Gamma
NK	Natural Killer
NOD	Non-Obese Diabetic
NSCLC	Non-Small Cell Lung Cancer
PyMT	Polyomavirus Middle-T oncogene
PSA	Prostate Tumor Antigen
RFP	Red Fluorescent Protein
RNA-seq	RNA sequencing
RT-qPCR	Reverve Transcriptase-quantitative Polymerase Chain Reaction
SSEA-1	Stage-Specific Embryonic Antigen 1
SCID	Severe Combined Immunodeficiency
SP	Side Population
SV40	Simian Virus 40
TAM	Tumor-Associated Macrophage
TK	Thymidine Kinase

Contents

1. Introduction

1.1 Neoplastic transformation

Cancer is a complex and heterogeneous genetic disease characterized by genomic instability and unregulated cell growth. Neoplastic transformation is a gradual process during which cells accumulate multiple genetic and epigenetic alterations that cause the loss of proliferation control, the ability to divide indefinitely and invade other tissue (Cooper 1992; Hahn 2002).

A central aim of cancer research has been to identify and characterize the genes mutated in cancer and their role in oncogenesis. Genes involved in cancer development are mainly regulators of cell proliferation, differentiation and survival and are primarily classified in two different classes: oncogenes and tumor suppressor genes. The first ones are generally positive inducers of cell growth, or negative regulators of differentiation and programmed cell death, and are activated by gain-of-function mutations, such as point mutations, translocations or gene amplifications (Croce, 2008). In contrast, the second ones are genes that normally act as brakes of cell growth and promote cell death in unfavorable conditions. These types of genes are generally inactivated by recessive loss-of-function mutations (Sherr, 2004). Many studies have also demonstrated the importance in the control of tumor growth of microRNAs, a class of short RNAs that regulates the expression of protein-coding genes. MicroRNAs can act either as oncogenic promoters or tumor suppressors, depending on their target genes that can thus be specifically up-regulated or down-regulated in tumors (Jansson and Lund 2012; Hayes et al. 2014).

Thus, tumorigenesis is a complex process consisting of many steps in which key genes gradually and progressively accumulate selective mutations, named “driver mutations”, which favor the transformation of normal cells to cancer cells. Together with driver mutations, cancer cells can also gather mutations that do not play a causative role in cancer development, defined “passenger mutations”. However, some of these mutations can actually confer a selective advantage in particular conditions. For example, mutations promoting drug resistance to chemotherapeutic agents can be selected during therapy and favor tumor recurrence (Stratton et al. 2009).

1.1.1 The hallmarks of cancer

To understand and rationalize the complexity of neoplastic transformation, in the last decade Hanahan and Weinberg (2011) highlighted ten traits or biological capabilities, named "hallmarks of cancer", which are common to most types of cancer (Figure 1).

Among these characteristics, the most fundamental is the ability of cancer cells to auto-sustain their growth, either deregulating the normal proliferative signaling pathways, or increasing the availability of growth factors, through their own production or stimulating their synthesis by tumor-associated stroma cells

(Cheng et al. 2008; Witsch et al. 2010; Lemmon and Schlessinger, 2010; Davies and Samuels, 2010). In addition, most cancer cells potentiate proliferation by acquiring the ability to evade anti-growth signals (Sherr, 2004; Burkhart and Sage, 2008; Seluanov et al., 2009).

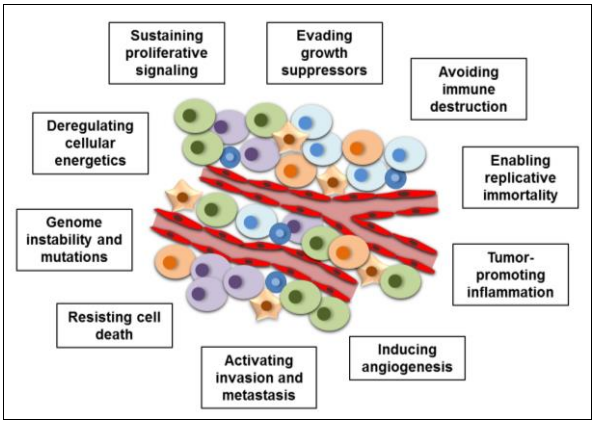

Figure 1. The hallmarks of cancer. Schematic illustration of the ten hallmarks of cancer described by Hanahan and Weinberg. Each of these cancer-driving features represents a candidate for anticancer treatments.

The process of neoplastic transformation also involves a series of events that allow cells to bypass senescence and to evade death by apoptosis, two processes that protect tissues from cancer development (Shay and Roninson, 2004; Campisi, 2013; Fernald and Kurokawa, 2013). Senescence is mainly related to telomere shortening and is overcome by cancer cells through the activation of telomerase or alternative telomere-maintenance mechanisms, which make them able to divide indefinitely (Shay and Wright, 2010). Moreover, senescence mechanisms can also be promoted by DNA damage or stressful conditions. In cancer, the inactivation of key genes associated to the DNA damage response can lead to the inhibition of senescence mechanisms and to the promotion of cell proliferation, thus supporting oncogenic transformation (d'Adda di Fagagna, 2008).

The highest pathological grade of malignancy is achieved when cancer cells become able to induce the development of blood vessels inside the tumor mass, a process named angiogenesis, which favors tumor access to nutrients and increases tumor cell migratory and invasive capacities (Hanahan and Folkman, 1996; Zetter, 1998; Talmadge and Fidler, 2010).

Another hallmark of cancer is genomic instability that, at least in sporadic cancers, is considered an initiating event together with the deregulation of growth-regulating genes and DNA damage/DNA replication stress. Genomic instability would then facilitate the establishment of all the other hallmarks (Negrini, 2010).

An emerging hallmark of cancer is the reprogramming of cancer cell energy metabolism, which was firstly described by Otto Warburg in 1930 (Warburg, 1930). Cancer cells change their bioenergetics program exhibiting rapid adaptive responses to hypoxia and hypo-nutrient conditions, potentiating the capacity to intake nutrients and anabolic pathways, to produce the macromolecules required to

sustain their high rate of proliferation (Yoshida, 2015; Pavlova and Thompson, 2016).

Finally, the two last hallmarks of cancer are strictly correlated with each other and are associated to the tumor microenvironment and the immune system. On one hand, tumor cells are able to evade the surveillance of the immune system through still unknown mechanisms and, on the other hand, promote tumor-associated inflammatory responses that enhance tumor development. These responses can contribute to multiple hallmark capabilities by supplying molecules to the tumor microenvironment, including growth factors, survival and proangiogenic factors and matrix-modifying enzymes, that are all together involved in tumor growth and in the increase of malignancy (Coussens and Werb, 2002; DeNardo et al. 2010; Gajewski et al. 2013).

It is now clear that the tumor microenvironment plays a very important role in tumor development and progression, together with the cancer associated changes that characterize tumor cells. To this regard, many studies have highlighted a high degree of genetic heterogeneity within tumor tissues that requires to be unraveled to defeat tumors (Marusyk and Polyak, 2010; Gerlinger et al. 2012).

1.1.2 Tumor heterogeneity

The advent and widespread use of next-generation sequencing approaches has shed light on the complexity of intra-tumor heterogeneity and its implications for cancer diagnosis, prognosis and therapeutic response (Lawrence et al. 2013; Easwaran et al. 2014).

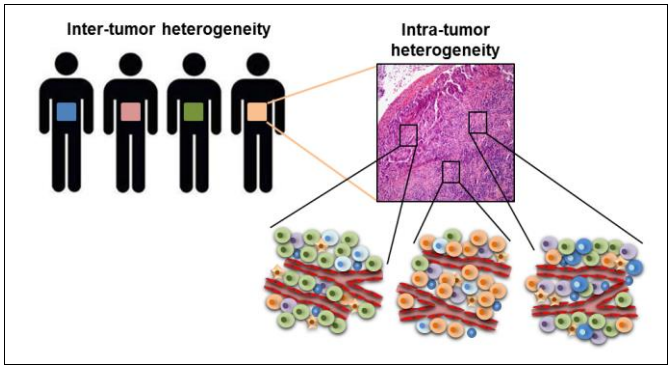

Figure 2. Tumor heterogeneity. Tumor heterogeneity is observed at different levels: among tumors of the same type (inter-tumor heterogeneity); among different areas within the same tumor (intra-tumor heterogeneity); within a single tumor area characterized by heterogeneous clonal populations.

Within a tumor, subclone diversity may be observed (intra-tumor heterogeneity); subclones may be mixed together or spatially separated by physical barriers such as blood vessels or microenvironmental variations. Tumor subclones may show differential gene expression due to genetic and epigenetic heterogeneity (clonal heterogeneity) (Fig. 2). Within a subclonal population, there are multiple routes to intercellular genetic and non-genetic diversification such as, for example, variations in chromosome copy number, somatic point mutations and epigenetic

modifications (Burrell et al. 2013).

Tumor heterogeneity is influenced by both cell-intrinsic and cell-extrinsic mechanisms. Intrinsic heterogeneity includes variations in genetic, epigenetic and biological properties of cancer cells, whereas extrinsic traits are related to the cancer microenvironment that mutually interacts with cancer cells and affects the development and progression of the neoplastic disease (Sun and Yu, 2015).

Recent studies revealed the presence of extensive variations in genomic aberrations within tumors. For example, in glioblastomas, copy number variations of two commonly amplified receptor tyrosine kinases, EGFR and PDGFRA, were identified among cells from the same tumor specimen using multicolor fluorescent *in situ* hybridization (FISH). The majority of the cells had a mutual exclusive amplification of these two genes, whereas co-amplification was only observed in a minority of the cancer cells. Moreover, gene amplifications in subclones seemed to also follow a spatial distribution, with one or the other type of gene predominating in certain areas of the same specimen (Szerlip et al. 2012; Little et al. 2012).

In 2012, Nik-Zainal and colleagues applied a mathematical model to genome-wide sequencing data obtained from 21 breast cancers identifying in each tumor a prominent subclonal diversification, with mutations present in just a fraction of the cells (Nik-Zainal et al. 2012). Recently, Gerlinger and coworkers (2014) performed a multi-region exome sequencing on multiple spatially separated biopsies obtained from ten primary clear cell renal cell carcinomas (ccRCCs). Among all the aberrations detected, the only ubiquitous events were the mutation in the tumor suppressor gene *VHL* and the chromosome 3p loss, which are associated with up to 90% of sporadic ccRCCs (Nickerson et al. 2008; Gatto et al., 2014); while several mutations occurring in potential driver genes of ccRCC, such as the tumor suppressor *PTEN*, *MTOR*, *TSC1* and *PIK3CA* of the MTORC1 pathway, the chromatin structure modulators *STED2* and *PBRM1* (Brugarolas, 2014), were identified in subclonal and spatially separated populations. Moreover, the number of driver mutations identified increased with the number of biopsies analyzed. For several genes, different mutations with similar functional consequences were detected, indicating that these genes have an important role in the progression of this type of cancer. This study clearly indicates that a deep evaluation of genomic topography of a tumor leads to a better understanding of its evolution and is highly important to drive possible targeted therapies.

Recent evidence has shown that genetic mutations are not the only source of intra-tumor heterogeneity and epigenetic changes also play an important role. For example, differences in DNA methylation have been described among tumor subpopulations. Analyzing multiple topographically distinct tumor sites, premalignant lesions, and lymph node metastases from five cases of prostate cancer, Brocks et al. (2014) demonstrated that distinct primary tumor and metastatic subclones showed specific methylation patterns in prostate-specific gene (*PTEN*, *TP53*, *GSTP1*) regulatory elements and the degree of methylation variability in these loci depended on their genetic and epigenetic context.

Intra-tumor heterogeneity can also be highlighted at the transcriptional level. Recently, studying gene expression profiles in several tumor foci of 11 patients with $ER^+/HER2^-$ multifocal/multicentric invasive lobular breast tumors, Norton and colleagues (2016) observed a significant variability, both within patients and

between-foci, in the expression of 466 genes, including *CDH1*, *FIGF*, *RELN*, *SFRP1*, *MMP7*, *NTRK2*, *LAMB3*, *SPRY2* and *KIT*, which are all together associated to an increase of invasiveness and metastasis formation.

In the last years, studies performed using single-cell RNA-sequencing (RNA-seq) increased the knowledge on intra-tumor heterogeneity. Using this approach, Patel and colleagues (2014) analyzed 430 cells isolated from five primary glioblastomas and revealed the presence of diverse transcriptional programs related to oncogenic signaling, proliferation, immune response, hypoxia and stemness. Importantly, they found that established glioblastoma subtype classifiers were variably expressed across individual cells within a tumor. Thus, tumor single cell analysis can reveal an intra-tumoral heterogeneity, which can have prognostic and therapeutic value.

Heterogeneity has also been described between primary tumors and metastases. Using next-generation sequencing techniques, Shah and coworkers (2009) identified 32 mutations in metastasis originated from a primary lobular breast cancer 9 years after its diagnosis and removal. Among these mutations, 5 were prevalent in the primary tumor, 6 were present at low frequency (1-13%) and 19 were not detectable. These findings suggest that mutational heterogeneity is present in primary tumors and increases during cancer progression.

More recently, Tirosh and colleagues. (2016) analyzed populations of cells derived from one patient with primary acral melanoma and 18 patients with metastatic melanoma at the single cell level, determing single-cell RNA-seq profiles from 4645 malignant, immune, and stromal cells. After distinguishing cell transcriptional states between malignant and non-malignant cells, they analyzed individual malignant cells and found transcriptional heterogeneity among cells of the same tumor in cell cycle and spatial organization programs. Moreover, a subpopulation of malignant cells with a transcriptional program associated with resistance to MAP-kinase targeted therapies was identified, which was actually enriched after MAP kinase inhibitor treatment, reinforcing recurrence of metastatic melanomas. In a subset of tumor associated cells, these authors also found the expression of specific genes that could influence the cellular composition of the tumor microenvironment. Thus, deepening the knowledge on cellular composition and specific transcriptional programs within a tumor could help to better understand data obtained from bulk tumor analysis and drive precision medicine interventions.

Intra-tumor heterogeneity can also be caused by the surrounding microenvironment, which can itself show different features in different regions. Multiple factors contribute to a variable microenvironment, such as for example the tumor's blood supply. An unequal distribution of blood vessels in a tumor may induce heterogeneous signal transduction, gene expression, and genomic instability in cancer cells either directly, through the supplied growth factors or hormones, or indirectly through oxidative stress, hypoxia, or acidosis. As a result, malignant cancers are dynamically evolving 'clades' of cells living in distinct microhabitats (Gillies et al. 2012).

In addition to endothelial cells, other stromal cells, including fibroblasts, inflammatory cells, and pluripotent mesenchymal cells, also contribute to the diversified genotypes and phenotypes of cancer cells through the secretion of

cytokines, growth factors, and extracellular matrix (ECM) components, which in turn play a role in chemoattraction of stromal cells, endothelial cells and inflammatory cells, further influencing the microenvironment, the diversification of cancer cells and consequently therapeutic response (Junttila and De Sauvage, 2013).

One of the clinical implications of intra-tumor heterogeneity is drug resistance. Functionally, cell-to-cell variability, either genetic or non-genetic, can compromise the efficacy of cancer therapies by increasing the repertoire of possible cellular responses (Zhang et al. 2014; Patel et al. 2014). A recent work on breast cancer using multiregion whole-genome sequencing revealed that resistance to chemotherapy and metastasis formation could be caused by detectable subclones with different somatic variations, suggesting that clonally dominant events are not necessarily more important in function than minor subclonal lesions (Yates et al. 2015).

1.2 Models of cancer evolution

Cancers evolve over variable time frames (~1–50 years) and, in each patient, the clonal structure, genotype and phenotype changes over time.

Two different models have been proposed for cancer development and progression based on the origin of its complexity and heterogeneity. The first, indicated as the classical model of cancer evolution, is the clonal evolution model which clearly reflects the Darwinian evolutionary system. The second is the cancer stem cell model, asserting a hierarchical organization of cells, such that only a small subset is responsible for sustaining tumorigenesis and establishing the cellular heterogeneity characteristic of tumors.

1.2.1 The clonal evolution model

The clonal evolution model was first proposed in 1976 by Peter Nowell in his manuscript '*The clonal evolution of tumor cell populations*' where he synthesized the view of cancer as an evolutionary process driven by stepwise somatic cell mutations with sequential subclonal selection (Nowell, 1976). According to this theory, tumors arise from a single mutated cell, accumulating additional mutations during their progression. These changes give rise to additional subpopulations, and each of these subpopulations has the ability to divide and mutate further. This heterogeneity may give rise to subclones that possess an evolutionary advantage over the others within the tumor environment, and these subclones may become dominant in the tumor over time (Merlo et al. 2006; Swanton 2012). This is a nonhierarchical model in which all the cells arising from the dominant clone have the same tumorigenic capacity. A large body of data from tissue section, small biopsy and the more recent single cell analyses indicate that tumor cells evolve through complex and branching trajectories, exactly as envisioned by Nowell, providing a striking parallel with Charles Darwin's iconic evolutionary speciation tree (Greaves and Maley, 2012). As for organisms, natural selection in tumors is based upon competition for space and resources. This landscape is made even more

complex when clinical treatment comes into play (Gatenby and Gillies, 2008). For example, angiogenesis is an attractive therapeutic target, however, angiogenesis inhibitors also alter the environment (through increased hypoxia and acidosis), producing strong Darwinian forces that rapidly promote adaptive strategies including increased invasiveness. Not surprisingly, anti-angiogenic therapies have shown little benefit as monotherapy (Iwamoto et al. 2009). Moreover, since many cancer therapeutics are genotoxic, they could induce new mutations in surviving cells, thus probably improving fitness and malignant potential (Zona et al. 2014).

The tumor microenvironment is a dynamic entity that could potentially promote clonal evolution and selection. For example, through the production of cytokines, which are crucial components of inflammatory lesions in a cancer ecosystem and regulate several cellular processes (Qian and Pollard, 2010), or via microvesicles and exosomes, originated in tumor niches, which can deliver nucleic acid and proteins conferring survival advantages to cancer cell subclones (Camussi et al. 2013; Martins et al. 2013). Moreover, these micro-habitats can be drastically modified by chemotherapy or radiotherapy, probably providing new selective pressures that can induce fitness advantages of cell variants that survive to therapy and cause cancer relapse.

The clonal evolution model supports the theory that, through the processes of clonal expansion, genetic and epigenetic diversification and clonal selection, cancers develop a variable clonal architecture within protected and adaptive tissue ecosystems.

1.2.2 The cancer stem cell model

The second model for cancer development and evolution is the cancer stem cell (CSC) paradigm. Unlike the clonal evolution model, where all cancer cells possess tumorigenic potential, the CSC hypothesis postulates that only a subpopulation of tumor cells have tumorigenic potential. These cells share features with normal stem cells, hence the name CSCs and, as normal stem cells, can generate cells with the same tumorigenic potential, through symmetric division, or more differentiated cells that constitute the bulk of the tumor, through asymmetric division (Reya et al. 2001; Dick 2008). This model of tumor development suggests a hierarchical cellular organization within a tumor compared to the stochastic model of clonal evolution.

The first evidence supporting the hierarchical nature of cancer originated from xenotransplantation experiments carried out with hematopoietic acute myeloid leukemia (AML) cells (Lapidot et al. 1994; Bonnet and Dick, 1997). Leukemic cells were sorted for the expression of specific surface markers and transplanted into immunodeficient mice, with the intention to discriminate phenotypically tumorigenic cells from the rest of the tumor cell population. In particular, Bonnet and Dick (1997) demonstrated that cells positive for CD34, a surface marker primarily associated with hematopoietic stem cells (HSCs), and negative for CD38, a surface marker of lineage commitment, were the tumorigenic cells responsible for the generation of AML xenografts in NOD/SCID mice. The authors also demonstrated that $CD34^{+}CD38^{-}$ leukemic cells were able to self-renew, generating

tumors in secondary recipient mice; furthermore, analyzing the entire leukemic cell population derived from the AML xenografts, they assessed that $CD34^{+}CD38^{-}$ cells were also able to differentiate into the heterogeneous leukemic lineages of the primary tumor. Thus, these tumor-initiating cells display stem cell properties such as self-renewal and multipotent differentiation, recapitulating and resulting in the heterogeneity of tumor cell phenotypes. Discovering that only $CD34^{+}CD38^{-}$ cancer cells could initiate leukemia suggested for the first time that cells expressing stem cell-associated markers and properties play a role in hematopoietic tumorigenesis and supported the hypothesis that a cellular hierarchy is involved in tumor development. After this seminal work, the research on CSCs was extended to solid tumors, initially on solid tumors of epithelial and neuroectodermal origin and, more recently, of mesenchymal origin too.

The first identification of CSCs in solid tumors was made by Al-Hajj and colleagues (2003). Analyzing the cell population of 9 human breast cancers, these researchers isolated putative CSCs which were characterized by the positive expression of CD44 and the negative or low expression of CD24 ($CD44^{+}$ $CD24^{-/low}$ cells), typical cell surface markers of normal mammary stem cells. Particularly, cells derived from breast cancer of 8 out 9 patients and expressing this phenotype were able to form tumors when injected into immunodeficient mice even in a very small number, whereas, $CD44^{-}$ $CD24^{+}$ cells derived from the same tumor mass did not form tumors after injection, even in a very high number. Tumors arising from $CD44^{+}$ $CD24^{-/low}$ cells resembled the phenotypic complexity of the tumors from which they were derived; furthermore, when $CD44^{+}$ $CD24^{-/low}$ cells were serially passaged through several rounds of tumor formation in mice, they maintained the same degree of tumorigenicity at each passage. This study provides evidence that $CD44^{+}$ $CD24^{-/low}$ tumorigenic cells undergo self-renewal and differentiation similarly to normal stem cells and there is a hierarchical cell organization in breast cancers, thus supporting the CSC model.

Further studies were conducted testing the applicability of the cancer stem cell model in many other solid tumors such as brain tumors (Singh et al. 2004; Galli et al. 2004; Dirks 2006), colorectal cancer (O'Brien et al. 2007; Ricci-Vitiani et al. 2007), melanoma (Fang et al. 2005; Schatton and Frank, 2008), lung cancer (Ho et al. 2007; Eramo et al. 2008), sarcomas (Gibbs et al. 2005), gastric cancer (Takaishi et al. 2009), hepatic cancer (Yang et al. 2008), pancreatic cancer (Li et al. 2007; Hermann 2007), ovarian cancer (Bapat et al. 2005) and prostate cancer (Collins et al. 2005). These studies suggest that many cancers follow the CSC model and contain a subset of high tumorigenic cells able to sustain tumor growth and maintenance.

The ability of CSCs to generate the bulk of more differentiated cells that form the tumor mass is a property that supports the link between the hierarchical organization proposed by CSC model and the intra-tumoral heterogeneity. Epigenetic mechanisms are involved in the regulation of embryonic and/or adult stem cells transcriptional programs, controlling differentiation as well as self-renewal processes. Multiple observations indicate that the establishment and maintenance of CSC features can be orchestrated in a similar way, switching on and off CSC epigenetic markers to generate heterogeneous populations of cells with distinct phenotypes and features (Muñoz et al. 2012). For example,

Trowbridge and colleagues (2012) demonstrated that haploinsufficiency of the DNA methyltransferase Dnmt1 correlates with impaired CSC self-renewal and delayed leukemogenesis. More recently, genome-wide DNA methylation profiling of pancreatic ductal adenocarcinoma CSCs revealed that these cells have a higher level of DNA methylation and showed overexpression of *DNMT1* compared to non-CSC populations. The inhibition of *DNMT1* expression via upregulation of the microRNA miR-17-92 cluster caused an epigenetic reprogramming that reduced CSC self-renewal and differentiation ability (Zagorac et al. 2016). Thus, these observations suggest that epigenetic factors, classically ascribed to govern normal stem cell differentiation, are important regulators of CSC status and differences between CSCs and their progeny are likely to be an important determinant of the heterogeneity of some cancers.

The CSC model has also received wide attention because it also provides an explanation for tumor recurrence. CSCs possess a property that makes them clinically relevant. These cells express resistant phenotypes to both ionizing radiation and chemotherapeutic agents (Bao et al. 2006; Woodward et al. 2007; Li et al. 2008; Diehn et al. 2009). This suggests that many cancer therapies, while killing the bulk of tumor cells, may ultimately fail because they do not eliminate CSCs, which survive and can eventually determine tumor relapse. Recent studies illustrate that a stem cell-like gene expression signature is related to relapse in glioblastoma and is predictive of patient outcome in human leukemia, breast cancer, glioblastoma and ovarian cancer, lending support to the clinical relevance of CSCs (Eppert et al. 2011; Wicha 2012; Liu et al. 2013; Balbous et al. 2014).

Despite there is clearly evidence supporting the presence of CSCs in several cancers, there are some caveats in the experimental methodologies used to demonstrate that cancer strictly follows the CSC model. The golden standard experiments to prove the presence of CSCs in cancers are based on xenograft limiting dilution assays and tumor-specific CSC markers to isolate the tumor initiating cells. However, xenograft models have some inherent limitations such as the need to control immune response in the transplanted animal and the different mircroenvironmet present at the xenograft site. Moreover, the use of surface markers is difficult to reproduce across multiple tumors and may not adequately delineate CSCs from non-CSCs, suggesting that CSC markers are not universal (Gunther et al. 2007; Beier et al. 2007; Hwang-Verslues et al. 2009). In addition, recent observations have shown that CSCs are heterogeneous and plastic entities, in fact they can undergo genetic evolution, can have different phenotypes among different patients, can be present in genetically and phenotypically distinct pools within tumors and metastases and, finally, can derive from the reversion of the phenotype of non-CSCs to CSCs (see pages 31-34). These observations indicate that CSCs are subjected to change and adaptation through clonal evolution or epigenetic plasticity (Shackleton et al. 2009), pointing to an overlap between the clonal evolution model, driven by genetic alterations, and the CSC model, based on non-genetic alterations. These two models are thus not mutually exclusive, but can operate together to generate intra-tumor heterogeneity (Fig. 3) (Visvander and Lindeman, 2012; Kreso and Dick, 2014; Cabrera et al. 2015).

Recent studies in different types of leukemia supported this view of cancer progression. Eppert and collegues (2011) showed that AML leukemia stem cells

(AML-LSCs) isolated from 16 primary human AML samples exhibited diverse surface marker profiles and frequency. Moreover, Notta and co-workers (2011) carried out combined genetic and functional studies of the LSCs from human AML and B-cell acute lymphoblastic leukemia (B-ALL) and the results revealed that genetic diversity occurred in LSCs defining multiple distinct subclones within the various AML patients. Also data from breast, renal and pancreatic cancers showed extensive genetic heterogeneity which would not be driven by merely differentiation of CSCs, but rather every CSC could form genetically distinct tumor populations (Campbell et al. 2010; Nik-Zainal et al. 2012; Gerlinger et al. 2012). Furthermore, CSC plasticity links clonal evolution and CSC models and suggests that CSC hierarchy can be seen as a bidirectional balance between CSCs and differentiated non-CSCs. However, if CSC plasticity is coordinated from microenvironment clues or stochastic processes depends on the type of tumor and its genetic background (Medema, 2013; Cabrera et al. 2015). Collectively, these observations indicate that there are evident commonalities between the clonal evolution and the CSC model of cancer development and progression.

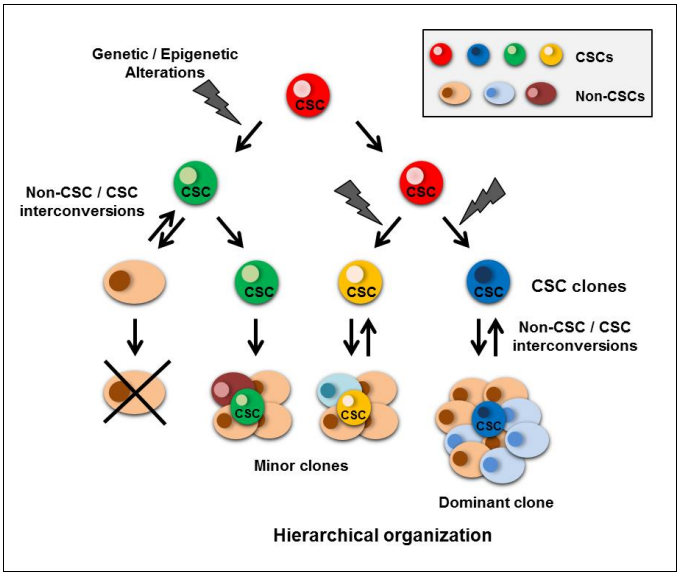

Figure 3. Schematic representation of the unified model of tumor development. The unified model reports at the apex a cancer stem cell (CSC) that after the acquisition of genetic and/or epigenetic mutations evolves, originating several CSC clones characterized by various phenotypic and functional features. Most of these clones grow, organizing the hierarchical structure of tumors. Moreover, non-CSCs can acquire CSC potential thus substaining CSC populations and increasing tumor heterogeneity, a concept known as tumor plasticity.

1.3 CSC isolation and characterization

The first step to study CSC biology implicates their identification and eventually isolation from tumor cell populations. Different methodologies are used to identify and then isolate CSCs. The most commonly used assays include

expression of specific markers, sphere formation assay, multipotency evaluation and *in vivo* tumorigenicity assay.

1.3.1 CSC detection and isolation by expression of specific markers

The identification and isolation of CSCs from a tumor cell population can be performed using various methods. The expression of specific cell surface antigens is the most common tag of CSCs used for their enrichment with FACS (Fluorescent Activated Cell Sorting). Different cell surface antigens have been identified in several cancers as candidate CSC biomarkers. However, no universal CSC markers exist, rather the identified markers are frequently tumor specific and often shared with the stem cells of the tissue of origin. Typically, these surface markers belong to the category of membrane proteins. As described in "The cancer stem cell model" paragraph, the first works describing isolation and characterization of cancer cells with stem-like features were performed in AML. In this tumor, using antibodies against the CD34 and CD38 surface glicoproteins and a cell sorting technique, researchers identified a small subpopulation expressing a $CD34^+$ $CD38^-$ profile that was able to propagate leukemia; in contrast, cells also expressing CD38 were not tumorigenic, despite having the morphological phenotype of leukemic blasts (Lapidot et al. 1994; Bonnet and Dick, 1997). However, further work showed that LSCs able to initiate tumor in mice models also resided in the $CD34^-$ $CD38^+$ cell fraction (Ishikawa et al. 2007; Sarry et al. 2011) and, furthermore, in certain genetically defined cases, such as AML mutated in nucleophosmin 1 (NPM1c), LSCs were found predominantly within the $CD34^-$ fraction in half of the cases (Taussig et al. 2010). Goardon and coworkers (2011) analyzed the immunophenotype of $CD34^+$ blasts of 100 primary AML samples and identified two LSC subpopulations. The first one was present in about 88% of cases and expressed the $CD34^+$ $CD38^-$ $CD45RA^+$ $CD90^-$ phenotype and defined "LMPP-like"(lymphoid multipotent primed progenitor) LSCs and the second one, less frequent, expressed the $CD34^+$ $CD38^+$ $CD123^+$ $CD45RA^+$ phenotype and defined "GMP-like" (granulocyte-macrophage progenitors). LSCs. Both LSC subpopulations were able to engraft immunodeficient mice, generating a leukemic cell progeny with restricted myeloid properties.

Afterward, a great number of other LSC surface markers were identified and intensively explored in human AMLs in the last years, contributing to determine the extensive variability of the AML-CSC surface markers (Pelosi et al. 2015).

These observations indicate that in most AML patients leukemogenic cells were present in at least another fraction of cells besides those $CD34^+$CD38, suggesting that a specific expression pattern of surface markers does not univocally identify cancer stem cells in AML.

The transmembrane glycoprotein CD44, which acts as a receptor for extracellular matrix elements, is another surface marker that has often been associated with the CSC phenotypes. CSCs showing expressions of CD44 were identified in several solid tumors such as breast (Al-Hajj et al. 2003), gastric and colorectal carcinoma (Dalerba et al. 2007), pancreatic cancer (Li et al. 2007), head and neck squamous cell carcinomas (Prince et al. 2007), ovarian cancer (Zhang et al. 2008), bladder malignancies (Gedye et al. 2010) and glioblastomas (Pietras et

al. 2014). The $CD44^+$ cell subset in these tumors was able to initiate tumorigenesis in immunocompromised mice and had the properties of self-renewal and multipotent differentiation. Different CD44 variants (CD44v) can originate from alternative splicing of the primary transcript. Given that many of these variants are preferentially expressed and are involved in several steps of cancer initiation and progression, CD44v isoforms might be better CSC markers than the CD44 standard isoform (Yan et al. 2015).

The transmembrane glycoprotein CD133, also known as prominin-1, has been identified as a peculiar surface marker of CSC populations in several tumors, including brain cancer (Singh et al. 2003; Bao et al. 2006), colorectal cancer (Ricci-Vitiani et al. 2007; Du et al. 2008), hepatocarcinoma (Yin et al. 2007), melanoma (Monzani et al. 2007), lung cancer (Eramo et al. 2008; Tirino et al. 2009) and prostate cancer (Rybak et al. 2011). Moreover, CD133 identifies CSCs in sarcomas, including osteosarcoma, chondrosarcoma, Ewing's sarcoma, and synovial sarcoma (Suvà et al. 2009; Terry and Nielsen 2010; Tirino et al. 2011).

Several other surface markers have been used to define CSCs (Greve et al. 2012; Medema 2013; Liu et al. 2015a) and the combination of different markers has been proposed to improve reliability of CSCs isolation by surface marker detection. For example, in glioblastoma multiforme (GBM), other markers are flanked to CD133 to isolate CSCs, such as EGF receptor (EGFR) and CD44 (Beier et al. 2007; Emlet et al. 2014).

The lack of a complete reliability of surface markers for CSC isolation can also depend on the fact that surface marker expression may vary during tumor growth *in vivo* and the different experimental conditions used in different laboratories may not always be suitable for their detection (Medema 2013). Moreover, the surface antigens used until now do not have a well-determined role in stemness (Welte et al. 2010; Magee et al. 2012). Thus, there is now a wide consensus that phenotypic characterization should be accompanied by functional validation of CSCs (Clevers 2011; Hjelmeland and Rich 2012).

ALDH1 (aldehyde dehydrogenase 1) is regarded as a functional biomarker for CSCs (Oliveira 2011). ALDH1 is a cytosolic enzyme that is responsible for oxidizing intracellular aldehydes and plays a role in drug detoxification (Yoshida et al. 1992). An increased expression of ALDH1 has been found in CSCs of several cancers, like breast (Charafe-Jauffret et al. 2010), pancreatic (Kim et al. 2011), lung (Jiang et al. 2009) and prostate cancers (Nishida et al. 2012), and its increased activity could be responsible for CSC chemotherapy resistance. To this regard Croker and Allan (2012) demonstrated that inhibition of ALDH1 activity reduced the chemotherapy and radiation resistance of human breast CSCs. However, a controversial result was observed in some breast cancer cell lines, where the inhibition of ALDH1 led to an enrichment in CSCs (Ginestier et al. 2009).

Another method used to detect and isolate CSCs is based on their high capacity to extrude Hoechst 33342, a vital DNA fluorescent stain (Golebiewska et al. 2011). At the basis of this property, there is the elevated expression in CSCs of a class of enzymes belonging to the ATP-binding cassette (ABC) transporter superfamily (Di and Zhao 2015). These enzymes are drug efflux pumps and also act in Hoechst 33342 extrusion. Thus, CSCs overexpressing these pumps can be identified by flow cytometry as a non-fluorescent side population (SP) of cells

(Bhagwandin et al. 2016). Indeed, many studies have demonstrated a crucial role of some members of the ABC superfamily, such as ABCB1, ABCC1, ABCC2 and ABCG2, in CSC therapeutic resistance in several tumors (Di and Zhao 2015).

Another useful method to isolate cancer cells with stem-like properties is based on the evaluation of the retention of two lipophilic molecules, PKH26 and PKH6, which label the cell membrane and, after a cell division, are partitioned equally between the daughter cells. While a slow-dividing cell effectively retains the dye, faster-dividing cells rapidly lose or dilute the dye from membrane. This method can be exploited to identify CSCs with slow proliferation rates. In addition, given that CSCs undergo asymmetric division, they retain the label for longer periods than rapidly dividing differentiated daughter cells. This technique has been used to isolate CSCs from osteosarcoma and breast cancer (Pece et al. 2010; Rainusso et al. 2011).

Although not restricted to CSCs, the expression of components of signaling pathways associated with cell pluripotency was also used to characterize these cells. Proteins whose expression was linked to the maintenance of the CSC phenotype include the Oct-4 (*POU5F1*), Sox2, and Nanog transcription factors, frequently overexpressed in CSCs and more specifically linked to self-renewal property, as well as Kfl4 and Myc, implicated in cell reprogramming, and Wnt/β-catenin, Notch, Hedgehog and Bmi1, whose pathway are often deregulated in CSCs (Hadjimichael et al. 2015; Borah et al. 2015). Compared with surface marker-based strategies, the analysis of these factors may provide a more target-specific tool to isolate CSCs. The use of FACS or reporter systems are the common methods to detect CSCs using these factors as targets. The use of flow cytometry could be limiting because these proteins have intracellular localization. Methods based on the use of reporter systems, which employ gene promoters responsive to CSC specific transcription factors (e.g. Oct-4, Sox2, Nanog) that drive the expression of a fluorescent protein, have been widely used and found to be reliable (Levings et al. 2009; Zbinden et al. 2010; Wu et al. 2012).

1.3.2 CSC enrichment by the sphere-formation assay

The sphere-forming assay is widely used to detect and culture cells with stemness features. Typically, this assay consists in culturing cells *in vitro* under non-adherent conditions using serum-free culture media supplemented with specific growth factors, such as epidermal growth factor (EGF), basic-fibroblast growth factor (bFGF), leukemia inhibitory factor (LIF), neural cell survivor factor-1 (NSF-1), used singly or in combination on the basis of the tissue of origin of the cells (Hirschhaeuser et al. 2010; Watanabe et al. 2014). In these conditions, most of the cells are not able to grow and consequently die, while a small percentage of them, endowed with stemness properties, responds to growth factors, grows in suspension and gives rise clonally to spherical cell cluster called spheres. Sphere-forming cultures were first used by Reynolds and Weiss (1992) to isolate normal stem cells from brain tissues. These authors plated cells in non-adherent culture conditions in serum-free medium supplemented with EGF. Only cells with stemness properties were able to grow in suspension forming the so-called "neurospheres". The majority of the cells within these neurospheres expressed

Nestin, a marker of neuronal stem cells. The authors also demonstrated the self-renewal potential of sphere-forming cells: after enzymatic dissociation of primary spheres and serial replating into serum-free/EGF containing medium, cells re-formed spheres. Moreover, they tested the differentiation ability of sphere cells demonstrating that these cells were able to acquire morphology and antigenic properties of mature neurons and astrocytes in adherent monolayer cultures.

The use of sphere-forming assay to eventually isolate and culture CSCs from tumors was achieved for the first time by Ignatova and colleagues (2002). They plated glial cells derived from primary tumors in serum-free medium supplemented with EGF, FGF and insulin. In these conditions, they isolated a small population of cells able to grow as tumorspheres and expressing Nestin and other stemness markers. Moreover, these sphere-forming cells were also able to differentiate into neuronal and glial cells, similarly to normal stem cells and cancer stem cells. Subsequently, exploiting this protocol, tumorsphere-forming cells were isolated from samples of patients affected by GBM (Yuan et al. 2004) and other types of brain tumor; these cells were able to form secondary spheres upon replating, differentiate and efficiently exhibited a high degree of tumorigenicity in nude mice, thus showing CSC properties (Singh et al. 2003; Bao et al. 2006; Wang et al. 2008a). Recently, Liu and colleagues (2015b) have isolated a subset of SP (side population) cells from medulloblastomas biopsies, which formed spheres with higher frequency compared to non-SP cells, and demonstrated that SP cells expressed several stemness properties as neural stem cell markers, like Nestin and Notch1, and ABCG2 transporters, thus supporting the CSC phenotype of these cells. The tumorsphere assay has been also applied to isolate stem-like tumor cells from other types of cancer and their metastasis, such as colorectal cancers, breast cancers, hepatocarcinomas and prostate cancers (Ponti et al. 2005; Ricci-Vitiani et al. 2007; Grimshaw et al. 2008; Cao et al. 2011; Sheng et al. 2013). In addition, spheres formed by cells expressing the stemness genes *POU5F1*, *NANOG* and *SOX2*, increased ALDH1 activity and high tumorigenicity *in vivo* were obtained from primary sarcomas and sarcoma cell models, pointing out that this approach can be useful for the isolation of cancer cells with self-renewal and high tumorigenic potential and to study the evolution of tumor progression (Salerno et al., 2013; Martinez-Cruzado et al. 2016).

The tumorsphere approach has also been used to isolate and characterize circulating cancer stem cells (cCSCs), a high aggressive subpopulation of circulating tumor cells that express stemness features and are a source of metastatic spread from the primary tumors (Barriere et al. 2014; Yang et al. 2015). Exploiting this assay, Pizon and colleagues (2016) analyzed the presence of cCSCs in the peripheral blood of 72 patients with breast cancer, including 23 patients with metastatic spread. They found that in 79% of patients there were circulating tumor cells able to form tumorspheres, which expressed markers typical of breast cancer CSCs, such as $CD44^{+}$ $CD24^{-/low}$ $EpCAM^{+}$, showed *SOX2*, *POU5F1* and *NANOG* overexpression and increased ALDH1 activity. Sphere cells were also endowed with self-renewal ability. Moreover, the total amount of tumorspheres obtained from cCSCs was higher in patients with metastases than in patients without metastasis and patients who did not receive chemotherapy after surgery compared

to patients who had done chemotherapy. Thus, tumorspheres can also be a way to monitor therapy efficacy.

1.3.3 CSC characterization by multipotency evaluation

Multipotency is an essential feature of normal stem cells. This characteristic is not a crucial dogma to define a canonical CSC. However, CSCs undergo symmetric or asymmetric division to differentiate into several cell types that can be found in the original tumor tissue and therefore are considered multipotent. For example, osteosarcoma and chondrosarcoma CSCs can be characterized via multipotency assays relying on relatively easy protocols for *in vitro* differentiation and identification of the differentiated cell types. Sarcoma CSCs, originated from transformed mesenchymal cells, exhibit multi-lineage differentiation ability. In fact, these cells can differentiate into mesenchymal cell types, including osteoblasts, chondrocytes, and adipocytes, through appropriate stimuli (Suvà et al. 2009; Tirino et al. 2011). Recently, Bao and colleagues (2015) showed that a subpopulation of luminal mammary cancer stem cells, isolated from a breast cancer mouse model, was able to develop well-differentiated carcinomas when implanted into the mammary fat pads of syngeneic immune competent mice. Moreover, *in vitro*, upon stimulation with dexamethasone and prolactin or adipogenic agents, these cells differentiated into mammary lineages and adipocytes, respectively.

1.3.4 CSC characterization by in vivo tumorigenicity evaluation

The main characteristic of CSCs is their high tumorigenic potential. The experimental approach used to study tumorigenic potential of CSCs generally includes the collection of putative CSCs through different methods and their xenotransplantation into immunodeficient mice to test their ability to form tumors. However, there are important technical and biological issues which need to be addressed about the use of xenotransplantation assays that could be unfavorable for CSC characterization and determination of their frequency (Nassar and Blanplain 2016). Firstly, the methodologies used to collect cells for mice inoculation, such as mechanical dissociation and enzymatic digestion, may disrupt surface molecules important first of all for cell identification at FACS analysis and then probably essential for their tumorigenicity. These conditions could alter the real number of tumor cells able to generate a tumor, possibly leading to misinterpretation of the results. Other important factors that require consideration are the tumor microenvironment and the site of injection, that can contribute to the efficiency of tumor initiation. The murine microenvironment is different from the human one in terms of architecture, stromal components and secreted molecules (Kuperwasser et al. 2004) and these factors can influence tumor growth and progression, not only in the cases of heterotopic transplantations but also in orthotopic ones. For example, some mouse growth factors and adhesion molecules do not bind human receptors (Manz, 2007; Rongvaux et al. 2013). Thus, some cancer cells that in the human microenvironment have tumorigenic potential can lose this ability in the microenvironment of xenograft mouse models. Another important issue in the xenotransplantation assay is the influence of xenogeneic immune responses evoked

in mice by human cells. The degree of immunodeficiency of the recipient mice can influence the correct measurement of the tumorigenic cell frequency in the cancer population. For example, the use of two different types of immunocompromised mice, such as NOD/SCID or NSG (NOD/SCID IL2Rγ^{null}) strains, less and more immunocompromised respectively, can provide a different estimation of the CSC frequency within melanoma cell populations. Specifically, the use of NSG mice improved the detection of melanoma tumorigenic cells, enhancing their frequency compared to NOD/SCID mice (Quintana et al. 2008, 2010). Similar results were obtained in mouse models of melanoma using *in vivo* single-cell tumor formation assays (Held et al. 2010). A very recent work shows tumor fragments of ccRCC engraft more efficiently than single cell suspensions in NSG mice, indicating that classical xenotransplantation methods can underestimate CSC frequency in ccRCCs (Gedye et al. 2016). Thus, xenotransplantation assays sometimes dramatically underestimate or overestimate the detectable frequency of human cancer cells with tumorigenic potential, also in high permissive mice models.

Although transplantation assays allow distinguishing CSCs within tumor cell populations, they do not allow following the fate of these cells within their natural microenvironment. In order to overcome the problems linked to transplantation and study tumorigenic potential of CSCs in native microenvironments, new approaches have been developed, creating new mouse models. These approaches are based on the principle of lineage tracing experiments, by which specific cell populations are labeled in mice and their fate is followed, for example, during cancer development and recurrence (Rycaj and Tang, 2015). Many studies were conducted using this system and specific engineered mice models were developed to trace and identify the cells originating the tumor. On the other hand, in the established, traced tumors, marked tumor cells can be purified and used in the limiting dilution assay and serial tumor transplantations to determine whether they have CSC properties, that is, self-renewing and long-term tumor-propagating activity. This latter tracing strategy can also be adapted to dissect tumor cell heterogeneity in cultured cancer cells and human xenograft tumors. For example, the promoter of the prostate tumor antigen (PSA) was used to drive reporter genes (GFP and RFP) in a lentiviral vector, which was used to infect cultured prostate cancer cells as well as cells generating tumors in mice, and then to separate the $PSA^{-/lo}$ and PSA^{+} cancer cells on the basis of the expression of the fluorescent marker. The analysis of $PSA^{-/lo}$ cells revealed that they showed stemness features and were able to undergo asymmetric cell division generating PSA^{+} cells both *in vitro* as well as in serially transplanted tumors (Qin et al. 2012). Similarly, a Wnt reporter gene allowed tracing colorectal CSCs and demonstrating that the Wnt signaling was activated in these CSCs by soluble molecules secreted by the neighboring myofibroblasts (Vermeulen et al. 2010).

Recently, three lineage-tracing studies provided support to the CSC model in different types of solid tumors, as brain, intestinal and breast cancers (Chen et al. 2012; Schepers et al. 2012; Kozar et al. 2013; Zomer et al. 2013). Chen and colleagues (2012), using a transgenic mouse model of glioblastoma, engineered with the Nestin promoter-ΔTK-IRES-GFP construct, demonstrated that glioblastomas contained a relatively quiescent populations of CSCs that originated from neural stem cells, which were responsible for tumor maintenance and

recurrence after chemotherapy. Schepers and coworkers (2012), exploiting lineage tracing experiments based on the use of Cre recombinase-expressing mice knock-in for the crypt stem cell marker LGR5, showed that a subpopulation of adenoma cells induced by the loss of *APC* were positive for the marker and demonstrated that these cells were able to self-renew and give rise to more differentiated $LGR5^-$ adenoma cells. Moreover, the authors found that $LGR5^+$ adenoma cells had a gene expression pattern similar to that of intestinal crypt stem cells from which the tumors arose. Using a novel lineage-tracing technique leading to continuous clonal labeling, Kozar and coworkers (2013) showed the appearance of large dominant clones within adenomas sustained by CSCs, but they suggested that only a small fraction of LGR5-expressing cells are acting as tumor stem cells in this model.

Using lineage tracing in an MMTV-PyMT mouse model of breast tumors, Zomer and colleagues (2013) observed tumor cell clonal dynamics over time using intravital imaging. Interestingly, some clones initially expanded and then contracted or disappeared, whereas other clones rapidly expanded and became dominant within 2 weeks of observation, consistently with important tumor heterogeneity and the existence of CSCs in this model. All together these observations are in agreement with the idea that tumors are heterogeneous and contain a subset of cells with CSC properties involved in cancer development and recurrence. Moreover, the last mentioned study demonstrated that tumor progression is supported by a dynamicity of CSC dominant clones, strengthening the idea of an unified model for tumorigenesis (Kreso and Dick, 2014).

1.4 CSC-related genes

CSCs share various similarities with stem cells, especially with normal stem cells of the tissue of origin of the tumor. One of these similarities is the ability to self-renew. Self-renewal is a special cell division process that enables a stem cell to produce another stem cell with essentially the same development and replication potential. Self-renewal allows the expansion of the stem cell compartment when systemic or local signals trigger massive proliferation, allowing the maintenance of a tissue-specific undifferentiated pool of cells in the organ or tissue. CSCs are endowed with the same self-renewal ability, although in an aberrant way respect to normal stem cells. Because self-renewal is required by both normal stem cells and cancer stem cells, it is reasonable to assume that the molecular mechanisms regulating this stem cell function are shared by the two cell types. However, in cancer stem cells the factors that regulate these mechanisms are often deregulated and altered through mutations and epigenetic modifications.

Pathways involved in self-renewal include the Wnt, Notch, Hedgehog, and Bmi1 pathways (Borah et al. 2015). Wnt is an ancient and evolutionary conserved pathway, which controls stem cells and determines cellular fate during development. Wnt proteins constitute a group of secreted signaling molecules that bind to the Frizzled family of transmembrane receptors on target cells. Once Wnt ligand binds to its receptor, a cascade of events occurs leading to stabilization of β-catenin, a cell adhesion molecule, which translocates into the nucleus and, through interactions with specific transcription factors, as TCF/LEF proteins, activates the

transcription of genes involved in cell proliferation, as c-*MYC*, cell migration and cell fate determination, which are crucial processes in embryonic development and self-renewal of adult stem cells. The relevance of Wnt/β-catenin signaling in human cancers is perhaps better known for its role in colon cancer (Morin et al. 1997); however, this pathway has also been linked to CSC biology. Consistent findings have shed light to the fact that Wnt/β-catenin pattern plays an important role in the regulation of CSC signatures in several cancers, as leukemia (Wang et al. 2010), colorectal cancer (Vermeulen et al. 2010), cutaneous squamous cell carcinoma (Malanchi et al. 2008) and breast cancer (Malanchi et al. 2012). More recently, Cheng and coworkers (2013) showed that overexpression of β-catenin in a nasopharyngeal carcinoma cell line led to the acquisition of stem-like properties such as sphere formation, *POU5F1*, *SOX2*, *KLF4* and *NANOG* overexpression, as well as an increase in the $CD44^+$ population. Similarly, Lee and colleagues (2014) found that ectopic β-catenin expression in head and neck squamous cell carcinoma (HNSCC) cell lines induced the up-regulation of CSC markers together with enhanced sphere formation capacity and chemotherapy resistance.

Notch is a transmembrane receptor that coordinates a signaling cascade widely conserved and shared by multicellular organisms for the regulation of cell-to-cell communications during embryogenesis, cellular proliferation, differentiation and apoptosis (Artavanis-Tsakonas et al. 1999). Notch activates the expression of many types of genes involved in several processes, including stemness genes such as c-*MYC* (Lobry et al. 2014; Zinin et al. 2014; Yashiro-Ohtani et al. 2014). Deregulation of Notch has been reported in several cancer types (Miyamoto et al. 2003; Santagata et al. 2004; Reedijk et al. 2005; Roy et al. 2007; Wang et al. 2009; Liao et al. 2011), where inappropriate activation of the pathway leads to uncontrolled proliferation, restricted differentiation and prevents apoptosis of cancer cells. However, its role as an oncogene in not well defined yet; in fact, many studies have demonstrated that it acts as tumor suppressor in some cancer tissues. To this regard, inhibition of *NOTCH* expression in some NSCLC (non-small cell lung cancer) cell lines resulted in increased cell proliferation, while its overexpression resulted in apoptosis activation. In other NSCLC cell lines, on the contrary, apoptotic events were stimulated by *NOTCH* down-regulation (Wael et al. 2014). Performing genomic analysis on diverse squamous cell carcinomas, Zhang and colleagues (2016a) identified several loss of function mutations in *NOTCH*, suggesting that Notch may function as tumor suppressor in these cancers. Aberrant Notch expression has also been linked to CSC self-renewal and differentiation (Dreesen and Brivanlou, 2007). In breast cancer, CSCs show high levels of Notch expression and Notch levels positively correlate with mammosphere forming efficiency and tumorigenicity (Farnie et al. 2007). Abel and colleagues (2014) demonstrated that pancreatic CSCs are characterized by high expression levels of Notch pathway components. Inhibition of Notch activation reduced tumorsphere formation and CSC frequency. Conversely, Notch activation increased pancreatic CSC self-renewal. *In vivo*, treatment of pancreatic cancer cell xenografts with the Notch inhibitor GSI inhibited tumor growth and reduced the CSC population of xenograft tumors.

It is known that the Hedgehog (Hh) signaling pathway, involved in the controlling of embryonic developmental but also in postnatal and adult tissue

morphogenesis, has also roles in the maintenance of normal stem cells and in cancer development (Ruiz i Altaba et al. 2002). Indeed, experimental evidence confirmed that many stemness properties, as self-renewal ability, of CSCs identified in many tumors depends on the Hh signaling pathway (Clement et al. 2007; Peacock et al. 2007; Feldmann et al. 2007; Dierks et al. 2008; Zhao et al. 2009a). Moreover, as investigated by Liu et al. (2006), Hh signaling has also been found to regulate self-renewal in breast CSCs acting in concert with Bmi1, another protein related to the CSC phenotype. Bmi1 is a member of the Polycomb-group protein family and is crucial for hematopoietic stem cell and neural stem cell self-renewal (Molofsky et al. 2003, Park et al. 2003) as well as for mouse LSCs (Lessard and Sauvageau 2003).

Several markers that were identified as inducers and regulators of pluripotency in stem cells play also a role in CSCs (Hadjimichael et al. 2015). As previously mentioned (see page 22), transcription factors Oct-4, Sox2 and Nanog constitute the "core pluripotency network" that regulates pluripotency of both mouse and human embryonic stem cells (ESCs). They synergistically bind to their own promoter/enhancer elements establishing an auto-regulatory circuit (Boyer et al. 2005; Loh et al. 2006). This master pluripotency network, including additional factors such as Klf4, Stat3 and the oncoprotein c-Myc, binds to and regulates the expression of two distinct groups of genes in ESCs: genes related to self-renewal (activate) and genes related to differentiation (silenced) (Jaenisch and Young 2008; Bourillot and Savatier 2010). The latter group of genes is co-regulated by the Polycomb repressor complexes (PRC1 and PRC2) (Boyer et al. 2006). These groups of genes often mutually regulate each other and interact physically and functionally with chromatin remodeling and modification complexes, constituting transcriptional networks for embryonic stem cell pluripotency, somatic cell reprogramming and cancer (Chen et al. 2008a; Orkin et al. 2008; Kim et al. 2010a; Orkin and Hochedlinger 2011; Young 2011).

Numerous studies have indicated that the three transcription factors constituting the core of the pluripotency network play also a crucial role, singularly or in combination, in several tumors, in particular in the maintenance of CSC features. For example, Oct-4 was shown to be up-regulated in many human cancers such as bladder cancer, lung cancer, prostate cancer, breast cancer and many others (Atlasi et al. 2007; Ben-Porath et al. 2008; Liu et al. 2011a). Hu and coworkers. (2008) reported that in murine lung carcinoma cells and human breast cancer MCF7 cells, ablation of Oct-4 led to apoptosis of CSC-like cells through the inhibition of the Oct-4/Tcl1/Akt1 pathway and reduced tumor growth. Another study confirmed that the reduction of Oct-4 expression in lung cancer cells decreased their tumorigenic capacity and increased chemotherapeutic sensitivity (Chen et al. 2008b). Chiou and colleagues (2008) enriched oral cancer CSCs by sphere formation and concluded that these cells highly expressed Oct-4 and had similar characteristics to stem cells and malignant tumors. Moreover, it has been shown that ectopic expression of Oct-4 into normal primary breast epithelial cells generated cell lines that formed triple-negative breast carcinomas in nude mice (Beltran et al. 2011). Recently, Wang and coworkers (2013a) demonstrated that cervical cancer cells expressed higher Oct-4 levels than normal cervix cells. They showed that Oct-4 promoted tumor formation *in vivo* and inhibited apoptosis by the

activation of miR-125b expression. In addition, Oct-4 has been suggested to regulate stemness of head and neck squamous carcinoma CSCs. The overexpression of Oct-4 in carcinoma cells activated cyclin E, leading to tumor growth, and promoted tumor invasion through Slug expression (Koo et al. 2015).

Sox2 is another critical transcription factor with a role in CSCs. Sox2 is important for osteosarcoma cell self-renewal and is an antagonist of the pro-differentiation Wnt pathway, which can in turn negatively affect its expression (Basu-Roy et al. 2012). Studies in gastric cancer showed that Sox2 expression inhibition reduced spheres formation and increased apoptosis of sphere cells (Tian et al. 2012). The contribution of Sox2 in pancreatic cancer CSC phenotype was suggested by the fact that its expression was associated with the promotion of stem cell-like features, like sphere formation. Moreover, spheres were enriched in cells overexpressing Sox2 and other CSC markers, as ALDH1, epithelial surface antigen (ESA) and CD44. Interestingly, Sox2 knockdown induced tumor growth inhibition by cell cycle arrest, indicating that Sox2 has a role also in promoting proliferation (Herreros-Villanueva et al. 2013). In prostate CSCs, the inhibition of EGFR signaling led to the decrease of Sox2 expression and self-renewal capacity. Moreover, Sox2 knockdown reduced the ability of prostate CSCs to grow under anchorage-independent conditions (Rybak and Tang 2013). In melanoma CSC studies, Sox2 expression was shown to be under control of the Hedgehog-GLI signaling pathway and to regulate melanosphere formation and self-renewal (Santini et al. 2014).

Nanog is the third member of the core pluripotency network in undifferentiated ESCs. Its expression was investigated in several types of cancer, including lung, breast, oral, kidney, gastric, cervix, brain, ovarian and prostate cancer (Bussolati et al. 2008; Amsterdam et al. 2013; Lu et al. 2014). In many of these cancers, abnormal high expression levels of Nanog were related to a poor prognosis (Lin et al. 2012; Lee et al. 2012). For example, in oral squamous cell and lung adenocarcinoma, high levels of Nanog, in combination with Oct-4 overexpression, were linked to advanced cancer stage and shorter patient survival (Chiou et al. 2008; 2010). Several groups have demonstrated that Nanog expression is much higher in CSCs than in non-stem cancer cells in many types of cancer. In colorectal cancer, Nanog-positive CSCs constitute approximately 2% of the total cancer cell population (Ibrahim et al. 2012). In osteosarcomas and NSCLCs, $CD133^+$ or $CD44^+$ cells express significant higher levels of Nanog than $CD133^-$ or $CD44^-$ cells indicating that high expression levels of Nanog are related to the CSC phenotype (Leung et al. 2010; He et al. 2012). Studies on several cancers have shown that Nanog is not only a CSC marker but also induces CSC-like characteristics. For example, overexpression of Nanog in prostate cancer increased tumor regenerative ability (Jeter et al. 2011). Exogenous Nanog expression in colorectal cancer cells drove cells to adopt a stem-like phenotype. Nanog-positive colorectal cancer cells showed increased sphere formation ability and tumor formation capacity in xenograft models (Ibrahim et al. 2012).

Recently, Olmez and colleagues (2015) successfully dedifferentiated two patient-derived GMB cell lines into CSC-like cells through ectopic expression of Oct-4, Sox2 and Nanog transcription factors. Transformed cells acquired sphere

formation ability, CD133, CD44 and ALDH1A1 expression, and exhibited significantly chemoresistance.

Besides *POU5F1*, *SOX2* and *NANOG*, other genes and pathways important in stem cells have been linked to cancer and in particular to CSCs. C-Myc is deregulated in many cancers and is a stemness transcription factor (Takahashi and Yamanaka, 2006; Takahashi et al. 2007). C-Myc is involved in numerous biological functions. It acts as an essential regulator of cell growth, proliferation and differentiation and is thought to be crucial for stem cell pluripotency and proliferation (Cole and Henriksson 2006; Laurenti et al. 2009). However, c-Myc has a dual role in neoplastic transformation. Indeed, on one hand, being an inducer of proliferation, it favors transformation, while on the other hand it can contrast this process through apoptosis activation (Evan et al. 1992; Meyer et al. 2006). Evidence of c-Myc involvement in CSCs were reported by Wang and coworkers. (2008b), who showed that a population of $CD133^+$ CSCs isolated from primary glioma surgical biopsies expressed higher levels of c-Myc compared to glioma non-CSCs. Moreover, the knockdown of c-Myc in glioma CSCs determined a reduction of their cell growth and an increase of apoptotic events. Finally, glioma CSCs with decreased levels of c-Myc failed to form neuropsheres *in vitro* and tumors after orthotopic xenotransplantation *in vivo*. In a recent study, it has been demonstrated that silencing c-Myc using siRNAs decreased prostate CSC maintenance and tumorigenicity and induced senescence in the prostate CSC subpopulation (Civenni et al. 2013). Despite the strong association between c-Myc deregulation and CSCs in prostate cancer, mechanisms involved in the modulation of its expression in this tumor are not well clear yet.

An essential trait of stem cells is linked to their ability to self-replicate without incurring into DNA damage. An important factor associated to self-renewal is the nucleolar GTP- binding protein nucleostemin (encoded by the gene *GNL3*, guanine-nucleotide- binding protein-like 3). This protein is known to be localized in nucleoli and has a role in cell-cycle progression and maintenance of stemness features in stem cells and cancer cells (Tsai and McKay 2002). Several studies have also demonstrated that this protein plays part in safeguarding processes of genomic integrity in stem and cancer cells (Tsai 2014). Therefore, it has been investigated its possible role in the CSC phenotype. Indeed, Tamase and coworkers (2009) using a reporter system in which the nucleostemin promoter directed GFP expression, identified nucleostemin-GFP^+ cells as tumor-initiating cells in a mouse brain tumor mode. Lin and colleagues (2010) demonstrated that nucleostemin is enriched in breast CSCs and its expression also increased during progression of mammary tumors in transgenic breast cancer mice models *in vivo* and during sphere propagation *in vitro*. Recently, $CD133^+$ cancer cells were isolated from a rare form of GBM involving the lateral ventricles of brain and the analysis of their molecular profile revealed an increase in nucleostemin expression (Li et al. 2012).

Collectively, a large body of results suggests that normal stem cells and CSCs share critical transcription factors. It is clear that pluripotency factors Oct-4, Nanog, Sox2, together with the other stemness factors mentioned above, as in particular Notch and c-Myc, play a crucial role in cancer development and specifically in CSC biology. However, further investigation of their role in

determining the CSC phenotypes, will provide the exact regulatory mechanisms and possibly new regulatory factors relating to tumorigenesis.

1.5 CSC-related miRNAs

In addition to genetic diversity and differential expression of genes and proteins among tumor cells, noncoding RNAs, as microRNAs (miRNAs), have emerged as crucial molecules involved in several issues of tumor development. MicroRNAs are a class of endogenous non-coding RNA molecules 18-22 nucleotides long. The majority of these short molecules acts inducing mRNA degradation by binding to the 3'-untraslated region (UTR) of the complementary mRNA target, through a conserved region at the microRNA designated 'seed sequence'. However, in some instances miRNAs can repress mRNA translation.

There are many works showing that miRNAs can exert a role in the regulation of several CSC features (Leal and Lleonart 2013; Sun et al. 2014). Yu and coworkers (2007) revealed the implication of let-7 in the regulation of some breast cancer CSC properties. In particular, they observed that let-7 is down-regulated in breast cancer CSCs and its exogenous expression reduced mammospheres and tumor formation capacity in $CD44^{+/high}CD24^{-/low}$ CSCs. Moreover, let-7 deregulation diminished the expression of the stemness gene c-*MYC*. MiR-30 is also down-regulated in breast cancer CSCs. Transfection of both let-7 and miR-30 into breast cancer CSCs further reduces their stemness properties (Yu et al. 2010). Other miRNAs are associated to breast cancer CSC phenotype. Using miRNA profiling, Iliopoulos and colleagues (2010) defined a set of 22 miRNAs that were differentially expressed in normal *vs* CSC, including let-7 and the miR-200 family. The role of the miR-200 cluster is important in the regulation of breast CSC properties. Shimono and coworkers (2009) have demonstrated that miRNA-220c strongly regulates the expression of the self-renewal regulator Bmi1 and suppresses clonogenicity and tumorigenicity of breast CSCs.

MiR-9/9*, miR-17 and miR-106b are the most expressed miRNAs in the glioblastoma CSC population. It was demonstrated that knocking down miR-9 and miR-17 caused a reduction in neurosphere formation (Schraivogel et al. 2011). In contrast, miR-199b-5p is a negative regulator of CSC maintenance in brain tumors; Garzia and coworkers (2009) showed that its overexpression in medulloblastoma, inhibited the self-renewal capacity of CSCs targeting HES-1, a transcription factor of the Notch signaling pathway. Similarly, miR-145 was found down-regulated in $CD133^{+}$ glioblastoma stem cells and its overexpression caused the inhibition of tumorigenic potential of this cancer cell population as well as the reduction of other CSC properties by targeting Oct-4 and Sox2 mRNAs (Yang et al. 2012).

A crucial role in the regulation of CSC features is conducted by the tumor suppressor miR-34a. The deregulation of this miRNA was found in CSCs derived from several types of tumors, including prostate, lung, brain, pancreatic, breast, colon and gastric cancer (Ji et al. 2009; Liu et al. 2011b; Bu et al. 2013; Shi et al. 2014; Kang et al. 2015). Firstly, miR-34a was shown to downregulate Notch expression and to inhibit cell proliferation in glioma and medulloblastoma cells (Li et al. 2009a), pointing out its role as a tumor suppressor. Liu and coworkers (2011b) analyzed miRNA expression profile in $CD44^{+}$ prostate CSCs isolated from

primary tumor or mouse xenograft and found that miR34a was strongly down-regulated; they also demonstrated that the overexpression of miR-34a in these cells impaired their proliferation, tumorigenicity and metastatic potential by targeting CD44. A similar action was obtained in NSCLC cell lines where miR-34a was found down-regulated and its overexpression in $CD44^+$ CSCs inhibited their tumorigenic capacity, while its knockdown in non-CSCs promoted tumor development (Shi et al. 2014). More recently, Zhang and coworkers (2016b) demonstrated the strong implication of miR-34a-Notch circuitry in the maintenance of CSCs isolated from murine breast cancer cell line. In fact, they showed that miR-34a caused a reduction of stemness properties of breast CSCs and induced the cytotoxic susceptibility of these cells to the natural killer (NK) cells *in vitro* by the down-regulation of Notch signaling molecules.

1.6 CSC origin and plasticity

The CSC hypothesis postulates that cancers are hierarchically organized and only a subset of cells, the CSCs, drive cancer growth (Clevers 2011). However, despite the existence of this small cell population is increasingly documented and accepted in several tumors, little is known about their origin and what is known is still a matter of discussion. Up to date, several hypothesis have been formulated. Studies on leukemia suggested that CSCs can originate from neoplastic transformation of normal stem cells, since these two types of cells share several stemness features, such as surface marker expression, self-renewal and multilineage differentiation ability. To this regard, already in 1978, Fialkow and colleagues showed that HSCs were the cells which acquired the *BCR-ABL* oncogenic mutation and gave rise to the major lineages of blood cells in chronic myeloid leukemia (CML) patients. A similar result was obtained in a CML mouse model, in which it was demonstrated that CML could be established by restricting *BCR-ABLp210* oncogene expression in murine $Sca1^+$ hematopoietic stem cells (Pérez-Caro et al. 2009). More recently, a study performed on AML patients showed that a mutated form of the gene *DNMT3a*, which encodes a DNA methyltransferase, was commonly found in myeloid cancer cells and in normal T- and B-lymphocytes and NK cells, suggesting that this mutation probably occurred in HSCs, which are precursors of all these types of cells (Shlush et al. 2014).

Also in some solid tumors, there is evidence that CSCs can derive from oncogenic transformation of adult stem cells. In a mouse model of colorectal cancer, Barker and coworkers (2009) demonstrated that *APC* loss in $Lgr5^+$ crypt stem cells led to neoplastic transformation in a shorter time and with a greater number of adenomas than *APC* deletion in progenitors or differentiated cells. In addition, the use of lineage tracing assays has permitted to demonstrate that several cancers can originate from transformation of stem cells. For example, transfer of prostate cancer basal cells, which show stem-like properties, from benign tumors to immunodeficient mice revealed that these cells were able to develop a typical human prostate cancer, with expansion of luminal cells and loss of basal cells. Thus, basal cells seem to be the cells of origin of prostate cancer, despite the luminal histological features of cancer cells (Goldstein et al. 2010). Using similar experiments, also glioblastomas and medulloblastomas have been shown to

originate from stem cells of distinct brain regions upon activating mutations in the proto-oncogene *N-MYC* (Swartling et al. 2012).

However, it has been shown that also early progenitor cells can acquire self-renewal ability, initiate and drive tumor progression as CSCs. Jaiswal and coworkers (2003) induced *BCR/ABL* oncogene expression specifically in myeloid progenitors leading to AML in mice. Similarly, Krivtsov and coworkers (2006) described the conversion of a committed GMP to LSC through the expression of the oncogenic fusion protein MLL-AF9. The obtained LSCs were capable of transferring leukaemia to secondary recipient mice when only four cells were injected, and possessed an immunophenotype and a global gene expression profile very similar to that of normal GMPs. However, a subset of genes highly expressed in HSCs was re-activated in LSCs. In another study, Goardon and colleagues (2011) showed that in several AML tumor samples, two populations with a progenitor immunophenotype could be isolated, which showed CSC properties and gave rise to hierarchical organized tumors. Gene expression patterns of the two cellular populations resembled more that of GMPs and LMPPs rather than that of HSCs. This suggests that AML can derive from the transformation of progenitor cells, which acquire self-renewal properties.

Indeed, analysis of LSCs in patients with CML provided the strong evidence that these cells arose from normal blood stem cells. However, in CML patients at advanced stages of the disease, blast crisis was shown to be due to the expansion of a GMP pool, which acquired self-renewal properties through the activation of the Wnt/β-catenin pathway. Thus, blast cells probably originate from differentiated cells derived from LSCs (Jamieson et al. 2004). These observations indicate that CSCs may not always originate from the same cells that give rise to the tumor, but can also derive from bulk tumor cells through the acquisition of additional mutations. Thus, it is conceivable that CSCs can arise from neoplastic transformation of mature cells, which can lead to cellular reprogramming with a switch from a differentiated cell state to a stem-like state.

This hypothesis has found support from studies conducted in normal tissues where differentiated cells can stably revert into replicating progenitors or even multipotent stem cells under specific conditions, such as for example injuries or stem cell ablation, regenerating tissues or stem cell niche (van Es et al. 2012; Tata et al. 2013; Zhao et al. 2016). Moreover, experiments of somatic cell reprogramming has been conducted *in vitro* by Takahashi and colleagues (2007) where they dedifferentiated fully mature fibroblasts into embryonic stem-like cells, also named induced pluripotent stem cells (iPSCs), through the ectopic expression of some stemness genes (Yamanaka factors), many of which are also involved in neoplastic transformation. If terminally differentiated cells can regain stem cell traits to maintain a balanced equilibrium between non-stem and stem cell compartments or to be able to regenerate damaged tissue, it is possible to assume that this process can be adopted also by cancers and, in particular, could offer a new insight into CSC origin.

One of the first works demonstrating that CSCs can originate from reprogramming of mature cells triggered by neoplastic transformation was that of Chaffer and coworkers (2011). These authors first showed that differentiated $CD44^-$ human mammary epithelial cells (HMECs) reverted to a stemness $CD44^+$

phenotype at low frequency. Then, they demonstrated that when cells were neoplastically transformed, through the exogenous expression of telomerase and the oncogenes simian virus 40 early region (SV40ER) and H-*ras*, $CD44^-$ cells converted into the $CD44^+$ state at a much higher rate compared to their untransformed counterparts. Moreover, tumors induced in NOD/SCID mice by transformed $CD44^-$ HMECs contained $CD44^+$ cancer stem-like cells, indicating that reprogramming of differentiated transformed cells can spontaneously occur either *in vitro* or *in vivo*.

Another evidence supporting this hypothesis was reported by Scaffidi and Misteli (2011). They induced *in vitro* neoplastic transformation of human fibroblasts through the exogenous expression of telomerase and H-*ras* and the inactivation of the p53 and pRB tumor suppressor pathways through the ectopic expression of SV40 antigens. Upon transformation, a small fraction of CSC-like cells, which was endowed with high tumorigenic potential in NSG mice, arose from the whole cell population. This subpopulation expressed the stage-specific embryonic antigen 1 (SSEA-1) stem cell marker, was able to self-renew and differentiate and maintained the hierarchical organization of tumors, generating non tumorigenic $SSEA\text{-}1^-$ cancer cells. In addition, the authors observed that $SSEA\text{-}1^-$ cells casually converted into $SSEA\text{-}1^+$, indicating that oncogenic reprogramming of differentiated cells into CSC-like cells is a stochastic process in *in vitro* transformed cell lines.

Friedmann-Morvinski and coworkers (2012) demonstrated that the development of gliomas in mice can be sustained by a subset of cancer stem-like cells, which originate from the dedifferentiation of primary cortical astrocytes transformed *in vitro* by transduction with shNF1-shp53 or H-RasV12-shp53 vector. In a mouse model of intestinal carcinogenesis, Schwitalla and colleagues (2013) showed that elevated levels of NF-κB induced the dedifferentiation of non-stem cells, which acquired CSC features.

In summary, these studies point out that CSCs are plastic entities, not only these cells can differentiate to originate the heterogeneous pool of bulk tumor cells, but can also be originated by bulk tumor cells through a dedifferentiation process. In this light, CSCs are a highly dynamic system and this implicates important consequences for the use of anticancer treatments. In fact, targeting CSCs might not be sufficient, if CSCs can be newly generated by bulk tumor cells. Thus, in the last years, the attention of researchers is drifted into the new established concept of the 'CSC plasticity', based on this inter-convertibility between CSCs and non-CSCs, in order to define the molecular mechanisms possibly involved, and still unknown. Moreover, the concept of CSC plasticity is increasingly seen as the true model of cancer development which links clonal evolution and CSC models, imposing that hierarchical organization of tumors should be seen as a bidirectional balance between CSC and differentiated non-CSCs.

1.7 Factors promoting CSC plasticity

1.7.1 The Epithelial-Mesenchymal Transition (EMT)

EMT is the cellular process occurring when epithelial cells acquire a mesenchymal phenotype and lose adhesion with neighboring cells increasing their migratory capacity. EMT is a natural process taking place during embryonic development, but is also crucial for tumor progression and expansion. It allows epithelial cancer cells to acquire the capacity to move and infiltrate surrounding tissues and eventually spread from the primary site to distant sites, where they can give rise to metastases (Thiery et al. 2009; Lamouille et al. 2014).

Mani and coworkers (2008) were the first researchers to report a correlation between EMT and the acquisition of the CSC phenotype. These authors, exploiting *in vitro* transformed HMECs, demonstrated that upon EMT induction these cells also acquired stemness features. To induce EMT, they infected cells with retroviral vectors expressing either Twist or Snail or treated them with recombinant TGF-β1, all well-known EMT inducers. Upon EMT induction, they found that, compared to mock or untreated cells, the resulting cells were enriched in $CD44^{high}$ $CD24^{low}$ cells, showed a significant increase in sphere-forming ability and tumorigenicity, and displayed differentiation capacities, indicating that these cells had acquired CSC features. In turn, these authors showed that primary tumor-derived $CD44^{high}$ $CD24^{low}$ cells expressed high levels of EMT markers, suggesting that human breast tumors undergoing EMT are enriched in CSCs, which probably originate from non-CSCs upon EMT engagement. The association between EMT and CSC plasticity was further demonstrated by Morel and colleagues (2012), exploiting a transgenic mouse model coexpressing Twist and oncogenic Ras. These authors demonstrated that the forced expression of Twist correlated with the generation of malignant mammary epithelial cells characterized by EMT traits and stem-like features.

A link between CSC and EMT is also shown by the observation that transcription factors that promote EMT can directly modulate the expression of stemness-related genes. For example, in pancreatic and colorectal cancers, the EMT-activator ZEB1 can induce the expression of the stemness-associated genes *SOX2* and *KLF4*, favoring the dedifferentiation of bulk tumor cells into CSCs and probably also promoting the dissemination of these cells (Wellner et al. 2009). In patients with head and neck carcinoma, Twist was shown to directly induce the expression of *BMI1* (Yang et al. 2010). Epigenetics also plays a crucial role in the regulation of the mechanisms involved in the link between EMT and CSC. To this regard, a very recent study performed on prostate cancer cell lines demonstrated that the knockdown of *DNMT1*, an important regulator of chromatin status, induced the expression of the EMT-related gene *ZEB2* and increased the expression of Sox2, Oct-4 and Klf4. Moreover, the *DNMT1*-silenced prostate cancer cells expressed mesenchymal markers, as N-cadherin and vimentin, and showed other CSC features as the ability to form tumorspheres *in vitro* (Lee et al. 2016a).

However, other studies showed that the relationship between EMT and CSCs is more complex than expected (Brabletz 2012). For example, Ocaña and

colleagues (2012) demonstrated that down-regulation of the EMT activator PRRX1 in breast cancer cell lines not only increased cells' metastatic potential, but also promoted the acquisition of stemness properties. These findings identify a distinct mechanism of metastatic colonization and uncouple stemness and EMT. Thus, EMT signals seem to be involved both in differentiation and dedifferentiation of cancer cells, constituting a dynamic process able to promote cell plasticity and tumorigenicity.

1.7.2 The tumor microenvironment

Cancer cells are closely associated with a dynamic environment constituted by neighboring cells, like stromal cells, inflammatory and other immune cells, extracellular components, soluble factors, vascular and lymphatic networks. All together these components are in relation with each other and give rise to the tumor microenvironment or niche (Chen et al. 2015). Several microenvironmental factors can regulate the CSC fate, as cellular and molecular components of the extracellular matrix, secreted molecules, such as cytokines and growth factors, endothelial cells, various immune cells, inflammation and hypoxia. The role of these factors in CSC maintenance has been demonstrated in several tumors.

Matrix metalloproteinases (MMPs), which represent a family of zinc-dependent endopeptidases with the function to degrade components of ECM and further facilitate angiogenesis, tumor cell invasion, and metastasis, can play a crucial role in the promotion and maintenance of CSC features. Overexpression of MMP13 was specifically found in tumorsphere-forming cells derived from brain cancer cell populations (Inoue et al. 2010). MMP10 is highly expressed in CSCs, and repression of MMP10 leads to the loss of stem cell-related gene expression in lung cancer stem-like cells (Justilien et al. 2012). In pancreatic carcinoma, breast cancer and colon cancer models, an interplay between neoplastic cells, CSCs, and the stroma is observed. In pancreatic carcinomas, stellate cells, myofibroblast-like cells found in the stromal compartment, have been shown to enhance CSC features, such as sphere-forming ability and self-renewal. The acquisition of these CSC properties resulted from the activation of the expression of CSC-related genes promoted by stellate stromal cells via the paracrine Nodal/Activin signaling pathway (Lonardo et al. 2012).

The role of mesenchymal stem cells in CSC plasticity is also important. These cells can provide an advantageous microenvironment for the restoration of CSC subpopulations through secretion of several cytokines, such as interleukin (IL)-6 and IL-8, and chemokines, as CXCL7 and CXCL12 with paracrine and autocrine actions (Liu et al. 2011c; Cabarcas et al. 2011). Furthermore, these stromal cells can induce up-regulation of miR-199a in breast cancer cells, which causes the repression of the transcriptional regulator FOXP2, an inhibitor of stemness gene expression, thus providing tumor cells with CSC features (Cuiffo et al. 2014).

The interaction between immune cells and cancer cells has been shown to promote tumor development and progression. A recent study has elucidated how the immune system can affect CSCs through paracrine signaling in colorectal cancer. In particular, using a model of colorectal cancer, Kryczek and colleagues (2014) showed that tumor infiltrated $CD4^+$ T cells secreted IL-22, which activated

the transcription factor STAT3 and induced the expression of the histone methyltransferase DOT1L. DOT1L promoted the expression of *SOX2*, *POU5F1* and *NANOG*, increasing cancer cell stemness and tumorigenicity.

A strict relationship exists also between tumor-associated macrophages (TAMs) and CSCs. In both human glioma samples and animal models, the distribution of TAMs in the microglia correlated with the localization of $CD133^+$ glioma stem-like cells, and these macrophages could significantly enhance the CSC features and the invasive capability of these cells through paracrine production of TGF-β1 (Ye et al. 2012). In pancreatic tumors, for example, the reduction of the number of TAMs can decrease the population of CSCs, causing an improvement in the response to anticancer treatments (Mitchem et al. 2013).

Tumor microvasculature and hypoxia represent important factors for the regulation of CSC plasticity. In various solid cancers, endothelial cells were shown to promote CSC self-renewal by direct cell-to-cell contact or by production of nitric oxide (NO) via the Notch signaling pathway (Charles and Holland 2010). More recently, Fessler and colleagues (2015) showed that tumor microvascular endothelial cells make primary GBM cells to dedifferentiate into glioma CSCs through the secretion of bFGF.

Hypoxia has been shown to increase the expression of stem cell markers in several cancer cell lines. For example, hypoxia-inducible factors (HIFs), particularly HIF2α, were able to regulate glioblastoma stem cell properties, including sphere formation capacity and tumorigenic potential (Li et al. 2009b).

Taken together, these experimental observations underline the role of the tumor microenvironment, including ECM, stromal components, immune cells, growth factors and cytokines, endothelial cells, hypoxic conditions, in the regulation of the plasticity of tumor cells and CSCs and indicate that the multiple factors of the tumor niche can constitute new targets for anticancer therapy.

1.8 The role of inflammation in CSC induction and maintenance

Inflammation has been associated with the development of cancer since a long time (Balkwill and Mantovani 2001; Coussens and Werb 2002). Generally, the tumor microenvironment is characterized by chronic inflammation, which can favor tumor formation by stimulating cell proliferation and promoting invasion and metastases. As discussed in the previous paragraph, the immune cells of the tumor microenvironment are part of the factors that can contribute to the regulation of CSC plasticity. Among these, inflammatory cells, which occupy an important role in tumor development, have been reported to have a potential role in CSC initiation, regulation and function. Evidence reported that several factors produced by inflammatory cells may directly affect normal stem cells and their properties. For example, tumor necrosis factor alpha (TNF-α), one of the most important pro-inflammatory cytokine, participates in the induction of neuronal stem cell proliferation and inhibits their differentiation by the activation of the transcription factor NF-κB, a central regulator of inflammation (Widera et al. 2006). Regarding cancer, there are many studies focused on the role of inflammation components in the induction of CSC plasticity. Pro-inflammatory mediators, such as cytokines,

secreted in the tumor microenvironment by various immune cells, as macrophages, NK cells and $CD4^+$ T cells, are considered inducers of tumor cell plasticity in melanoma, breast and lung cancer, because they can affect the differentiation state of tumor cells by the up-regulation of EMT traits and stemness features (Ostyn et al. 2014; Sanguinetti et al. 2015; Liu et al. 2015c). Similarly, iperactivation of NF-κB signaling enhanced Wnt activation and induced dedifferentiation of non-stem cells in cancer stem-like cells endowed with high tumorigenic potential (Schwitalla et al. 2013).

An important inflammatory signal that occupies a central role in the induction and maintenance of CSC phenotype in several cancers is that mediated by IL-6. Iliopoulos and colleagues (2011) were the first to identify the role of this cytokine in CSC promotion. Particularly, using a cellular model of *in vitro* transformed breast cancer cells, primary breast and prostate cancer cells, they demonstrated that CSCs derived from these populations expressed higher levels of IL-6 respect to non-CSCs; furthermore, IL-6 was secreted in the medium and induced the conversion of non-CSCs in sphere-forming CSCs. More recently similar results were obtained in hepatocellular and ovarian carcinomas, demonstrating the crucial role of IL-6 in the promotion of CSC features, in particular enhancing tumorsphere formation efficiency and tumorigenicity of a subpopulation of tumor cells (Ding et al. 2016; Wang et al. 2016).

Other inflammatory cytokines that compose the CSC niche can affect features of these cells as self-renewal and tumorigenic potential. Recently, Xiang and coworkers (2015) demonstrated that IL-17, a pro-inflammatory cytokine produced by a subclass of T helper 17 (Th17) $CD4^+$ lymphocytes and $CD68^+$ macrophages, plays a crucial role in the promotion and maintenance of CSC phenotype derived from A2780 ovarian tumor cell line and ovarian primary tumors. They identified $CD133^+$ cancer stem-like cells and demonstrated that the exposition of these cells to IL-17 significantly enhanced their sphere formation ability and tumorigenic potential. In another recent work, elevated levels of pleiotropic IL-13, a key Th2 lymphocyte-derived cytokine usually associated to increased CRC risk in patients with inflammatory bowel disease, promotes stem-like phenotypes in colorectal cancer cell lines through STAT6/EMT-traits activation (Cao et al. 2016). Additional evidence indicates that some chemokines and their respective receptors, which are key chemotactic factors regulating the recruitment of several types of cells in the tumor microenvironment, mark CSC populations (Ye et al. 2014; Blaylock 2015; Zou and Wicha 2015). These observations suggest a continuous crosstalk between CSCs and inflammatory components, which regulates CSC homing, maintenance and dissemination at distant sites.

The local inflammatory response that characterizes the tumor microenvironment is also regulated by another group of soluble factors belonging to the interferon (IFN) cytokine family, which are essentially produced by stromal, immune and also cancer cells. Human IFNs are essentially classified into three groups: type I, II and III IFNs. Type I IFNs, which include the best known IFN-α and IFN-β molecules, are part of the innate immune system and occupy an essential role in response against viral and microbial infections. Canonically, type I IFN signaling activates the JAK/TYK-STAT1/2-IRF9 pathway, which leads to the transcriptional activation of IFN-stimulated genes (ISGs) and IFN inducible genes,

such as IFI6, IFI16 and IF27 (Decker et al. 2005; Zhao et al. 2009b; Ivashkiv and Donlin 2014). IFN-γ is the unique member of type II IFN group and plays a crucial role in immune responses associated to Th1 lymphocytes and mediates essentially JAK1/2-STAT1 pathway which leads to the expression of ISGs and INF-responsive genes (IRFs), such as IRF1, IRF5 and IRF7 (Schroder et al. 2004).

The role of IFN response in cancer has mostly been ascribed to antitumor function by a direct action against tumor cells or activating immune responses, so that these molecules have been approved by the Food and Drug Administration for clinical applications against many tumors and still have an important role in a lot of current anticancer therapies (Minn 2015; Parker et al. 2016). However, despite this asserted role, deregulation of IFN signaling was recently described in many tumors as one of the key networks involved in tumorigenicity. Recently, Forys and coworkers (2014) identified a protumorigenic signaling cascade mediated by IFN-β in human triple-negative breast cells. IFN-β signaling mediated the activation of the transcription factor STAT1, which regulates the transcription of ISG genes, among which *ISG15*; in these cells this IFN-responsive axis was found up-regulated and associated to enhanced tumorigenicity *in vivo*.

The IFN-responsive gene *ISG15* encondes an ubiquitin-like protein that can be conjugated to proteins in a process named ISGylation, remain free in cytosol or even secreted in the extracellular space. This gene has a well-known antiviral activity, but recently has been found up-regulated in several cancers and seems to play a role in the regulation of the CSC phenotype (Zuo et al. 2016). Sainz and colleagues (2014) demonstrated that pancreatic cancer cell secretion of IFN-β stimulated TAMs to produce and secrete ISG15, which in turn induced stemness features in pancreatic tumor cells and enhanced self-renewal and tumorigencity capacities of CSCs. Thus, this protein appears to play a key role in the promotion and maintenance of pancreatic CSC phenotype. More recently, ISG15 was found overexpressed in nasopharyngeal carcinomas compared to non tumoral tissues and its expression levels were shown to be inversely correlated to patients' survival. Moreover, exogenous expression of ISG15 in two nasopharyngeal cancer cell lines induced CSC features, as increased tumorsphere formation ability, overexpression of stemness genes and high tumorigenic potential *in vivo* (Chen et al. 2016).

Among the molecules that belong to the IFN pathway, several IFN alpha-inducible proteins were found deregulated in several cancers (Suomela et al. 2004; Wenzel et al. 2008; Gupta et al. 2016). Recently, Li and colleagues (2015a) showed that IFN alpha-inducible protein 27 (IFI27) was overespressed in ovarian carcinomas and its levels were positively related to the expression of mesenchymal markers, as vimentin. Ectopic IFI27 overexpression induced stemness features in ovarian cancer cells as the ability to form tumorspheres, self-renewal, high *in vivo* tumorigenicity and drug resistance. All these results suggest the importance of inflammation components for the regulation of CSC plasticity, indicating new potential targets for developing novel diagnosis and therapeutical strategies.

1.9 CSC and metabolism

Cancer cell metabolism reprogramming is one the emerging hallmarks of cancer (Pavlova and Thompson, 2016). Thus, cancer metabolic pathways have become new possible targets for more effective anticancer treatments. An intensive metabolic reprogramming has also been shown in CSCs and is related to the high versatility of these cells to adapt to several tumor microenvironment changes (Peiris-Pagès et al. 2016). In contrast to bulk tumor cells, which preferentially follow the glycolytic pathways both in presence or absence of oxygen, CSCs from several tumor types have been shown to rely alternatively on glycolytic or mitochondrial oxidative metabolism (Dando et al. 2015). For instance, Liu et al. demonstrated (2012) that the SP cells isolated *in vitro* from human lung and colon cancer cell lines exhibited altered expression of genes involved in glycolysis. These cells showed higher glycolytic activity compared to non-SP cells, and glucose deprivation or the inhibition of glycolysis by 3-bromo-2-oxopropionate-1-propyl ester (3-BrOP) treatment significantly decreased the SP population and impaired their ability to induce *in vivo* tumor formation. Moreover, CSCs derived from a glioblastoma mouse model were shown to display a decreased mitochondrial oxidative metabolism, a high glycolytic activity to produce ATP, and a preference for a low oxygen microenvironment. Treatment of tumor cells with both glycolytic inhibitors and standard chemotherapeutic agents effectively killed CSCs and decreased tumor formation in mice (Zhou et al. 2011).

However, other studies showed that CSCs can also follow a mitochondrial oxidative metabolism. Exploiting an inducible mouse model of pancreatic carcinoma, Viale and coworkers (2014), identified a subpopulation of resistant tumor cells responsible for tumor relapse, which relied on oxidative phosphorylation to grow and survive. Another study performed on CSCs isolated from patients with epithelial ovarian cancer showed that these cells overexpressed genes involved in glucose uptake, oxidative phosphorylation and fatty acid β-oxidation compared to non-CSCs. These CSCs were resistant to glucose starvation both *in vivo* and *in vitro,* maintaining stemness features and oxidative metabolism in this condition (Pastò et al. 2014). Recently, Farnie and coworkers (2015), studying breast cancer cell lines and metastatic breast cancer tumor samples, identified a subpopulation of cells with high mitochondrial mass that was specifically enriched in CSC markers, formed mammospheres with high frequency and showed high chemo-resistance to paclitaxel treatment.

Menendez and Alarcon (2014) hypothesized a metabolic model for CSCs that predicts that biochemical changes triggered in the tumor microenvironment by nutrient availability or acidic as well as hypoxic conditions could promote epigenetic changes in non-CSCs that in turn allow the expression of stemness genes, thus to promote or reinforce CSC population.

Amino acid and lipid metabolism are also involved in cancer cell stemness. Li and collaborators (2015b) demonstrated that pancreatic CSCs are dependent on glutamine availability to grow and when starved for this aminoacid they down-regulated the expression of pluripotent genes and lost the ability to form spheres, self-renew capacity and became more sensitive to drug treatments.

Alterations in lipid metabolism have recently been recognized to play a role in generating and maintaining the CSC phenotype. Ginestier and colleagues (2012) demonstrated the overexpression of genes enconding enzymes of the mevalonate pathway in tumorspheres from breast cancer cell lines. The mevalonate pathway leads to the synthesis of isoprenoids that are used in many biological processes, as cholesterol biosynthesis and steroid biosynthesis, protein farnesylation and geranylgeranylation (GG). The authors showed that the inhibition of this pathway led to a reduction in tumorsphere formation in the breast cancer cell lines, which was dependent on the impairment of the protein GG pathway, and not on a deficiency in cholesterol biosynthesis or protein farnesylation. Recently, Brandi et al. (2016) showed that the mevalonate pathway is also important for the survival of pancreatic cancer CSCs; in fact, its inhibition caused negative effects on their self-renewal properties. These results suggest that components of the mevalonate pathway could be potential targets for tumor therapy, being important for CSC biology.

2. Aims of the research

The cancer stem cell model of tumor progression postulates that a specific subpopulation of tumor cells endowed with stemness features, the cancer stem cells (CSCs), is the main responsible for cancer initiation and development. This cancer cell subpopulation would be able to sustain the hierarchical organization of tumor tissue, generating both new CSCs and the more differentiated bulk tumor cells (Kreso and Dick, 2014). CSC origin is elusive, many studies have demonstrated that CSCs can originate from transformation of adult stem cells. However, recent evidence has indicated that CSCs can also originate from bulk tumor cells through a dedifferentiation process, leading to the acquisition of stem-like properties. In addition, some works reported that CSCs can be generated *in vitro* during oncogenic transformation of differentiated cells, pointing to a high degree of plasticity of tumor cells (Chaffer et al. 2011; Scaffidi and Misteli, 2011). However, little is known about the molecular mechanisms involved in the dedifferentiation programs that can promote a CSC phenotype in transformed cell. To this regard, CSCs generated *in vitro* can be an easy to handle tool to add pieces of information on this process.

The aim of this thesis was to investigate the possible presence of cells with the CSC phenotype in *in vitro* transformed cells and study their molecular features. To this purpose, we exploited the cen3tel model system, a cellular system developed in our laboratory from telomerase immortalized fibroblasts, which recapitulates the neoplastic transformation of human fibroblasts (Ostano et al. 2012). In particular we used cells (cen3tel 600 and cen3tel 1000) able to induce tumor in immunocompromised mice with decreasing latency, and thus with increasing aggressiveness. To assess for the presence of CSCs within the transformed cell populations, we used the sphere formation assay. This method has been widely used to enrich tumor cell populations in CSCs, independently of the expression of specific markers. In fact, a large body of evidence indicates that cells able to respond to growth factors and grow in suspension as spherical aggregates in the absence of serum are endowed with stemness features (Reynolds and Weiss, 1992; Ignatova et al. 2002; Hirschhaeuser et al. 2010). Indeed, cells able to grow as spheres were detected in both populations. We thus characterized sphere cells compared to their adherently growing counterparts for the presence of stemness features and then we performed genome-wide studies by microarray analysis in order to compare gene expression profiles of sphere cells and adherent cells and eventually define specific molecular signatures possibly involved in the induction of stemness and tumorigenic properties of sphere cell populations.

3. Materials and methods

3.1 Cell lines and cell cultures

3.1.1 The cen3tel cellular system: cen3tel 600 and cen3tel 1000 cells

The cells used in this study belong to the cen3tel cellular system, which was developed in our laboratory. This cellular system was obtained from primary fibroblasts, isolated from the skin of a centenarian individual, by infection with an hTERT-containing retrovirus (Mondello et al. 2003). hTERT-expressing cen3tel cells escaped from cellular senescence and acquired the ability to proliferate indefinitely, becoming immortal. During propagation in culture, hTERT-immortalized cen3tel cells gradually and spontaneously underwent neoplastic transformation (Zongaro et al. 2005; Belgiovine et al. 2010; Ostano et al. 2012; Chiodi et al. 2013). Characterizing cen3tel cells at the cellular and molecular level during propagation in culture, we could identify different phases along the road to transformation. At the initial stages after hTERT introduction, cen3tel cells maintained an elongated morphology and a behaviour similar to that of parental primary fibroblasts. After about 100 population doublings (PD), cen3tel cells started showing features of transformed cells, as the ability to grow in the absence of a solid surface and the down-regulation of *CDKN2A* expression, but they were not able to induce tumors when injected into immunocompromised mice (Mondello et al. 2003). Cells around PD 160 switched to a rounded morphology, increased their growth rate and acquired important cancer-associated changes, as the overexpression of c-*MYC* and the loss of p53 function, because of a mutation in the codon 161 of the DNA binding region. Moreover, at this stage, cen3tel cells became tumorigenic, forming tumors within 1 month after injection under the skin of immunocompromised mice. Once become tumorigenic, during further propagation *in vitro*, cells became progressively more aggressive, as shown by a decrease in the time required to form tumors in immunocompromised mice (Zongaro et al. 2005; Belgiovine et al. 2010). In particular, cen3tel cells around PD 600 and 1000 (cen3tel 600 and 1000 cells) induced sarcomas into immunocompromised mice 8 days and 2 days after inoculation, respectively. Moreover, cen3tel 1000 cells were also able to give metastases when injected into the tail vein of nude mice (Belgiovine et al. 2010). A comparison of gene expression profiles of cen3tel cells at different stages of transformation revealed that these cells showed the progressive modulation of the expression of several cancer-related genes, leading to a more and more aggressive neoplastic phenotype (Ostano et al. 2012). In this study we used cen3tel cells around PD 600 and PD 1000.

3.1.2 Cell Cultures

Cen3tel 600 and 1000 cells were propagated in adherent culture conditions using 10 cm diameter Petri dishes (Corning) in high glucose Dulbecco's Modified

Eagle's Medium (DMEM, Euroclone) supplemented with 10% Fetal Bovine Serum (FBS, Lonza), 2 mM L-Glutamine, and 1X Non-Essential Amino Acids (Euroclone), 100 U/ml penicillin, and 0.1 mg/ml streptomycin (Euroclone) (We will refer to this medium as complete DMEM) at 37°C in a 5% CO_2 humidified incubator. When cells reached confluence, they were accurately washed with PBS (Phosphate Buffered Saline, Oxoid) and detached from the dish and separated from one another by incubation at 37°C for 1-2 min. with about 600 µl of 0.25% trypsin-0.22 mg/ml EDTA in PBS (Euroclone). Then, cells were split and re-seeded in the same conditions up to confluence. Cell cultures were usually split either 1:2 or 1:4, and at each division one or two PDs, respectively, were added to the counting of the population doublings. For RNA and protein extraction, cellular pellets were prepared from actively growing cells and stored at -80°C.

3.2 Sphere formation assay

To perform sphere formation assays, cen3tel 600 and 1000 cells were plated in Petri dishes at a concentration of about 10^4 cells per ml of sphere-forming medium consisting in a 1:1 mixture of high glucose DMEM and Ham's Nutrient Mixture F-12 (Euroclone) supplemented with 20 ng/ml recombinant human Epidermal Growth Factor (EGF, Life Technologies), 20 ng/ml recombinant human Fibroblast Growth Factor-basic (FGFb, Life Technologies), 1X Insulin-Transferrin-Selenium (ITS 100X: Insulin 1 g/L, Transferrin 0.55 g/L, Sodium Selenite anhydrous 0.00067 g/L, Life Technologies), 4 mg/ml Bovine Serum Albumin (BSA, Sigma), 2 mM glutamine (Euroclone), 50 U/ml penicillin, and 0.05 mg/ml streptomycin (Euroclone). Spheres formed by adherent growing cen3tel cells, called primary spheres (I spheres), were counted and collected 6 or 7 days after seeding. Spheres were collected by gentle centrifugation (500 x g for 1 min. at room temperature) and, after removal of the supernatant, were enzymatically dissociated with trypsin-EDTA to obtain single cells. Sphere cells were then either replated in sphere forming medium to obtain secondary spheres (II spheres; the same procedure was used to obtain tertiary (III spheres) from secondary spheres), or used to prepare cellular pellets that were stored at -80°C for subsequent RNA and protein extraction. Sphere forming efficiency was calculated by dividing the number of spheres obtained for the number of cells plated.

To analyze gene expression during I and II sphere propagation, cells were collected 2, 6 or 7 days after seeding in sphere forming medium. 6-day spheres were smaller than spheres at 7 days of growth, but had a well-defined spherical morphology as 7-day spheres; moreover, single cells were almost totally absent at these stages of culture in sphere-forming medium. At day 2 of growth in sphere forming conditions, small clusters of about 4-6 cells were observed together with a lot of single cells. For the analysis, 6- and 7-day spheres were collected and disaggregated as described above. 2-day sphere cells were centrifugated at 500 x g for 1 min. and resuspended in serum-free DMEM without trypsinization. Cell samples were pelleted and stored at 80°C.

To characterize sphere cells differentiated in adherent culture conditions, 7-day cen3tel 600 and 1000 spheres were disaggregated and the derived cells were

seeded and propagated in serum containing medium (complete DMEM) up to 7 days. Differentiated adherently sphere-derived cells were collected at different time intervals after plating and cellular pellets were prepared and stored at -80°C.

3.3 Induction of adipoblasts and osteoblasts differentiation

To analyze adipoblast and osteoblast differentiation capacity of cen3tel 600 and 1000 adherent and sphere cells, the STEMPRO adipogenic or osteogenic differentiation kits were used according to the manufacturer instructions (Gibco). Briefly, cells were seeded into 12-well plates (Corning), at a density of $10^4/cm^2$ for adipogenesis and $3x10^3/cm^2$ for osteogenesis in 800 µL/well of differentiation medium. The media were replaced every 3-4 days. All experiments were performed twice. Adherent and sphere-derived cells were grown in parallel in complete DMEM and used as control cells.

3.3.1 Oil red O staining

To identify adipocytes, Oil Red O, which stains lipid droplets, was used. Adherent and sphere-derived cells were stained after 19 days of adipogenic induction. Control cells were stained after 15 days of growth in normal conditions. Cells were washed with PBS and fixed with 2 successive passages (10 min. and 3 hours, respectively) in 10% PBS-diluted formalin at room temperature. Formalin was then discharged and cells were washed with 60% isopropanol and incubated for 10 min. at room temperature in Oil Red O (Sigma-Aldrich), prepared as a 100% w/v solution in isopropanol and diluted in water to final concentration of 60%. Cells were then rinsed 4 times with distilled water and left at 4°C till samples were observed in phase-contrast with the Eclipse TS100 Nikon inverted microscope for a qualitative analysis of lipid accumulation. For a quantitative analysis, the Oil Red O was then eluted from each sample incubating the cells with 1 ml of 100% isopropanol for 10 min. and its amount quantified by measuring the absorbance of the solution at 500 nm. For each sample, the absorbance value was then normalized for the amount of DNA extracted, to correct for possible differences in cell number. To extract DNA after Oil Red O elution, cells were air-dried and then incubated overnight at 55°C with 1 ml/well of lysis buffer (200 mM NaCl; 100 mM Tris HCl pH 8.5; 5 mM EDTA; 0.2% SDS; 0.5 mg/ml Proteinase K). The lysis buffer was then recovered, DNA precipitated according to standard procedures, resuspended in water at 55°C for 1 hour and finally quantified reading the absorbance at 260 nm using Implen P330 nanophotometer.

3.3.2 Von Kossa staining

Calcium deposits were analyzed in adherent and sphere-derived cells grown in osteogenic differentiation medium for up to 28 days using Von Kossa Staining. Cells were fixed in 10% PBS-dissolved formalin for 30 min. at room temperature, rinsed with distilled water for 3 successive passages and then incubated in 5% silver nitrate (Sigma-Aldrich) under the light of a 60 W bulb. After 3 washes with

distilled water, cells were treated with 5% sodium thiosulfate (Sigma-Aldrich) for 5 min. at room temperature to remove unreacted silver nitrate, washed 3 times with distilled water and air-dried in a fume cupboard. The calcified extracellular matrix appeared as brown/black crystals at the Eclipse TS100 Nikon inverted microscope using phase-contrast.

3.4 Cell treatments

3.4.1 Etoposide treatment

To induce apoptosis, $2x10^6$ cen3tel 600 and 1000 cells were seeded in 10 cm diameter Petri dishes (Corning) in complete DMEM. After 24 hours, cells were incubated in complete DMEM supplemented with 100 μM etoposide (Sigma-Aldrich) for 24 hours. Afterwards, cells were collected, pelleted and stored at -80°C.

3.4.2 Treatment with the proteasomal inhibitor MG-132

In order to test protein expression after inhibition of proteasomal activity, cen3tel adherent cells and 6-day sphere cells were exposed to 25 μM MG-132 (Sigma-Aldrich) for 2 or 4 hours At the end of the treatment, cellular pellets were then prepared and stored at -80°C.

3.4.3 Simvastatin, cholesterol and mevalonate treatment

To investigate the possible role of cholesterol/mevalonate biosynthetic pathway on sphere formation, $3.5x10^5$ cen3tel 600 or cen3tel 1000 cells were seeded in 6 cm diameter Petri dishes (Corning) in complete DMEM. After 24 hours, cells were incubated either in complete DMEM supplemented with 0.8 (cen3tel 1000) or 1.2 (cen3tel 600) μM simvastatin (Sigma-Aldrich), or with simvastatin and 10 μM cholesterol (Sigma-Aldrich), or with simvastatin and 1 mM mevalonate (DL-mevalonolactone, Santa Cruz Biotechnology) for 72 hours. Then, cells were detached, counted using Trypan blue staining that allows distinguishing viable and dead cells and $4x10^3$ viable cells/well were seeded in sphere forming medium in 24 well-plates (Costar). Spheres were counted 6-7 days after plating.

3.4.4 IL-1β, IL-6 and ISG15 treatment

To analyze the effect of IL-1β (Peprotech) on adherent cell viability, $4x10^5$ cells were plated in 3 cm diameter Petri dishes (Corning) in complete DMEM. After 24 hours, the medium was replaced with complete DMEM supplemented with increasing concentrations of IL-1β (from 0.02 to 20 ng/mL) and cells grown for 72 hours. Cell viability was then assessed counting the cells after Trypan Blue staining.

To analyze the effect of IL-1β and IL-6 (Prepotech) and ISG15 (Abcam) on sphere formation, $4x10^3$ cen3tel 600 or cen3tel 1000 cells/well were seeded in 24

well-plates (Costar) in sphere-forming medium supplemented with 10 ng/mL recombinant human IL-1β or 10, 20 or 50 ng/mL recombinant human IL6 or 100 ng/mL of ISG15. Spheres were counted 6-7 days after plating.

3.5 *In vivo* tumorigenicity experiment

To test cell tumorigenic ability, cen3tel 600 cells were bilateraly injected into the leg muscle of NOD Scid Gamma (NSG) mice (The Jackson Laboratory) (from 4 to 6 mice for each cell sample). Mice were monitored for about 35 days assessing tumor appearance and measuring the tumor volume 1-2 times a week. Animal experiments were performed in collaboration with Dr. Belgiovine at the Istituto Clinico Humanitas di Rozzano, Milan. Mice and tumors were used in compliance with national (4D.L.N.116, G.U., suppl. 40,18-2-1992) and international law and policies (EEC Council Directive 86/609,OJ L 358, 1, 12-12-1987; NIH Guide for the Care and Use of Laboratory Animals, US National Research Council, 1996). This investigation was approved by the Animal Care and Use Committee of the Humanitas Clinical and Research Center.

3.6 Flow cytometric analysis

The percentage of cells expressing Sox2 was assessed using flow cytometric analysis. To this purpose, 10^6 cells, obtained by trypsinization of 6- or 7-day spheres or adherent cells, were collected in 1.5 ml tubes and centrifuged at 300 x g for 7 min. at 4°C. In this procedure, all the incubation steps were performed for 20 min. at 4°C, while centrifugations were carried out at 200 x g for 5 min. at 4°C. Firstly, cells were incubated with 50 µl of Fixation/Permeabilization solution (BD Biosciences). After the addition of 200 µl of 10 X BD Perm/Wash™ Buffer (BD Biosciences), cells were centrifuged, the supernatant was discarded and cells were resuspended in 50 µl of blocking solution constituted of 1% BSA prepared in 10X BD Perm/Wash™ Buffer. At the end of the incubation, 200 µl of 10X Perm/Wash™ Buffer were added, cells were centrifuged and then incubated in 50 µl of rabbit anti Sox2 primary antibody (S9072, Sigma-Aldrich) diluted 1:200 in 10X Perm/Wash™ Buffer. After that, 200 µl of 10X Perm/WashTM Buffer were added, cells were centrifuged to remove unreacted antibody and incubated in the dark with 50 µl of donkey anti-rabbit Alexa Fluor® 647-conjugated secondary antibody (Thermo Fisher Scientific) prepared at a 1:500 dilution in 10X Perm/Wash™ Buffer. Finally, for preserving immunofluorescence staining, cell samples were fixed in 50 µl of 1% PFA/PBS and stored at 4°C in the dark until cytofluorimetric analysis. As negative control, cell samples were also prepared according to the same procedure, but omitting the incubation with the primary antibody. Flow cytometric analysis was performed using BD FACSCanto™ (BD Biosciences) and results were acquired by BD FACSDiva™ Software (BD Biosciences).

3.7 RNA isolation

Total RNA isolation from cellular pellets was performed using the phenol/guanidine-based lysis reaction and standard isopropanol precipitation. Cells were homogenized at room temperature in QIAzol lysis reagent (Qiagen) at a concentration of about 3-5x10^6 cells/ml of reagent. After the addition of 200 µl of chloroform per ml of lysis reagent, the homogenate was centrifuged at 12000 x g for 15 min. at 4°C and the upper RNA-containing aqueous phase was recovered. RNA was then precipitated from the aqueous phase adding 500 µl of isopropanol per ml of lysis reagent. After centrifugation at 12000 x g for 10 min. at 4°C, the RNA pellet was washed with 1ml of 75% ethanol, centrifuged at 8000 x g for 5 min. at 4°C, air-dried, resuspended in 60-40 µl of RNase-free water and incubated for 10 min. at 65°C. RNA samples were purified from possible contaminant genomic DNA using the TURBO DNAfree™ kit (Ambion) as described by manufacturer's instructions. Briefly, 1 µl of TURBO DNase (2 U/µl) was added to 15 µg of RNA, together with 5 µl of 10X TURBO DNase buffer and RNase-free water to reach a final volume of 50 µl volume. Each reaction was incubated for 30 min. at 37°C. After that, in order to block enzymatic activity, each reaction was incubated with 5.5 µl of DNase inactivation reagent for 2 min. at room temperature, with frequent mixing. Finally, samples were centrifuged for 2 min. at 10000 x g and the RNA-containing supernatant was recovered and stored at -80°C. RNA concentration and purity were determined reading the sample absorbance at 230, 260 and 280 nm with the Implen P330 nanophotometer.

3.8 Reverse Transcription-Quantitative PCR

Reverse Transcription-quantitative PCR (RT-qPCR) was performed to analyze the expression levels of *POU5F1* (Oct-4), *NANOG*, *SOX2*, c-*MYC*, *GNL3* (nucleostemin), *NOTCH1* and the microRNA miR-34a on total RNA from cen3tel 600 and 1000 spheres and adherent cells. The same analysis was used to validate a subset of differentially expressed transcripts identified by microarray analysis. The list of the genes analyzed by RT-qPCR is reported in Table 1, together with the primer used for the PCR. For the analysis, 1 µg of each RNA sample was firstly converted into cDNA using QuantiTect and miScript Reverse Transcription kits (Qiagen), for mRNAs and miRNA, respectively, following the manufacturer's instructions. qPCR reactions were performed using the SYBR green chemistry (QuantiTect and miScript SYBR Green PCR kits, Qiagen, for mRNAs and miRNAs respectively). For each gene under investigation, the specific QuantiTect Primer Assay (Qiagen) (Table 1A) or custom primers (Table 1B) were used, while for miR-34a the miScript Primer Assay (Hs_miR-34a_1, Qiagen), detecting the mature sequence hsa-miR-34a-5p, was used. The housekeeping gene *GUSB* was used as reference to correct for possible differences in the amount of cDNA among different samples. For the normalization of miR-34a expression the expression of the small non-coding RNA U6 was determined, using the miScript Primer Assay Hs_RNU6B_12 (Qiagen).

Table 1. List of the qPCR primers. The length of the expected amplicons is also reported. (**A**) QuantiTect Primer Assays, (**B**) Custom primers

A

Gene Symbol	Gene Name	Primer Name	Accession Number	Amplicon length (bp)
GNL3	guanine nucleotide binding protein-like 3 (nucleolar)	Hs_GNL3_1_SG	NM_014366 NM_206825 NM_206826	141
GUSB	glucoronidase, beta	Hs_GUSB_1_SG	NM_000181 NM_001284290 NM_001293104 NM_001293105 XM_005250297	96
HMGCR	3-hydroxy-3-methylglutaryl-CoA reductase	Hs_HMGCR_1_SG	NM_000859 NM_001130996	87
HMGCS1	3-hydroxy-3-methylglutaryl-CoA synthase 1 (soluble)	Hs_HMGCS1_1_SG	NM_001098272 NM_002130	123
IFI6	interferon, alpha-inducible protein 6	Hs_IFI6_1_SG	NM_002038 NM_022872 NM_022873	108
IL13RA2	interleukin 13 receptor, alpha 2	Hs_IL13RA2_1_SG	NM_000640	82
MMP1	matrix metallopeptidase 1 (interstitial collagenase)	Hs_MMP1_1_SG	NM_001145938 NM_002421	103
MVK	mevalonate kinase	Hs_MVK_1_SG	NM_000431 NM_001114185 NM_001301182	124
c-MYC	v-myc avian myelocytomatosis viral oncogene homolog	Hs_MYC_1_SG	NM_002467	129
NANOG	Nanog homeobox	Hs_NANOG_2_SG	NM_024865 NM_001297698	164
NOTCH1	notch 1	Hs_NOTCH1_2_SG	NM_017617	92
POU5F1	POU class 5 homeobox 1	Hs_POU5F1_1_SG	NM_001173531 NM_002701 NM_203289 NM_001285986 NM_001285987	77
SOX2	SRY (sex determining region Y)-box 2	Hs_SOX2_1_SG	NM_003106	64

B

Gene Symbol	Gene Name	Primer sequence (5' - 3')	Accession Number	Amplicon length (bp)
*ID1**	Inhibitor of DNA binding 1	Fw:CGCTCCTCTCTGCACACC Rev:GATTCCACTCGTGTGTTTCTATTTT	NM_002165.3	72
*ID3**	Inhibitor of DNA binding 3	Fw:CGTGTCCTGACACCTCCAG Rev:CCACTTGACTTCACCAAATCC	NM_002167.4	132
MMP7[§]	Matrix metallopeptidase 7	Fw:ATGGGGAACTGCTGACATCAT Rev:CCAGCGTTCATCCTCATCGAA	NM_002423.4	153
MMP14[§]	Matrix metallopeptidase 14	Fw:CTAAGACCTTGGGAGGAAAAC Rev:AAGCCCCATCCAAGGCTAACA	NM_004995.3	192

[*] synthetized by BMR Genomics
[§] synthetized by Sigma-Aldrich

Each reaction was prepared and run in triplicate and all the experiments were repeated at least twice. qPCRs were done in the Light Cycler 480 apparatus (Roche), using 96-well reaction plates, following the protocols reported in Table 2.

Table 2. Amplification protocols for qPCR analysis.

mRNAs	
Number of cycles	**Settings**
1	95°C for 15 min.
45	95°C for 20 sec. 55°C for 20 sec. 72°C for 20 sec.

miRNAs	
Number of cycles	**Settings**
1	95°C for 15 min.
50	94°C for 15 sec. 55°C for 30 sec. 72°C for 30 sec.

For each qPCR run, the LightCycler 480 software (Roche) provides the C_t (threshold cycle) value obtained from the amplification curve. For each sample, the average value of the C_t of the three replicates, with the corresponding standard deviation (SD), are calculated. The quantification of the relative change of the expression of the gene of interest between sphere and adherent cells is performed using the $\Delta\Delta C_t$ method. This method consists in calculating the difference of the threshold cycle (ΔC_t) between the target gene and reference one. Then, the $\Delta\Delta C_t$ is determined as the difference of (ΔC_t)s of sphere cells and adherent cells. The relative gene expression of each sample is expressed as fold change (FC), calculated as $2^{-\Delta\Delta Ct}$, or as $\log_2$ FC.

3.9 mRNA profiles at genome-wide scale

3.9.1 Microarray probe preparation, hybridization, and scanning

Gene expression profiling of sphere cells *versus* adherent cells was done at the Cancer Genomics Laboratory of the Fondazione Edo ed Elvo Tempia Valenta in Biella directed by Dr Chiorino using Agilent Whole Human Genome Microarray 4x44k glass slides (containing 41000 probes corresponding to 19596 Entrez Gene RNAs) (Agilent Technologies). Microarray probe preparation, hybridization, and scanning for gene expression analysis were performed as described in previously published works (Deaglio, 2007; Belgiovine et al. 2010; Ostano et al. 2012). In brief, mRNA obtained from each sample was amplified to obtain amino allyl antisense RNA (aaRNA) (Amino Allyl MessageAmp I aRNA Kit, Ambion). The modified RNA was then labeled using NHS (N-hydroxysuccinimide) ester Cy3 or Cy5 dyes (Amersham Biosciences). Equal amounts of labeled RNA from each sample and reference were put together, fragmented and hybridized to oligonucleotide glass arrays. For each sample, two biological replicates were analyzed. Comparative hybridization of cen3tel sphere cell RNA *versus* the RNA from their corresponding adherent cells and a flourescent-reversal combination analysis were performed. After hybridization, slides were washed following the Agilent procedure and scanned using an Agilent C dual-laser microarray scanner (G2505C, Agilent Technologies).

3.9.2 Microarray data analysis and gene selection

Images were analyzed using the Feature Extraction software version 10.7 (Agilent Technologies). Raw data elaboration was carried out with Bioconductor (www.bioconductor.org) (Gentleman et al. 2004), using R statistical language. Background correction was performed with the *normexp* method with an offset of 50, *loess* was used for the within-array normalization and *A-quantile* for the between-array normalization. Separate channel analysis was then performed in order to analyse two-color data in terms of the individual channel intensities. The LIMMA (LInear Models for Microarray Analysis) package was used to identify differentially expressed genes in sphere cells *versus* adherent cells. The empirical Bayes method was used to compute a moderated *t*-statistics (Smyth, 2004). *p*-values were adjusted for multiple testing by using a false discovery rate (FDR) correction (Benjamini and Hochberg, 1995).

Relative changes in sphere cells *versus* adherent cells were expressed as base 2 logarithm of the ratio ($\log_2$ FC) and only those transcripts with $\log_2$ FC values greater than 0.58 or lower than -0.58 and an adjusted *p*-value lower than 0.05 were considered as differentially expressed in sphere cells compared to adherent cells, and thus selected for further analyses.

3.9.3 Cluster analysis

The R environment for statistical computing was used for unsupervised hierarchical clustering, performed on the global expression profiles of adherent and sphere cells. Euclidean distance as similarity metrics and ward linkage as linkage method were used. MeV version 4.6.1 (Saeed et al. 2006) was used for heatmao generation of subsets of genes according to their ontological classification.

3.9.4 Gene Ontology and network enrichment analysis

For the Gene Ontology (GO) analysis, a functional enrichment of the differentially modulated genes both in cen3tel 600 and 1000 sphere cells was performed using the tool available within DAVID website (http://david.abcc.ncifcrf.gov/). By this analysis, the biological processes with a *p*-value lower than 0.05 were considered as significantly enriched. Moreover, the PANTHER (Protein ANalysis THrough Evolutionary Relationships) Classification System (http://www.pantherdb.org/index.jsp) was used for pathway enrichment analysis ($p < 0.05$), that was applied to the lists of deregulated genes in both sphere cell samples in order to further identify pathways and assemble genes with common molecular functions.

3.9.5 Gene set enrichment analysis (GSEA)

GSEA was used on the lists of differentially expressed genes in sphere vs adherents cells in order to evaluate significant enrichment in predefined curated

sets of genes from online pathway databases and publications in PubMed (Subramanian et al. 2005).

3.10 Western blot analysis

Whole protein extraction was performed from cellular pellets using the RIPA lysis buffer (50 mM Tris HCl pH 8, 140 mM NaCl, 1% NP-40, 0.1% deoxycholate, 0.1% sodium dodecyl sulfate) supplemented with 1X phosphatase inhibitor cocktail (Roche) and 1X protease inhibitor cocktail (Thermo Scientific) (70 µl of buffer per 10^6 cells). Protein extracts were quantified using the Bradford Reagent (Sigma-Aldrich). For each sample, about 40 µg of proteins were loaded onto Sodium Dodecyl-Sulfate Polyacrylamide Gels and separated by electrophoresis (SDS-PAGE). Proteins were then transferred onto nitrocellulose blotting membranes (GE Healthcare Life Science), which, after 1 hour of saturation in 6% skimmed-milk/1X TBS blocking solution, were incubated with the primary antibody overnight at 4°C. The antibodies used are listed in Table 3. All the antibodies were diluted in 3% skimmed milk/1X TBS except the anti-phospho-Stat1(Tyr701) antibody, which was prepared in 5% BSA/1X TBS 0.1% Tween 20. After the incubation with the primary antibody, membranes were washed and incubated with the appropriate HRP-conjugated secondary antibodies (Jackson Immunoresearch, 1:5000 or 1:10000 in 3% skimmed milk/1X TBS) for 1 hour at room temperature. Immunoreactive signals were obtained using the Clarity Western ECL Substrate (Bio-Rad) chemiluminescent solution and then acquired with the Chemidoc XRS apparatus (Bio-Rad), which is equipped with a CCD (Charge-Coupled Device) camera. Signals were converted into a digital image by the QuantityOne software (Bio-Rad). The same software was used for band intensity quantification. γ-Tubulin was used as a loading control to correct for possible differences in the amount of proteins loaded for the different samples. Relative protein levels in sphere samples were then determined by normalizing the intensity values of their bands for those of the bands in the corresponding adherent cells. At least three independent experiments were carried out for each analysis and in several experiments more than one independent sample was analyzed both for adherent and sphere cells.

To assess for the presence of ISG15 (MW 17 KDa) in the culture medium (CM),about 4 mL of medium were collected from a 7 day sphere culture (about 1500 spheres/ml) and processed. To concentrate the medium and to eliminate BSA, which has a MW around 70 KDa, the medium was firstly loaded onto an Amicon Ultra-4 50K centrifugal filter unit. After two successive centrifugation at 3000 x g at 4°C, the CM passed through the filter, which contained proteins of MW < 50 KDa, was collected and loaded on an Amicon Ultra-4 10K centrifugal filter. After repeated centrifugations at 3000 x g at 4°C, the culture medium retained in the reservoir, which was enriched in the fraction of proteins ranging between 10 and 50 KDa, was collected. The final volume of the CM recovered was 50-70 µl, thus the medium was concentrated about 70 fold. 20 µl of concentrated culture medium were analyzed by western blotting using an antibody against ISG15 (Table 3).

Table 3. List of antibodies used in western blot analysis, with details about their manufacturer and antibody dilution.

TARGET	CATALOG NUMBER	HOST	SUPPLIER	DILUTION
γ-Tubulin	T6557	Mouse	Sigma-Aldrich	1:5000
BCL2A1	ab33862	Rabbit	Abcam	1:500
Cleaved caspase-3	ALX-210-807-C100	Rabbit	Enzo Life Sciences	1:500
Cleaved caspase-9	#9505	Rabbit	Cell Signaling	1:500
c-Myc	ab32072	Rabbit	Abcam	1:10000
ISG15	A-4	Mouse	Santa Cruz Biotechnology	1:500
IL-1β	MAB601	Mouse	R&D Systems	1:500
Notch1	ab52627	Rabbit	Abcam	1:1000
Nucleostemin (GNL3)	A300-600A	Rabbit	Bethyl	1:2000
PARP-1	ab191217	Rabbit	Abcam	1:1000
Poly(ADP-ribose) PAR	ALX-804-220	Mouse	Enzo Life Sciences	1:1000
RhoE	R6153	Mouse	Sigma-Aldrich	1:500
Stat1 p84/p91	C-136	Mouse	Santa Cruz Biotechnology	1:500
Phospho-Stat1 (Tyr701)	D4A7	Rabbit	Cell Signaling	1:1000

3.11 Statistical analysis

Results are presented as the mean ± standard deviation (SD) and analyzed using Student's *t*-test. *P*-values lower than 0.05, 0.01 or 0.005 were considered significant.

4. Results

4.1 Cen3tel 600 and 1000 cells contain a subpopulation able to form spheres in non adherent culture conditions

In preliminary results obtained in the laboratory, it was shown that cen3tel 600 and 1000 cells contain a subpopulation able to form spheres when plated in the absence of serum and in the presence of growth factors as EGF and bFGF (Fig. 4).

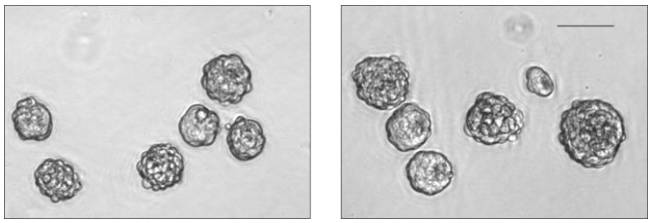

Figure 4. Cen3tel 600 (left panel) and cen3tel 1000 (right panel) tumorspheres. Cells were grown for 7 days in serum-free medium supplemented with growth factors. Images were taken with a phase contrast with a 4X objective. Bar: 100 μm.

Moreover, successive replatings of sphere cells in sphere forming conditions led to the formation of spheres with increasing frequency, suggesting that spheres were enriched in sphere forming cells (Fig. 5).

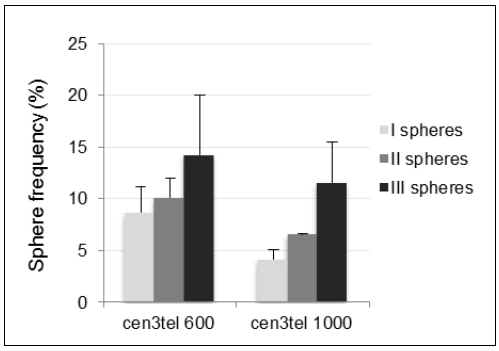

Figure 5. Spheres are enriched in sphere forming cells. Frequencies of primary (I), secondary (II) and tertiary (III) cen3tel 600 and 1000 spheres. Frequencies were measured after 7 days. Mean and standard deviation (error bars) values were calculated from three independent experiments.

We replated cen3tel 600 and cen3tel 1000 sphere cells for up to six times and we obtained spheres with increasing frequencies (data not shown). In addition, we did obtain spheres plating single cells. In fact, when we plated single cen3tel 600 or 1000 adherently growing cells in sphere forming conditions, we obtained spheres with a frequency of 15.6% and 2.9%, respectively; while plating single sphere-derived cells, frequencies increased up to about 60-70% in both cell lines, confirming that spheres are enriched in sphere forming cells. The frequency of sphere formation was higher in cen3tel 600 cells than in cen3tel 1000 cells, while

the dimension of the spheres was greater in the latter. The average number of cells/sphere was about 100 and 125 in cen3tel 600 spheres and cen3tel 1000 spheres, respectively. Cen3tel 1000 spheres show a larger size than 600 spheres probably because cen3tel 1000 cells proliferate slightly more than cen3tel 600 counterpart (Donà et al. 2013).

4.2 Cen3tel sphere cells are enriched in Sox2-positive cells

SOX2, *POU5F1* (encoding for Oct-4) and *NANOG* are master regulators of stemness properties and are frequently found overexpressed in CSCs (Hadjimichael et al. 2015). Thus, we analyzed whether the expression of these genes was modulated in sphere cells. By RT-qPCR, we did not find significant differences between sphere and adherent cells in *POU5F1* and *NANOG* expression (data not shown), while we found that the mRNA levels of *SOX2* were significantly higher in cen3tel 600 and 1000 sphere cells (FC 4.7 and 3.5, respectively) compared to their adherently growing counterparts (Fig. 6A).

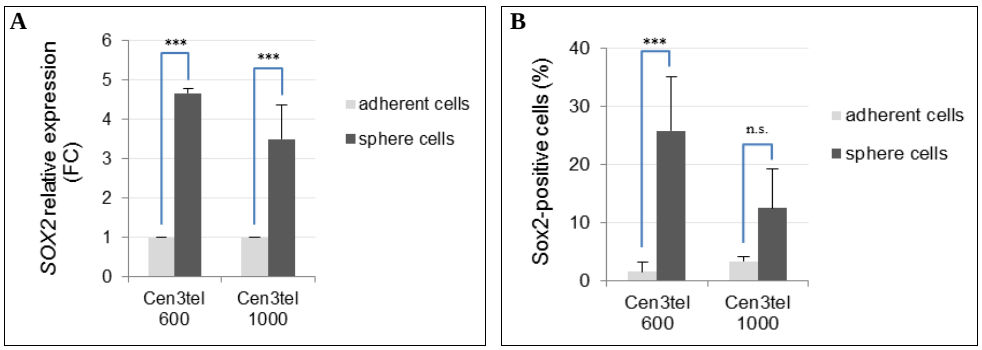

Figure 6. *SOX2* expression in cen3tel 600 and 1000 sphere cells. (**A**) RT-qPCR analysis of *SOX2* expression in cen3tel 600 and 1000 sphere cells. *SOX2* expression in each sphere sample is expressed as fold change (FC) relative to the expression in the corresponding adherent cells. The plot shows the average (FC) of three independent experiments. (**B**) Cytofluorimetric analysis of Sox2 expression showing the percentage of Sox2 positive cells in cen3tel 600 and 1000 sphere cells and adherent cells. Values are the average of the results of three independent experiments. Error bars: standard deviations. ***: $p < 0.005$; n.s. = not significant.

We then analysed *SOX2* expression at the protein level by cytofluorimetric analysis. Using this technique, we observed that cells grown in adhesion contained a small percentage of cells positive to Sox2, about 1.5% and 3% in cen3tel 600 cells and cen3tel 1000 cells, respectively. The percentage of Sox2 positive cells was increased in sphere cells and was higher in cells derived from cen3tel 600 spheres than in those derived from cen3tel 1000 spheres (about 26% *vs* 12%) (Fig. 6B). In spheres derived from both cen3tel cell types, the percentage of cells positive to Sox2 was quite variable among experiments, probably because Sox2 positive and negative cells could be generated with different frequencies during sphere growth. This variability can explain the lack of statistical significance between Sox2 expression in cen3tel 1000 spheres and adherent cells.

Taken together the results presented so far indicate that among cen3tel 600 and 1000 populations a subset of cells expressing CSC features is present, being able to respond to growth factors and grow in suspension forming spherical clusters of cells. Moreover, cen3tel sphere cells are endowed with self-renewal capability and spheres appear to be enriched in Sox2 expressing cells.

4.3 Cen3tel 600 and 1000 sphere cells show the same ability as adherently growing cells to differentiate *in vitro* into adipocytes and osteoblasts.

To further explore the possible stemness nature of cen3tel sphere cells, we investigated their ability to differentiate into different lineages, being this an important features of CSCs (Vermeulen 2008; Clevers 2011). In particular, we tested whether spheres were enriched in cells able to differentiate in adipocytes or osteoblasts compared to bulk cen3tel cells. To this purpose, cen3tel 600 and cen3tel 1000 cells, adherently growing or derived from spheres, were plated either in adipogenic or in osteogenic differentiation medium.

Adipogenic differentiation was assessed using Oil Red O stain, as indicator of intracellular lipid accumulation. A similar extent of differentiated cells was observed among cells grown in adhesion and spheres cells (Fig. 7 A and B).

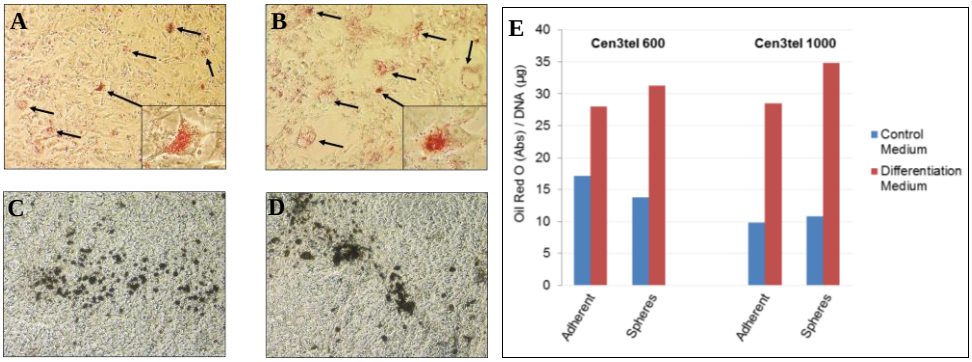

Figure 7. ***In vitro*** **adipogenic and osteogenic differentiation of cen3tel sphere and adherent cells. A-D**: Examples are shown of differentiated cen3tel 600 cells; the same results were obtained for cen3tel 1000 cells (not shown). Cen3tel 600 adherent (**A**) and sphere (**B**) cells cultured in adipogenic differentiation medium and stained with Oil Red O. Arrows indicate examples of adipocytes, large cells characterized by the presence of red spots corresponding to lipid droplets. In the inlets, an enlargement of an adipocyte is shown. Images were taken with a 10X objective, images in the inlets were taken with a 40X objective and enlarged digitally. **C-D**: Cen3tel 600 adherent (**C**) and sphere (**D**) cells cultured in osteogenic differentiation medium. The brown spots represent hydroxyapatite depositions stained by $AgNO_3$. Images were taken with phase contrast microscope with a 10X objective. (**E**) Quantitative analysis of intracellular lipid accumulation in differentiated cen3tel 600 and 1000 adherent and sphere cells grown in control of differentiated medium. Values are the ratio between the absorbance (Abs) at 500 nm of the Oil Red O extracted from each sample and the corresponding amount of total DNA.

Moreover, measuring the amount of Oil Red O incorporated in the different cell samples, we found that it was higher in cells grown in adipogenic

differentiation medium compared to control cells, but it was comparable in sphere and adherent cells (Fig. 7 E).

Osteogenic differentiation was analysed by $AgNO_3$ staining, as indicator of calcium deposition, and in all the cell samples we observed a massive and similar deposition of hydroxyapatite crystals (Fig. 7 C and D).

Thus both cells grown in adhesion and spheres contain cells capable of differentiating in various lineages and spheres does not appear to be enriched in cells able to undergo differentiation.

4.4 *In vivo* tumorigenicity of sphere cells

Given that a distinctive feature of CSCs is a higher tumorigenicity compared to the bulk of the tumor population, we performed *in vivo* tumorigenic assays to test the capacity of sphere cells to induce tumors in immunocompromised mice. We tested the tumorigenic potential of cen3tel 600 adherent and sphere cells inoculating $2.5x10^4$, $5x10^4$ or $5x10^5$ cells bilaterally into the leg muscle of NSG mice and following the development of the tumors (2, 3 and 2 mice were injected with each amount of cells, respectively). As shown in Fig. 8, tumors induced by $5x10^4$ or $5x10^5$ sphere cells showed a greater growth rate compared to those derived from adherent cells.

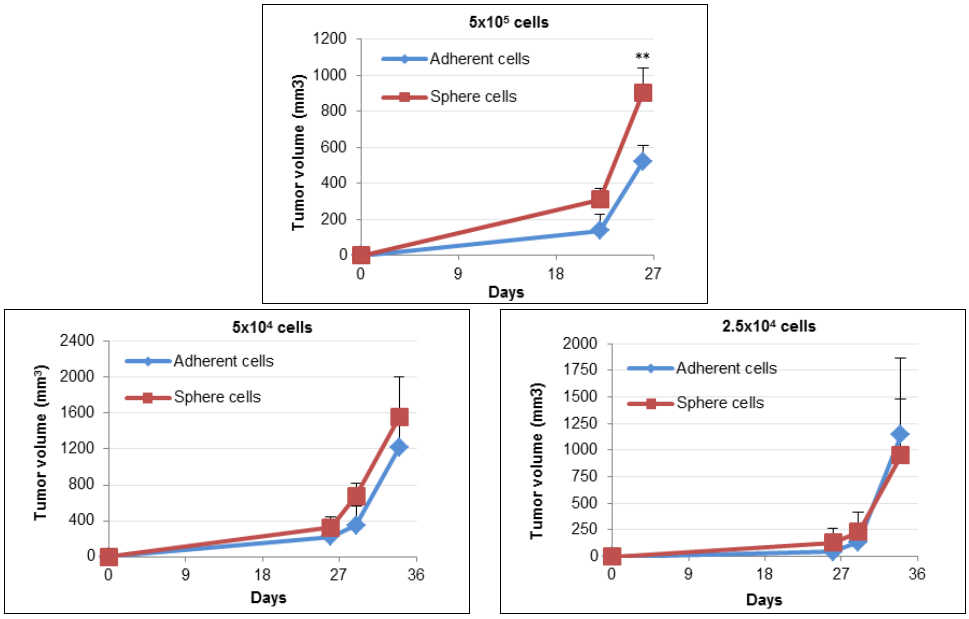

Figure 8. *In vivo* tumorigenicity of cen3tel 600 sphere cells. NSG mice were injected with three different amounts of cen3tel 600 sphere cells or adherent cells ($5x10^5$, $5x10^4$ or $2.5x10^4$). Injections were performed bilaterally into the leg muscle. Tumor growth was periodically monitored, tumor volume (mm^3) was measured and plotted against the time since injection. Error bars: standard deviations. **: $p < 0.01$.

In addition, tumors induced by $5x10^4$ sphere cells appeared earlier than tumor

induced by the same number of adherent cells (after 22 days, tumors were detectable in 5 out of 6 and 2 out of 6 sites of injection after inoculation with sphere or adherent cells, respectively).An earlier time of tumor appearance for sphere cells was also detected inoculating $2.5x10^4$ cells. In this case, tumors were developed at 3 out of 4 sites of injection 26 days after sphere cell inoculation, while only at 1 out of 4 of sites when adherent cells were inoculated. However, tumors induced by both types of cells then showed a similar growth rate. This observation was confirmed in a second experiment, in which at the first time of tumor detection (19 days after inoculation), tumors were present at 8 out of 8 sites of inoculation when $2.5x10^4$ sphere cells were injected and only in 1 out of 8 sites, when the same number of adherent cells was implanted. Thus, sphere cells obtained from cen3tel 600 cells show a slight increase in tumorigenicity compared to adherent cells. In particular, when a small number of cells is inoculated, sphere cells are able to engraft tumors more efficiently than adherent cells. The same analysis will be conducted with cen3tel 1000 sphere cells.

4.5 Expression of stemness genes and miR-34a in cen3tel 600 and 1000 sphere cells

To better characterize the molecular features of cells growing in spheres, we analysed the expression of genes known to be linked to stemness, such as c-*MYC*, *GNL3*, which encodes for nucleostemin, and *NOTCH1*.

We collected and disaggregated spheres from cen3tel 600 and cen3tel 1000 cells both at 6 and 7 days of growth and we first analysed the expression of these genes at protein level by western blotting.

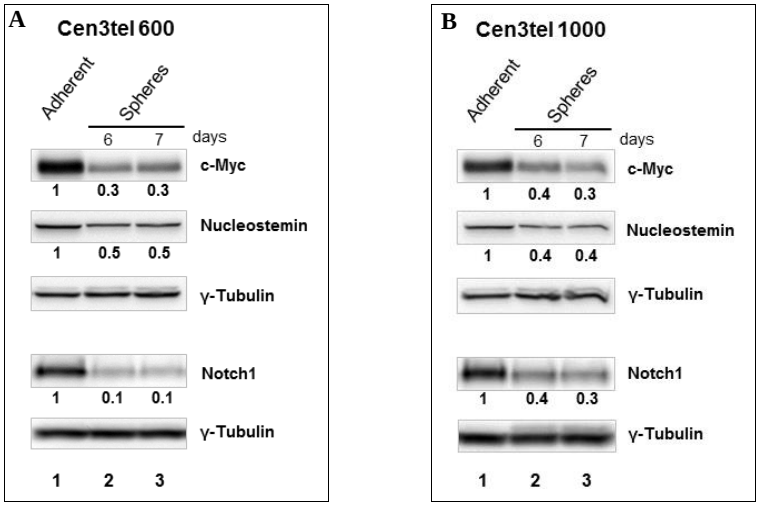

Figure 9. Western blot analysis of c-Myc, Nucleostemin and Notch1 expression in cen3tel 600 and 1000 spheres and adherent cells. Sphere cells were collected at 6 or 7 days of growth in serum free medium. For each protein, the relative intensity of the band in each sphere sample respect to the corresponding adherent cells is reported in bold below the corresponding lane. γ-Tubulin was used as loading control.

Surprisingly, we found a decreased level of all the three proteins in sphere cells compared to adherently growing cells (Fig. 9 A and B, lanes 2 and 3 vs lane 1), with a similar extent of expression reduction at both times of analysis.

Given that c-Myc expression decreases when cells stop proliferating (Bretones et al. 2015), we tested whether c-Myc down-regulation was linked to the exit from the cell cycle of cen3tel sphere cells, monitoring cell proliferation during sphere formation. At different time intervals (day 5, 6, 7 and 8), we collected and disaggregated spheres and determined the total number of cells, which was found to increase daily. The ratios between the number of cells at d6 and d5, d7 and d6, d8 and d7, were 1.7, 1.5 and 1.5, respectively, in cen3tel 600 cells, and 2.1, 1.6 and 1.9, respectively, in cen3tel 1000 cells. Albeit this increase in cell number is slightly lower than that observed in proliferating adherent cells (cells double their number every 24 hours, data not shown), we can conclude that c-Myc down-regulation was observed in a population of cells that were still proliferating.

We then analyzed the expression of miR-34a, which has a cross talk expression regulation with c-*MYC* and *NOTCH1* and is often down-regulated in cancer stem cells (Li et al. 2009a; Christoffersen et al. 2010; Liu et al. 2011b). By RT-qPCR, we found that it was significantly overexpressed in sphere cells compared to adherently growing cells (Fig. 10).

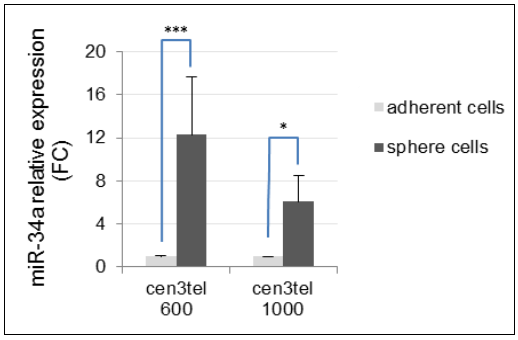

Figure 10. Expression of miR-34a in cen3tel 600 and 1000 sphere cells. Expression analysis of miR-34a was performed by RT-qPCR. MiR-34a expression in each sphere sample is indicated as fold change (FC) relative to the expression in corresponding adherent cells. Values are the mean of the results of three independent experiments. Error bars: standard deviations. *: p <0.05, ***: p < 0.005.

4.6 C-Myc, Notch1, Nucleostemin deregulation and miR-34a overexpression are reversible when sphere cells are replated in serum containing medium

We then investigated whether the expression modulation of these genes was reversible once sphere cells were plated in serum containing medium, spheres from both cen3tel 600 and 1000 cells were disaggregated, cells plated in adherent culture conditions and analysed at different time intervals. As shown in Figure 11, already one day after plating, the expression levels of c-Myc, nucleostemin and Notch1 regained values comparable to those found in control adherent cells (Fig. 11 A and

B, lanes 3-5 *vs* lane 2). Also miR-34a levels decreased after replating sphere cells in adherent culture conditions, but with a slower kinetics (Fig. 11 C and D).

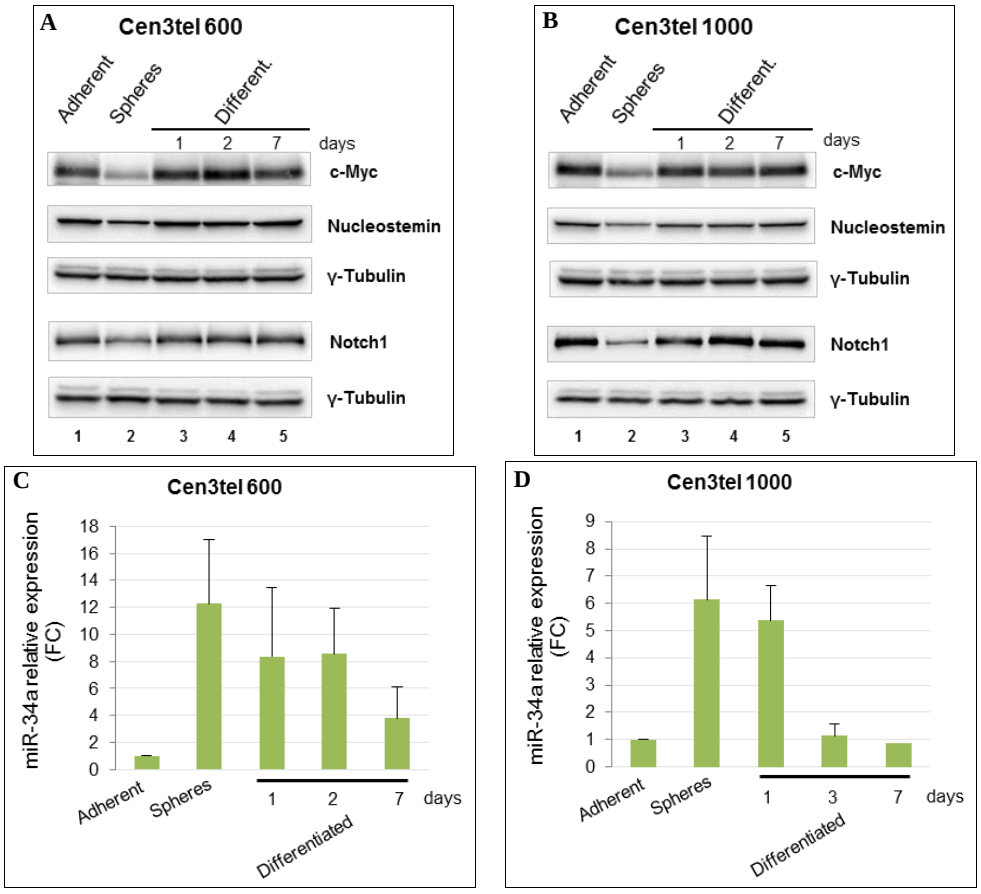

Figure 11. Expression of c-Myc, Nucleostemin, Notch1 and miR-34a in spheres and differentiated sphere cells. A, **B**. Western blot analysis of c-Myc, Nucleostemin and Notch1 expression in cen3tel 600 (**A**) and cen3tel 1000 (**B**) adherent cells, sphere cells and sphere cells grown for different time intervals in serum containing medium (differentiated). γ-Tubulin was used as control for protein loading. **C**, **D**. Analysis by RT-qPCR of miR-34a expression in cen3tel 600 (**C**) and cen3tel 1000 (**D**) adherent cells, sphere cells and sphere cells grown for different time intervals in serum containing medium. miR-34a expression levels in sphere cells are indicated as Fold Change (FC) relative to the corresponding adherent cells and are the mean of the results of three independent experiments. Error bars: standard deviations.

Thus, deregulation of the expression of c-Myc, nucleostemin, Notch1 and miR-34a in sphere cells is reversible when they are allowed to differentiate in adherent culture conditions.

In contrast, when spheres were disaggregated and sphere cells re-plated in non-adherent culture conditions, the levels of c-Myc, nucleostemin and Notch1 (lanes 3-4 and 7-8) remained comparable to that observed in primary spheres (lane 2 and lane 6) (Fig. 12), suggesting that this deregulation is linked to cell growth in suspension. Moreover, it is worthwhile noticing that the expression of these genes

appears to be concerted, since all the genes are regulated in the same way in the different culture conditions.

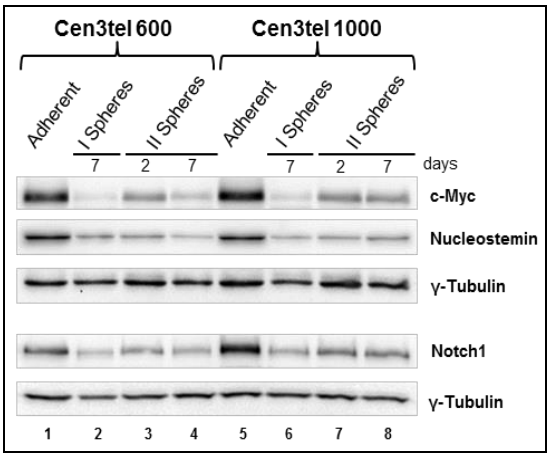

Figure 12. Western blot analysis of c-Myc, Nucleostemin and Notch1 expression in primary and secondary spheres. c-Myc, Nucleostemin and Notch1 expression were analyzed in cen3tel 600 and 1000 primary spheres (I Spheres) and secondary spheres (II Spheres) at different days of growth in sphere-forming medium. II spheres were obtained by replating I sphere cells in sphere-growing medium. γ-Tubulin was used as control for protein loading.

4.7 Expression regulation of c-*MYC*, *GNL3* and *NOTCH1* in sphere cells

To investigate the possible mechanisms of c-*MYC*, *GNL3* and *NOTCH1* expression regulation in cen3tel sphere cells, we analysed the expression of these genes at the transcriptional level by RT-qPCR. As shown in Fig. 13, significantly reduced levels of the transcripts was observed for c-*MYC* and *GNL3* in sphere cells compared to cells grown in adhesion, indicating that there is a layer of regulation for these genes at the transcriptional level. For *NOTCH1* a transcript reduction was observed but not significant, suggesting that other mechanism of expression regulation could be active.

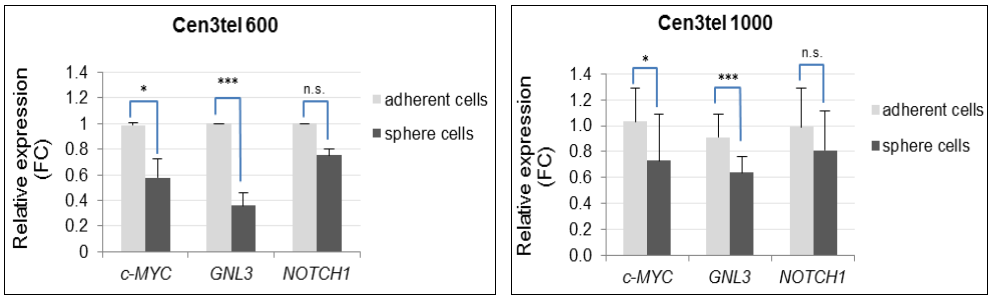

Figure 13. RT-qPCR analysis of c-*MYC*, *GNL3* and *NOTCH1* expression in cen3tel 600 and 1000 sphere cells. Expression levels in sphere cells are indicated as fold change (FC) relative to the corresponding adherent cells and are the mean of the results of three independent experiments. Error bars: standard deviations. *: $p < 0.05$, ***: $p < 0.005$; n.s. = not significant.

We thus tested whether proteasomal degradation could contribute to Notch1

decreased levels in sphere cells. Cen3tel 600 and cen3tel 1000 adherently growing cells and spheres grown for 6 days were incubated for 2 or 4 hours with the proteasomal inhibitor MG-132 and then Notch1 levels were analysed by western blotting. In parallel, we also analysed the levels of c-Myc, which is known to be subjected to proteasomal degradation.

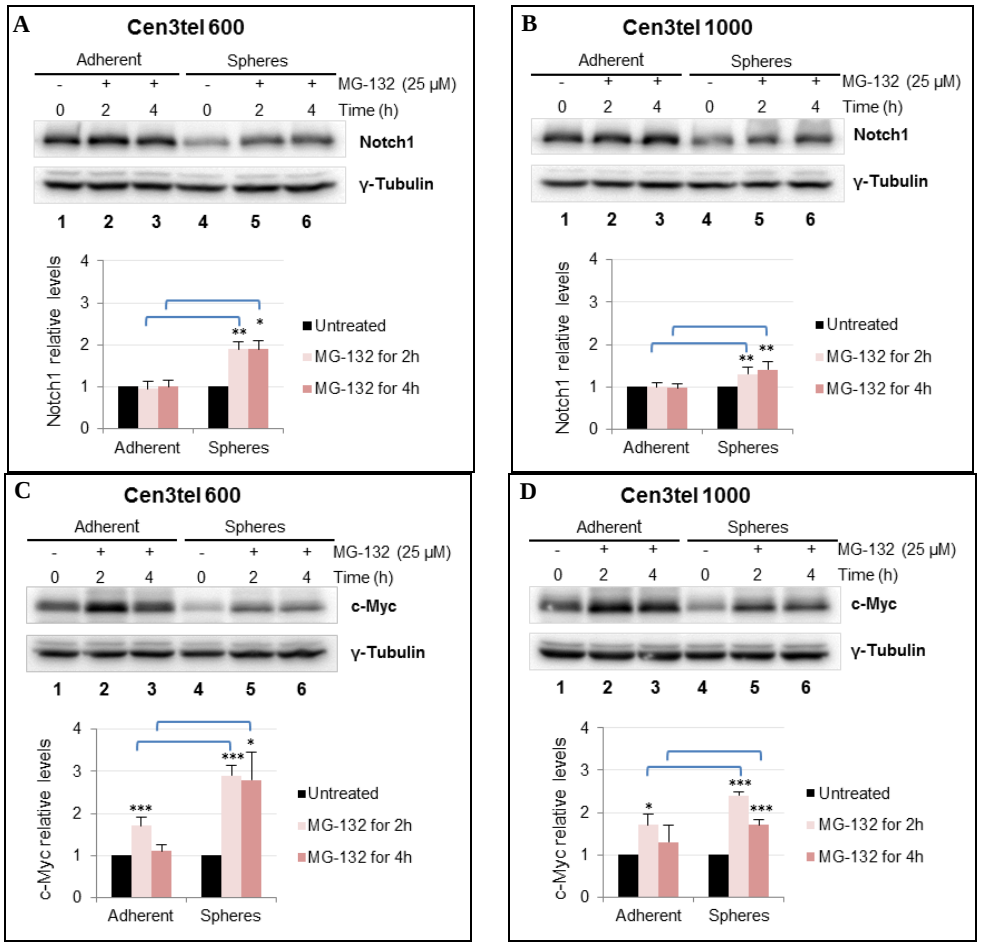

Figure 14. Western blot analysis of Notch1 (A and B) and c-Myc (C and D) expression in cen3tel 600 and 1000 adherent and sphere cells treated with the proteasome inhibitor MG-132. Cen3tel cells were seeded in sphere-forming medium and after 6 days of growth were exposed to 25 μM MG-132 for 2 or 4 hours. In parallel, the same treatment was used for adherently growing cells. MG-132-untreated adherent and sphere cells were used as control. Histograms show the relative intensity of the bands in treated cells respect to the corresponding untreated control samples. Values are the mean of the results of three independent experiments. γ-Tubulin was used as loading control. Error bars: standard deviations. *: $p < 0.05$, **: $p < 0.01$, ***: $p < 0.005$.

The analysis of Notch1 expression revealed that MG-132 did not affect the levels of this protein in both cen3tel 600 and 1000 adherent cells (Fig. 14 A and B, lanes 2 and 3 *vs* lane 1 and respective quantification histograms), while led to its accumulation in sphere cells (Fig. 14 A and B, lanes 5 and 6 *vs* lane 4 and

respective quantification histograms), suggesting that proteasomal activity can contribute to the reduction of Notch1 levels observed in sphere cells compared to adherent cells.

C-Myc levels increased both in cen3tel 600 and 1000 adherent and sphere cells upon MG-132 treatment (Fig. 14 C and D). In MG-132 treated sphere cells, the levels of c-Myc did not reach those observed in adherently growing cells (Fig. 14 C and D, lanes 5 and 6 vs lanes 2 and 3). However, the accumulation of the protein was greater in sphere cells compared to adherent cells (Fig. 14 C and D respective quantification histograms) suggesting that, also for c-Myc, proteasomal degradation can contribute to its decreased expression in sphere cells.

4.8 Sphere cells do not undergo apoptosis

It is well known that c-Myc promotes apoptosis (Meyer et al. 2006), thus decreased c-Myc levels in sphere cells could be functional to protect cells from death, which could occur because of the peculiar structure of spheres, in which cells grow in a highly compact way. Analyzing markers for the apoptotic process, as cleaved caspase 9 and 3 and the proteolytic poly (ADP-ribose) polymerase 1 (PARP-1) fragment in cen3tel 600 and 1000 sphere cells, we did not find detectable levels of these markers in sphere cells (Fig. 15 A, lanes 3 and 6; B, lanes 2 and 4).

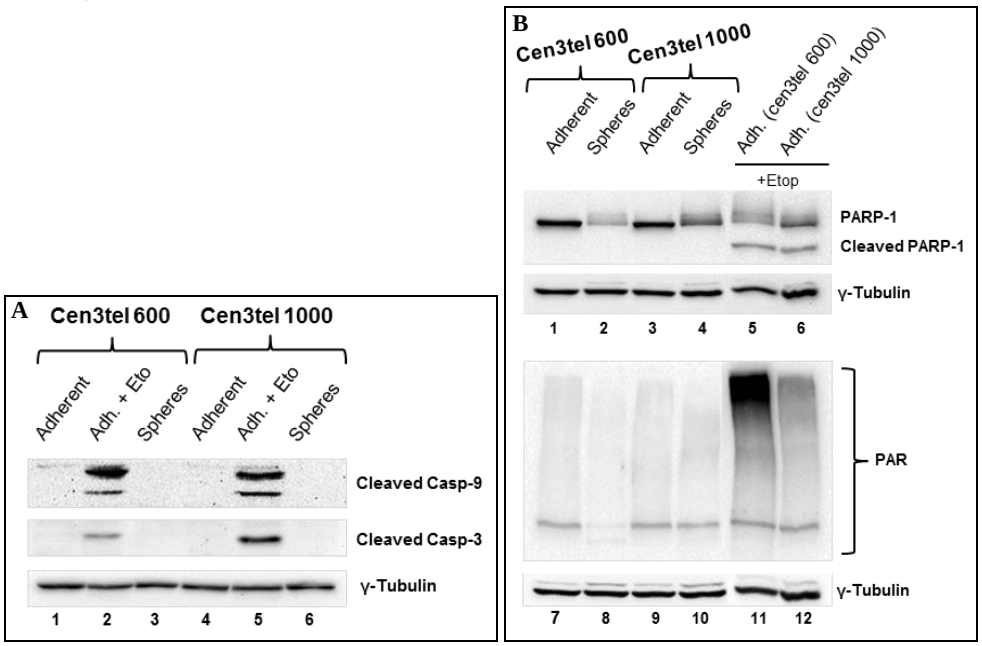

Figure 15. Western blot analysis of apoptotic markers in cen3tel 600 and 1000 sphere and adherent cells. Antibodies recognizing the cleaved active forms of caspases 9 and 3 (**A**) were used, as well as an antibody recognizing both the full-length and the apoptotic cleaved fragment of PARP-1 and an antibody anti-poly ADP ribose (PAR) (**B**). As apoptosis control, adherent cen3tel cells treated with 100 μM etoposide for 24 hours (+Etop) were used. γ-Tubulin was used as loading control.

As expected, in adherent cells the apoptotic markers were not observed (Fig. 15 A, lanes 1 and 4; B, lanes 1 and 3), but were induced after etoposide exposure (Fig. 15 A, lanes 2 and 5; B, lanes 5 and 6).

Thus, we can conclude that in sphere cells there is no evidence of activation of apoptosis and c-Myc down-regulation could contribute to the restraining of this process.

PARP-1 plays a role in several cellular processes, among which DNA repair and transcription, and can be activated by different stimuli. Once activated, PARP-1 becomes able to add poly(ADP-ribose) (PAR) residues to itself and to several other proteins (Muthurajan et al. 2014). Interestingly, the analysis of PARP-1 expression in sphere cells and etoposide treated cells, revealed the presence of a series of bands (Fig. 15 B, lanes 2, 4-6), which probably correspond to poly-ADP-ribosylated PARP-1, suggesting that in sphere cells a stimulus, still to be defined, activates the protein. However, analysing the global levels of protein poly-ADP-ribosylation in the different samples by western blotting with an antibody recognizing PAR residues, we found a similar extent of modifications in adherent and sphere cells, and a higher level in etoposide-treated cells, suggesting that etoposide induces a PARP-1 response different from that observed in sphere cells. Further investigations are required to better understand the possible meaning of PARP-1 modification in sphere cells.

4.9 Genome wide gene expression analysis by microarray

To get a better insight into sphere cell features, we compared genome wide gene expression profiles of cen3tel 600 and cen3tel 1000 sphere cells with those of their adherent counterparts. Gene expression profiling was performed using Agilent oligonucleotide glass arrays containing about 40,000 probes that correspond to about 20,000 transcripts. RNA samples prepared from two biological replicates of sphere cells were hybridized in duplicate against the RNA extracted from their corresponding adherent cells. Global gene expression profiling showed that adherent cen3tel 600 and 1000 cells were separated in two clusters (Fig. 16). Cen3tel 1000 sphere cells fell in the same cluster as their adherent counterpart. Cent3tel 600 sphere cells were closer to cen3tel 1000 adherent and sphere cells than to cen3tel 600 adherent cells, indicating that cen3tel 600 sphere cells switch towards a gene expression profile mainly similar to that of the more aggressive cen3tel 1000 cells.

Transcripts of sphere cells with $\log_2$FC versus adherent cells greater than 0.58 or lower than –0.58 and adjusted *p*-value less than 0.05 were considered as differentially expressed. 5867 probes were up-regulated in cen3tel 600 primary spheres compared to adherent cells, while 4354 were down-regulated. In cen3tel 1000 sphere cells, the number of deregulated transcripts relatively to adherent cells was lower, including 751 up-regulated and 184 down-regulated probes. In support to the observation that cen3tel 600 sphere cells were closer to cen3tel 1000 adherent cells than to cen3tel 600 adherent cells (Fig. 16), the number of genes differentially expressed between these two cell samples was about 3000 (~2200 up-regulated, ~800 down-regulated), compared to the ~10000 genes deregulated in

cen3tel 600 spheres *vs* their adherent counterpart. Most of the genes deregulated in cen3tel 1000 spheres were also deregulated in cen3tel 600 sphere cells. In fact, out of 751 probes up-regulated in cen3tel 1000 spheres, 643 were also up-regulated in cen3tel 600 spheres, and 142 probes out of the 184 down-regulated ones were also down-regulated (Table S1 and S2, respectively). We decided to carry on our investigation by analysing the genes commonly deregulated in cen3tel 600 and cen3tel 1000 sphere cells. Therefore, when we refer to sphere cells, we mean sphere derived from both cen3tel 600 and cen3tel 1000 sphere cells, unless otherwise specified.

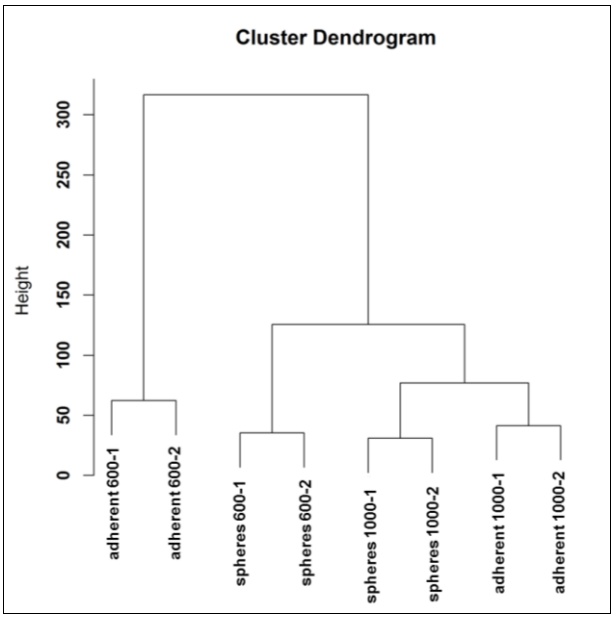

Figure 16. Global gene expression profiling of cen3tel 600 and 1000 adherent and sphere cells. Dendrogram represents the relationship of similarity among the global gene expression profiles of cen3tel 600 and 1000 adherent and sphere cells. The tree diagram was obtained from unsupervised hierarchical clustering using Euclidean distance as similarity metrics and ward linkage as linkage method. Each branch of the dendrogram is represented by the global gene expression profiles of the analyzed cell samples. For each cell samples, the two biological replicates are shown. The vertical axis indicates the Euclidean distance (Height) between samples/clusters.

4.10 Deregulation of cell movement genes in sphere cells

Comparing gene expression modulation during transformation of cen3tel cells and between spheres and adherent cells, we could observe that in sphere cells most of the genes differentially expressed relatively to adherent cells were up-regulated, while during transformation there was a trend towards gene expression up-regulation only at the initial phases of transformation (Ostano et al. 2012). For many genes, we actually found that the down-regulation observed during transformation was reversed in sphere cells.

Among these genes there are genes encoding proteins involved in cellular movement, such as several metalloproteinases (MMP) and the Rho GTPase Rnd3

(Belgiovine et al. 2010). During cen3tel transformation, we found that the deregulation of these genes was associated with a switch from the mesenchymal movement to the ameboid motility; in fact, tumorigenic cells were characterized by a movement dependent on the activity of the RhoA-dependent kinase ROCK and independent of MMPs (Belgiovine et al. 2010). In sphere cells, we observed the up-regulation of the expression of *MMP1*, *MMP7* and *MMP14*, as well as the overexpression of *RND3* (Fig. 17 A). Microarray results were confirmed either by RT-qPCR (for MMPs, Fig. 17 B) or by western blotting (for Rnd3, Fig. 17 C). Thus, cells growing as spheres show a reversion towards a more mesenchymal phenotype compared to adherent cells.

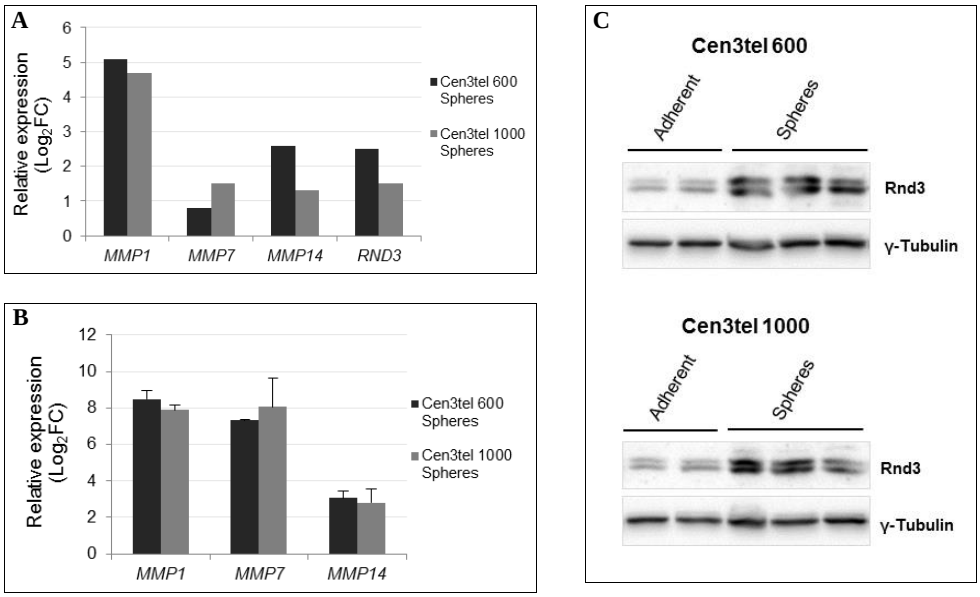

Figure 17. *MMP1, MMP7, MMP14* and *RND3* expression in cen3tel 600 and 1000 sphere cells (A) Expression of *MMP1, MMP7, MMP14* and *RND3* by microarray analysis. (**B**) Analysis of *MMP1, MMP7* and *MMP14* expression by RT-qPCR. In the plots of panels A and B, the expression of each gene in sphere cells is indicated as Log_2FC relative to its expression in the corresponding adherent cells. Error bars: standard deviations. (**C**) Evaluation of Rnd3 expression levels in cen3tel 600 and 1000 adherent and sphere cells by western blot analysis. γ-Tubulin expression was used as loading control.

4.11 Functional enrichment analysis of the genes differentially expressed in sphere cells vs adherently growing cells

To investigate the possible functional meaning of the molecular changes found in sphere cells, functional annotation of the lists of genes commonly up-regulated or down-regulated between cen3tel 600 and 1000 sphere cells *vs* their corresponding adherent cells were separately analysed using David (http://david.abcc.ncifcrf.gov/). The gene lists were analysed using the David functional annotation tool and the classification implemented by Panther within David to determine the overrepresented biological processes. The results of these

analyses considering the terms with *p*-value < 0.01 are reported in Tables S3-S7.

The analysis with David gave 69 level 5 biological processes of the GO overrepresented considering the up-regulated genes and 15 considering the down-regulated ones (p-value < 0.01, Table S3 and S4, respectively). The analysis with the Panther tool gave 14 and 6 overrepresented biological processes for the up-regulated and down-regulated genes, respectively (*p*-value < 0.01, Table S6 and S7). The work of this thesis has focused mainly on the processes linked to the up-regulated genes.

In Fig. 19 A, the 15 BP5 with the most significant *p*-values considering the up-regulated genes are shown. The first 15 terms actually represent 3 major processes.

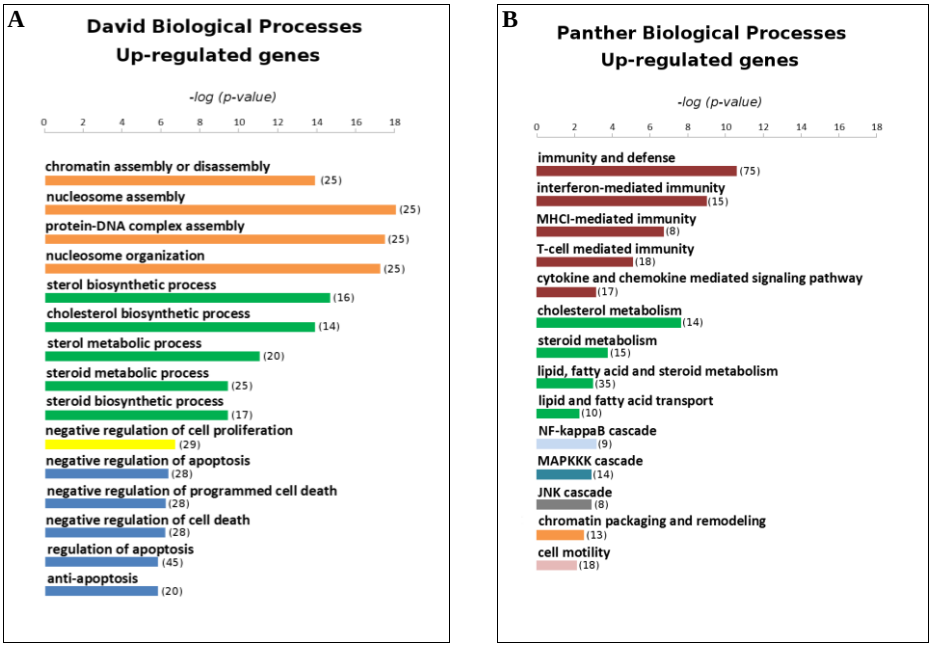

Figure 18. GO enrichment analysis on the list of the commonly up-regulated genes in cen3tel 600 and 1000 sphere cells. (**A**) Representation of 15 biological processes with the most significant *p*-value identified using the annotation tool David. (**B**) Representation of the 14 biological processes with *p*-value < 0.01 identified using the classification implemented by Panther annotation tool within David. Terms belonging to the same biological items are indicated with the same color. Within brackets, the number of deregulated genes falling in each biological processes is reported.

The first 4 terms (Fig. 19 A, orange bars) concern chromatin organization. The genes falling in these terms encode for several replication-dependent histone variants and for the replication-independent histone variant–H2AFJ (Table S5). Deregulation of these genes suggests that a reorganization occurs at the chromatin level in sphere cells, which could in turn have consequences on gene expression.

The second class of processes (green bars) includes genes related to cholesterol metabolism, mostly to the mevalonate/cholesterol biosynthetic pathway; we will discuss, this pathway in the next paragraph.

The third class of processes (blue bars) concerns the regulation of apoptosis,

mainly the negative regulation of this pathway, in agreement with the evidence previously reported that pathways preventing cell death are activated in sphere cells. The antiapoptotic *BCL2A1* gene is among the most up-regulated genes both in cen3tel 600 and 1000 sphere cells (Fig. 19 A); its up-regulation was confirmed by western blotting (Fig. 19 B).

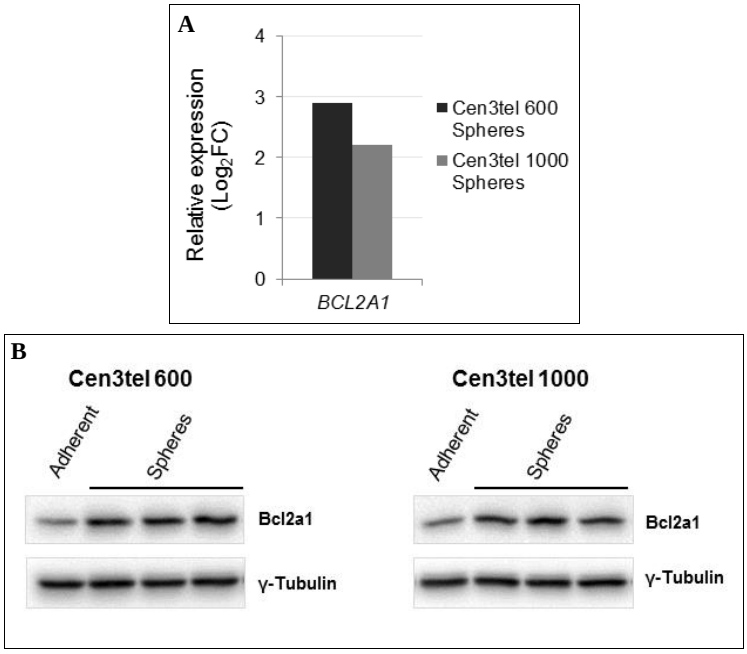

Figure 19. *BCL2A1* expression in cen3tel 600 and 1000 sphere cells. (**A**) Expression of *BCL2A1* in sphere cells by microarray analysis. In the plot, the expression of *BCL2A1* in sphere cells is indicated as Log2FC relative to its expression in the corresponding adherent cells. (**B**) Western blot analysis of Bcl2a1 expression in cen3tel 600 and 1000 adherent and sphere cells. γ-Tubulin was used as loading control.

"Negative regulation of cell proliferation" is also an overrepresented process, whose involvement in sphere cell phenotype can be in agreement with the slight decrease in cellular proliferation observed in spheres.

4.12 Deregulation of mevalonate/cholesterol biosynthetic pathway genes in sphere cells

Fig. 20 A shows the genes of the mevalonate/cholesterol biosynthetic pathways up-regulated in sphere cells. By RT-qPCR, we confirmed the overexpression of three genes of the pathway, namely *HMGCS1*, *HMGCR*, which encodes for the rate limiting enzyme of the pathway, and *MVK* (Fig. 20 B). Interestingly, this biosynthetic pathway was found to be up-regulated in tumorpheres formed by cell lines of the basal/mesenchymal subtypes and fundamental for the maintenance of breast cancer CSCs (Ginestier et al. 2012).

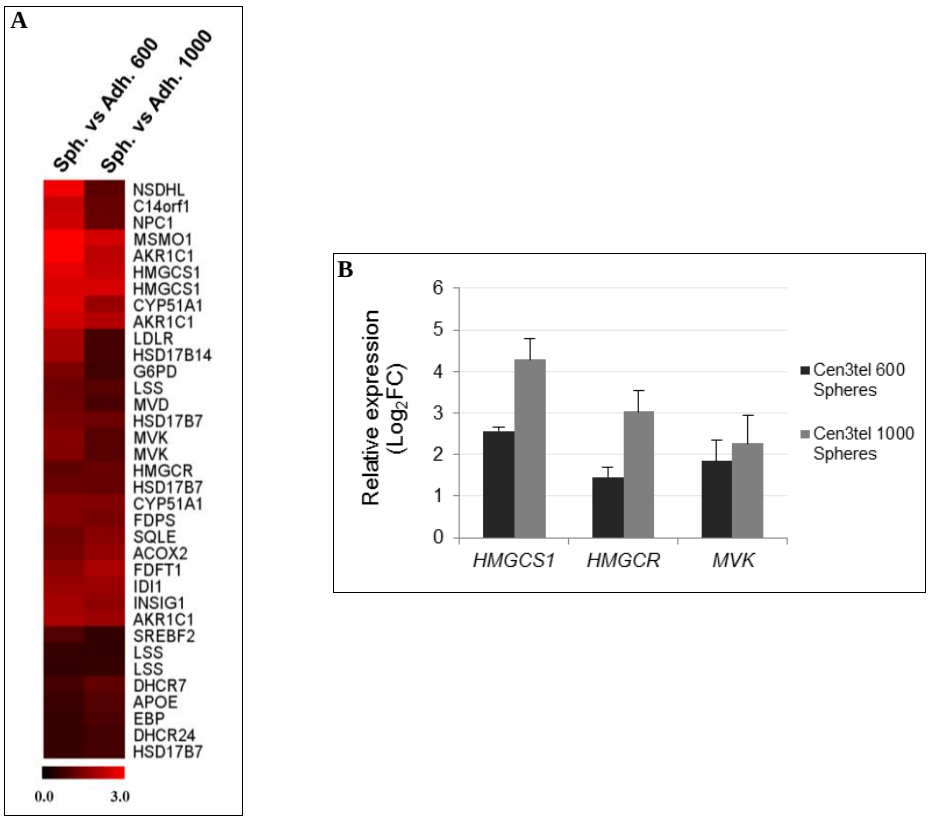

Figure 20. Expression of mevalonate/cholesterol biosynthetic pathway genes in cen3tel 600 and 1000 sphere cells. (**A**) Heatmap of mevalonate/cholesterol pathway genes up-regulated in cen3tel 600 and 1000 sphere cells. A red gradient was used to indicate up-regulation levels for each gene in sphere cells relative to adherent cells, indicated as Log_2FC. (**B**) RT-qPCR analysis of *HMGCS1*, *HMGCR* and *MVK* expression in sphere cells. The expression of each gene in sphere cells is indicated as Log_2FC relative to its expression in the corresponding adherent cells. Error bars: standard deviations.

We thus tested whether the up-regulation of these genes could play a role in sphere formation in cen3tel cells. To this regard, we analyzed the effect of

simvastatin on sphere formation. Simvastatin is an inhibitor of the HMGCR enzyme, which blocks the biosynthesis of mevalonate, an early intermediate in the cholesterol biosynthetic pathway (Gauthaman et al. 2009). Cen3tel 600 and 1000 cells were treated in adherent conditions for 3 days with a simvastatin concentration reducing survival to 50% (1.2 µM and 0.8 µM simvastatin, respectively), and then seeded in sphere-forming medium. As shown in Fig. 21, simvastatin reduced the number of spheres derived from treated cen3tel 600 and 1000 cells of about 5 times and 6 times respectively, compared to untreated samples. We then investigated whether the addition of cholesterol, which represents one of the final products of the pathway, or mevalonate during the simvastatin treatment could revert the effect of this drug. As shown in Fig. 21, the addition of cholesterol did not prevent the effect of simvastatin on sphere formation in both cen3tel cell populations, while the addition of mevalonate rescued sphere formation capacity. These results indicate that mevalonate plays a crucial role in the regulation of sphere formation capacity of cen3tel cells.

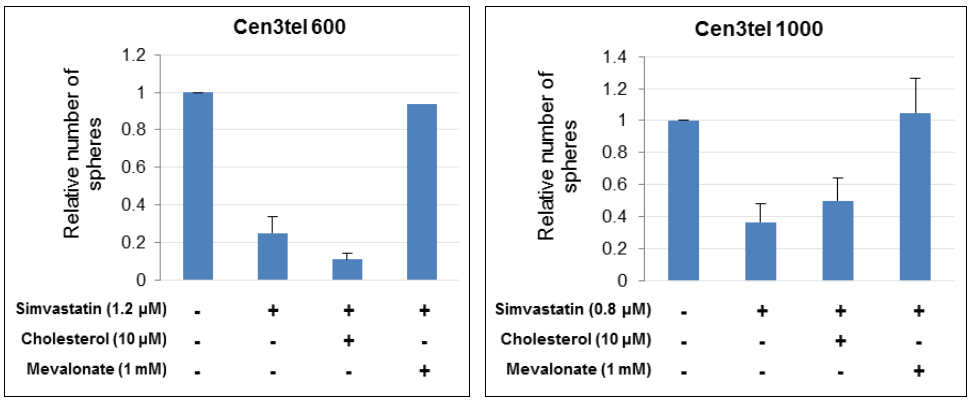

Figure 21. Sphere formation in cen3tel 600 and 1000 cells after inhibition of mevalonate metabolism. Sphere formation was assessed in cells treated for 3 days with the mevalonate metabolism inhibitor simvastatin and in cells exposed to simvastatin together with either cholesterol or mevalonate. In the plot, the number of spheres relative to the untreated control samples is reported for each treatment. Error bars: standard deviations.

4.13 Deregulation of cytokine genes in sphere cells

The analysis of the up-regulated genes in sphere cells performed with the Panther tool highlighted the overrepresentation not only of terms related to cholesterol and steroid metabolism and chromatin organization, but also to immunity and defense, interferon mediated immunity, cytokine and chemokine mediated signalling pathway (Fig. 18 B), suggesting a link between sphere formation, inflammation and immune response. We focused our attention on chemokine and interleukin genes up-regulated in cen3tel 600 and 1000 sphere cells (Fig. 22 A). Similarly to *MMP* and *RND3* genes, these cytokines showed a peculiar pattern of regulation during transformation of cen3tel cells. In fact, most of them displayed an increased expression relatively to primary fibroblasts in cells at the initial phase of transformation but not tumorigenic yet (cells around PD 100) and a

decrease in the overt tumorigenic cells (Ostano et al. 2012). Thus, in the tumorigenic background of cen3tel 600 and 1000 cells, sphere cells showed an increase in the expression of several cytokines, which are often associated with tumorigenesis (Grivennikov et al. 2010).

As shown in Fig. 22 A, in cen3tel 600 and 1000 spheres, *IL1B* and *IL13RA2* are the most up-regulated cytokines and among the most up-regulated genes (log_2FC 3.0 and 4.3, in cen3tel 600 spheres, respectively and log_2FC 3.2 and 3.0 in cen3tel 1000 spheres, respectively).

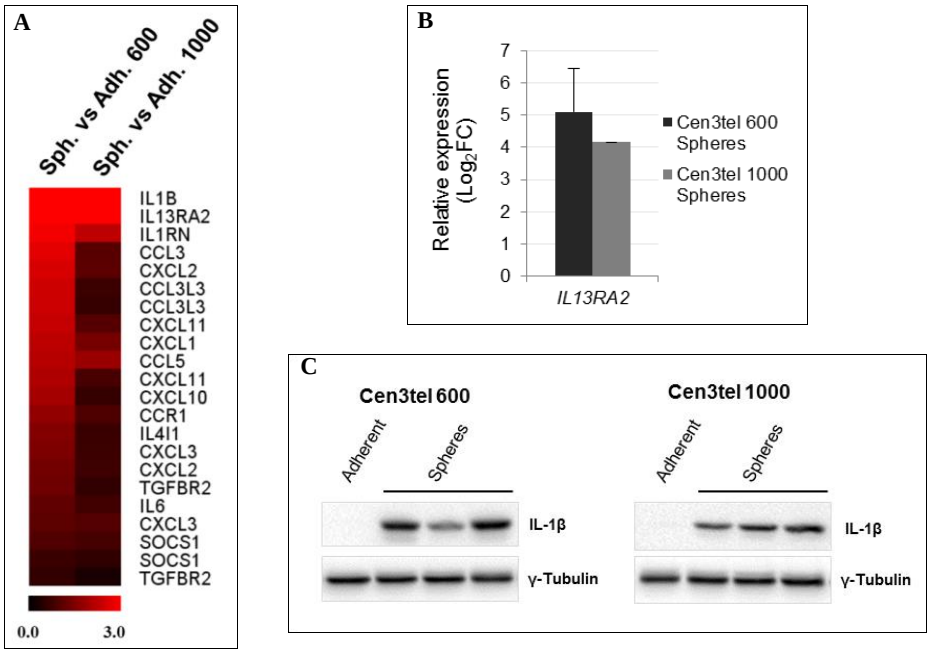

Figure 22. Chemokine expression in cen3tel 600 and 1000 sphere cells. (**A**) Heatmap of chemokine and interleukin genes up-regulated in cen3tel 600 and 1000 sphere cells. A red gradient was used to indicate up-regulation levels for each gene in sphere cells relative to adherent cells, indicated as Log_2FC. (**B**) RT-qPCR analysis of *IL13RA2* expression in sphere cells. The expression of *IL13RA2* in sphere cells is indicated as Log_2FC relative to its expression in the corresponding adherent cells. Error bars: standard deviations. (**C**) Western blot analysis of IL-1β expression in cen3tel 600 and 1000 adherent and sphere cells. γ-Tubulin expression was used as loading protein control.

During cen3tel transformation, *IL13RA2* was down-regulated at all phases (Log_2FC ~ -4, Ostano et al. 2012) and by RT-qPCR we did confirm its up-regulation in sphere cells (Fig. 22 B). Interestingly, elevated levels of *IL-13RA2* have been described in several cancers and have been implicated, for example, in metastatization and poor patients' survival in colorectal cancer and ERα-negative breast cancer (Barderas et al. 2012; Zhao et al. 2015).

IL1B econdes IL-1β, an inflammatory cytokine that plays a critical role in cancer progression, in particular in colorectal cancer (Lasry et al. 2016). IL-1β is synthesized as a precursor protein and then cleaved by caspase 1 to generate the secreted active molecule. The *IL1B* gene showed a modest deregulation during

cen3tel cell transformation (+0.3 in cen3tel 600 cells and -0.6 in cen3tel 1000 *vs* primary fibroblasts, respectively), while it was highly up-regulated in sphere cells, as shown in the heatmap (Fig. 22 A). By western blot, we showed that the IL-1β precursor form is undetectable in adherent cen3tel 600 and 1000 cells, while is overexpressed in sphere cells (Fig 22 C). However, despite the presence of high levels of pro-IL-1β in the cellular protein extracts, we did not detect secreted IL-1β in sphere culture medium (data not shown), suggesting that the protein is not processed to the active form, even if microarray analysis revealed the overexpression of caspase 1, caspase 4 and caspase 5, which are known to be involved in cytokine processing (Table S1; Man and Kanneganti, 2016).

Given that it is known that interleukins, such as IL-6, can drive the conversion from bulk tumor cells to stem cells in mammary tumor cells (Iliopoulos et al. 2011), we wondered whether IL-1β, despite being undetectable in the culture medium, could have a similar effect, possibly at very low concentrations. To test this hypothesis, we grew cent3tel cells in sphere forming conditions in the presence of IL-1β and we found that it actually had a detrimental effect (Fig. 23 A); in fact, in the presence of 10 ng/mL IL-1β, the number of spheres was decreased of about 50% both in cen3tel 600 and cen3tel 1000 cells compared to untreated cells. In cen3tel 600 cells we analysed the effect of concentrations as low as 0.02 ng/mL and again we found a decrease in sphere formation of about 50% (data not shown). Thus, mature IL-1β negatively affects sphere formation in cen3tel cells in a concentration independent manner.

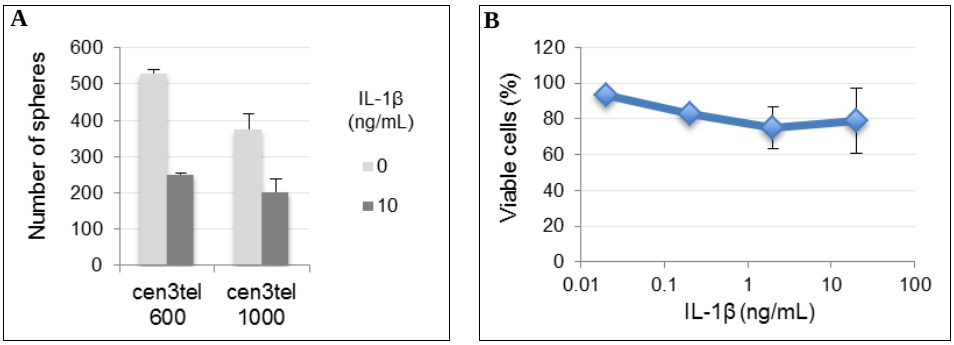

Figure 23. Effect of IL-1β on the growth of cen3tel 600 and 1000 sphere and adherent cells. (**A**) Evaluation of the effect of IL-1β on the sphere formation capacity of cen3tel 600 and 1000 cells. Cen3tel cells were seeded in sphere-forming medium in presence of 10 ng/mL IL-1β. After 7 days of growth, the average number of spheres in control samples and treated cells cells was determined. Bars: standard deviation. (**B**) Determination of the IL-1β effect on cen3tel 600 adherent cells' viability. Cells were seeded in adherent growing conditions and treated for 3 days with increasing concentrations of IL-1β. The percentage of viable cells relative to untreated control cells is shown. Error bars: standard deviations.

We then analyzed whether IL-1β inhibited cell growth also in cells plated in adherent culture conditions. To this purpose cen3tel cells 600 were plated in the presence of increasing concentrations of IL-1β for 7 days and viable cells were then counted as Trypan blue negative cells. As shown in Fig. 23 B, IL-1β has a modest effect on adherent cells' viability, in particular at very low concentrations

(0.02 ng/mL), at which more than 90% of the cells are still viable. This suggests that IL-1β might have a preferential negative effect on the cells that are prone to form spheres, despite the *IL1B* gene is up-regulated in sphere cells. To our knowledge, nothing is known about a possible function of the endocellular IL-1β precursor protein and it cannot be excluded that divergent roles might be played by the mature and the precursor form of this cytokine.

IL-6 was also overexpressed both in cen3tel 600 and cen3tel 1000 spheres (Log_2FC 0.78 and 1.15, respectively). Incubating cen3tel 600 and 1000 cells with increasing concentrations of IL-6, we found a significant increase in sphere formation in cen3tel 600 cells exposed to 20 and 50 ng/ml, while in cen3tel 1000 cells a modest increase was observed at the highest IL-6 concentration, but it was not significant (Fig. 24). This suggests that IL-6 has a sphere formation promoting effect also in cen3tel cells.

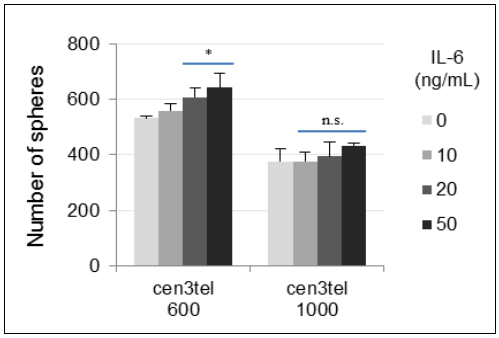

Figure 24. Effect of the IL-6 treatment on the sphere formation in cen3tel 600 and 1000 cells. Cen3tel cells were seeded in sphere-forming medium in the presence of increasing IL-6 concentrations (10, 20 or 50 ng/mL). After 7 days of growth, the average number of spheres in control samples and treated cells was determined. Error bars: standard deviations. *P*-values refers to IL-6-treated cells *vs* untreated controls. *: $p < 0.05$; n.s.: not significant.

4.14 Deregulation of INF pathway genes in sphere cells

Gene ontology analysis of the genes up-regulated in sphere cells revealed an enrichment for functions associated with the interferon pathway. Out of 168 genes related to this pathway found in the annotation database Amigo (http://amigo.geneontology.org/amigo/search/annotation), 37 genes were found significantly overexpressed in cen3tel 600 and 1000 spheres ($Log_2FC > 0.58$, adjusted $p < 0.05$) (Fig. 25 A).

Many of the genes belonging to the IFN pathway showed a peculiar pattern of expression during cen3tel transformation, being mainly up-regulated only at the initial phase of transformation. We choose three genes to confirm microarray results, namely *IFI6*, *ISG15* and *STAT1* (Fig. 25 B and 26).

IFI6 belongs to the group of INF inducible genes and was reported to be important for the development and growth of several cancers (Kim et al. 2010b; Gupta et al. 2016). It was found among the genes mostly up-regulated associated to the interferon pathway both in cen3tel 600 and 1000 sphere cells (Log_2FC 3.5 and 2.3, respectively). By RT-qPCR analysis we validated its overexpression in both

sphere cell populations (Fig. 25 B).

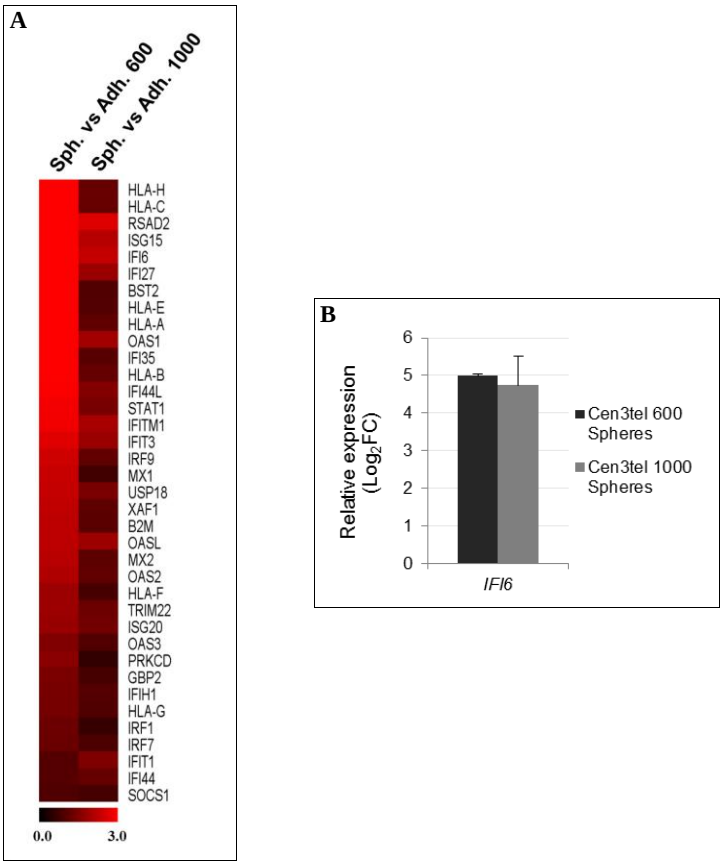

Figure 25. Expression of interferon-related genes in cen3tel 600 and 1000 spheres. (**A**) Heatmap of interferon-related genes up-regulated in cen3tel 600 and 1000 sphere cells. A red gradient was used to indicate up-regulation levels for each gene in sphere cells relative to adherent cells, indicated as Log_2FC. (**B**) RT-qPCR analysis of *IFI6* expression in sphere cells. *IFI6* expression in sphere cells is indicated as Log_2FC relative to its expression in the corresponding adherent cells. Error bars: standard deviations.

In different tumors, Stat1 can have either a tumor suppressor or a tumor promoting function; together with ISG15, it has been shown to promote transformation in cells deficient in p53 and ARF (Forys et al. 2014). We did confirm *STAT1* up-regulation in sphere cells, together with its increased activation, as shown by the high levels of phospho-Stat1^{Tyr701} in sphere cells compared to adherent cells (Fig. 26 A).

ISG15 has been shown to be up-regulated in several solid tumors (e.g. Li et al. 2014; Chen et al. 2016) and involved in cancer stem cell genesis and maintenance (Sainz et al. 2014). Its expression is mainly regulated by type I IFN through the transcription factor Stat1. *ISG15* encondes a small protein that can be covalently linked to several proteins in a process known as intracellular ISGylation, but also can be free in the cytosol or secreted in the extracellular space (Sgorbissa and

Brancolini, 2012).

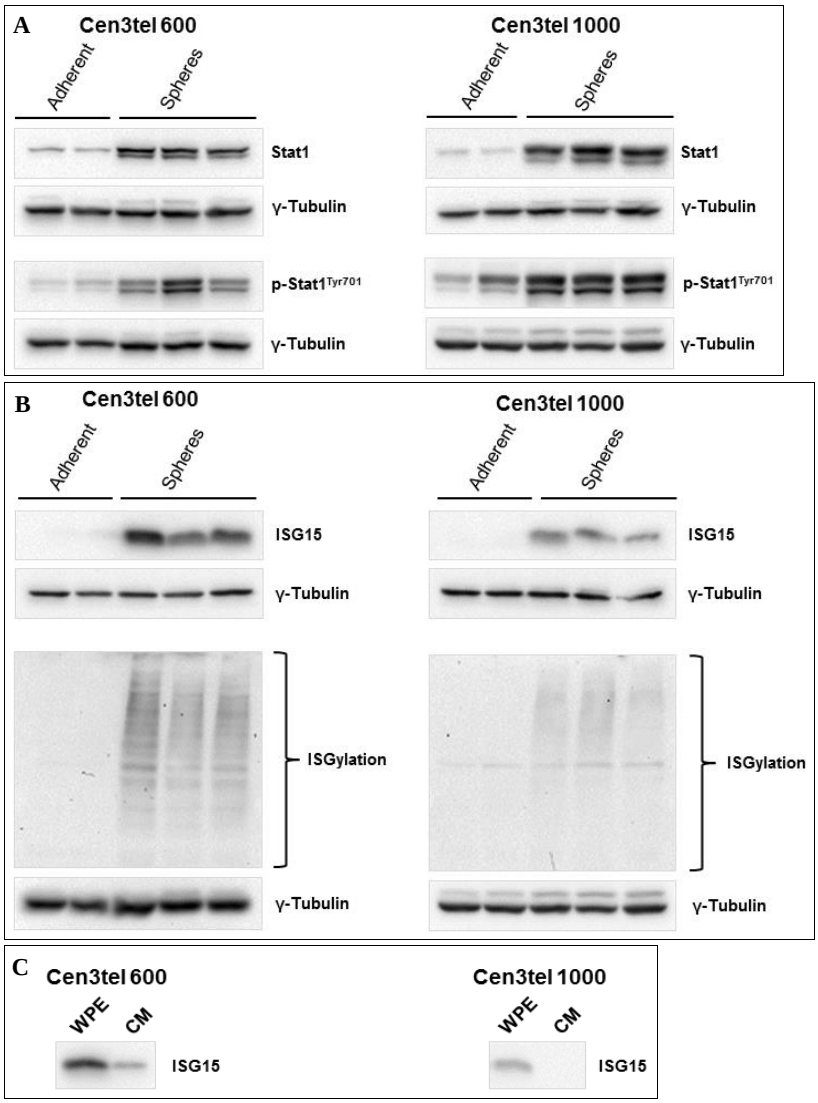

Figure 26. ISG15 and Stat1 expression in cen3tel 600 and 1000 sphere cells. Western blot analysis of the expression of Stat1 (**A**), ISG15 and ISGylated proteins (**B**) in cen3tel 600 and 1000 sphere cells and adherent cells. Phospho-Stat1^{Tyr701} is the active form of the transcription factor Stat1. (**C**) Analysis of the secretion of ISG15 in the culture medium (CM) of cen3tel 600 and 1000 sphere cells. The CM was processed as described in Materials and Methods and analyzed by western blotting with an antibody against ISG15; in the lane of the left, a sample of whole-protein extract (WPE) from sphere cells was loaded as positive control. γ-Tubulin expression was used as loading protein control.

By western blot analysis we confirmed ISG15 overexpression in sphere cells; as shown in Fig. 26 B, ISG15 is barely detectable in adherent cen3tel 600 and 1000 cells while is highly expressed in sphere cells, at a higher extent in cen3tel 600 spheres than in cen3tel 1000 spheres. A similar result was obtained analysing

protein ISGylation, which was much more prominent in sphere cells than in adherent cells and higher in cen3tel 600 spheres than in cen3tel 1000 spheres (Fig. 26 B). Thus in sphere cells there is the activation of a Stat1-ISG15 axis, which can have oncogenic potentiality (Forys et al. 2014).

As mentioned above, ISG15 can be secreted by the cells in the intercellular space. We thus tested whether ISG15 could be detected in the culture medium of sphere cells. The culture medium of cen3tel 600 and 1000 sphere cells was concentrated and analysed by western blotting with an anti-ISG15 antibody (see Materials and Methods). As shown in Fig. 26 C, a band corresponding to ISG15 was visible in the culture medium of cen3tel 600 sphere cells, but not of cen3tel 1000 cells, probably because it was under the detection limit.

Then, given that ISG15 can foster CSC generation (Sainz et al. 2014), we tested whether secreted ISG15 could promote sphere formation in cen3tel 600 and 1000 cells. We thus plated cen3tel cells in sphere forming medium in presence of 100 ng/mL of recombinant ISG15 and counted the number of spheres after 7 days of growth. As shown in Fig. 27, exogenous ISG15 has a modest but significant positive effect on sphere formation in both cen3tel 600 and 1000 cells.

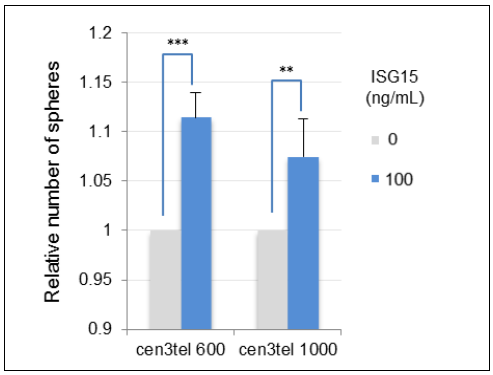

Figure 27. Exogenous ISG15 increases the sphere formation in cen3tel 600 and 1000 cells. Cen3tel 600 and 1000 cells were cultured in sphere-forming medium in the presence of 100 ng/mL ISG15. Spheres were counted 7 days after seeding. The number of spheres in ISG15-treated samples is reported relative to untreated samples. The data are the average of the results of three independent experiments. Error bars: standard deviations. **: $p < 0.01$; ***: $p < 0.005$.

4.15 Down-regulation of *ID1* and *ID3* in sphere cells

ID1 and *ID3* are transcription factors that play a role in the inhibition of the differentiation process and a positive role in self-renewal (Lasorella et al. 2014). Despite an up-regulation of these genes could be expected in sphere cells, microarray analysis revealed that these genes are down-regulated in both cen3tel 600 and 1000 sphere cells (Fig. 28 A and B). It is worthwhile mentioning that *ID1* and *ID3* were progressively down-regulated during neoplastic transformation of cen3tel cells, thus, in this cellular system, down-regulation of these genes might be functional to the tumorigenic capacity.

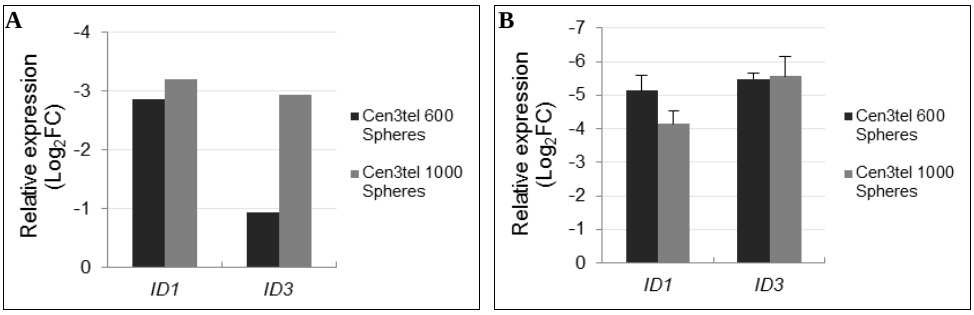

Figure 28. *ID1* and *ID3* expression in cen3tel 600 and 1000 spheres. (**A**) Expressions of *ID1* and *ID3* by microarray analysis. (**B**) RT-qPCR analysis of *ID1* and *ID3* expression in cen3tel 600 and 1000 spheres. The expression of each gene in sphere cells is indicated as Log_2FC relative to its expression in the corresponding adherent cells. Error bars: standard deviations.

5. Discussion

According to the CSC model, tumorigenesis is mainly driven by a subset of cancer cells with stemness properties and a high tumorigenic potential, which are able to initiate and sustain the hierarchical organization of tumors, similarly to stem cells in normal tissues (Medema, 2013). A key point of CSC biology regards CSC origin, an issue that is not well-defined and is still object of debate. CSCs can originate from neoplastic transformation of stem cells of the tissue of origin of the tumor (Reya et al. 2001), but recent findings indicate that CSCs may also derive from differentiated tumor cells through a genetic reprogramming that can induce their dedifferentiation toward a CSC-like phenotype (Schwitalla et al. 2013; Friedmann-Morvinski and Verma, 2014). Studies performed on *in vitro* transformed human cell lines have demonstrated that CSCs can also be generated *in vitro* after neoplastic transformation of differentiated human somatic cells (Scaffidi and Misteli, 2011; Chaffer et al. 2011; Friedmann-Morvinski et al. 2012), indicating a high plasticity of tumor cells.

In the work of this thesis, we used a cellular system of *in vitro* transformed human fibroblasts to study the heterogeneity of neoplastically transformed cell populations and the possible presence of cells with CSC features within these tumor cell populations. Here we show that *in vitro* transformed fibroblasts contain a subpopulation of cells able to form spheres when plated in the absence of serum and in the presence of growth factors, a capacity generally ascribed to cells with stemness features. Sphere cells were endowed with self renewal capability and showed an extensive variation in gene expression compared to the bulk of the populations, including genes involved in tumorigenesis and stemness. However, they showed only a limited increase in the tumorigenic potential compared to the bulk of the population.

We performed our study on cen3tel 600 and cen3tel 1000 cells, which represent two subsequent stages of transformation within the cen3tel cellular system, defined on the basis of the decreasing time required to develop tumors in immunocompromised mice. Respect to parental fibroblasts, cen3tel 1000 cells showed an increased modulation of the transcriptional program compared to cen3tel 600 cells; particular hallmarks of the more tumorigenic cen3tel 1000 cells were alterations in cell cycle, apoptosis, and cancer testis antigen gene expression (Belgiovine et al. 2010; Ostano et al. 2012). This system allowed us not only to study transcriptional variations associated with sphere formation, but also to verify whether and how the expression of the genes deregulated in spheres were modulated during the stepwise process of *in vitro* transformation.

Sox2, Oct-4 and Nanog are key transcription factors regulating stemness features in normal stem cells and are frequently found overexpressed in CSCs of several tumors (Hadjimichael et al. 2015). We thus analyzed the expression of the genes encoding for these factors in cen3tel 600 and 1000 sphere cells. By RT-qPCR analysis, we found that *POU5F1* and *NANOG* were expressed at similar levels in cen3tel 600 and 1000 tumorspheres and adherent cells, while *SOX2* was overexpressed in sphere cells. Moreover, by cytofluorimetric analysis, we showed

an enrichment in Sox2-positive cells in spheres compared to adherent cells, suggesting that spheres are enriched in cells with stemness features. Despite these stemness features, cen3tel sphere cells did not show an increased capacity to differentiate into adipocytes or osteoblasts compared to adherent cells, suggesting that multilineage differentiation capacity is a characteristic of the entire cen3tel population. However, it has to be pointed out that the differentiation assays require to seed cells in the presence of serum, thus it cannot be excluded that in these conditions sphere cells lose some of their features, including a peculiar differentiation capacity.

We then tested the expression in sphere cells of genes, as c-*MYC*, *NOTCH1*, *GNL3*, which are known to play an important role in stemness and tumorigenicity and are frequently found overexpressed in CSCs (Wang et al. 2008b; Abel et al. 2014; Tin et al. 2014), together with the expression of the tumorsuppressor microRNA miR-34a, which is often down-regulated in CSCs (Liu and Tang, 2011). There is evidence that these genes are able to cross-regulate their expression. Indeed, c-*MYC* has been identified as a transcriptional target of Notch1 (Satoh et al. 2004), while *GNL3* expression has been shown to be positively regulated by c-Myc (Zwolinska et al. 2012). MiR-34a can down-regulate *NOTCH1* (Li et al. 2009a; Bu et al. 2013) and undergoes a reciprocal negative regulation with c-*MYC* (Christoffersen et al. 2010; Yamamura et al. 2012a; Yamamura et al. 2012b; Chang et al. 2008). Surprisingly, we demonstrated that c-Myc, nucleostemin and Notch1 were down-regulated both in cen3tel 600 and 1000 sphere cells, while miR-34a was significantly up-regulated respect to adherently growing cells. In cen3tel spheres, we found that deregulation of these genes is actually concerted; in fact, all of them regained the pattern of expression observed in adherent cells when sphere cells were allowed differentiating in serum containing medium, while maintained the same pattern of expression when sphere cells where replated in sphere forming medium. These observations suggest that these genes are connected in a circuitry and probably act in the same functional process during sphere formation. Moreover, the reversibility of the deregulation of these genes indicates that their modulation is under the control of epigenetic mechanisms.

As far as the mechanism of c-*MYC*, *GNL3* and *NOTCH1* expression regulation in sphere cells is concerned, we demonstrated a significant transcriptional down-regulation for *GNL3* and c-*MYC*, while the level of *NOTCH1* transcription was not significantly lower in sphere cells than in adherent cells. Exposing adherent and sphere cells to the proteasome inhibitor MG-132, we found significant greater accumulation of Notch1 in sphere cells compared to adherent cells, suggesting that proteasomal degradation is increased in sphere cells and contributes to decrease the levels of this protein. A similar result was found for c-Myc, which thus seems to be subjected to multiple layers of expression regulation in spheres.

c-*MYC* is not only an oncogene, but participates also in the apoptotic process, acting as an apoptotic inducer (Hoffman and Liebermann, 2008). Thus, given its role as promoter of cell death, it is possible that the decreased c-Myc levels observed in sphere cells are functional to protect cells from apoptosis, in particular the cells located in the inner part of the spheres, which could receive less nutrient and/or oxygen given the compact structure of the spheres. Indeed, in sphere cells we did not find the presence of apoptotic markers, as the activated fragments of

caspase 9 and caspase 3 and the PARP-1 proteolytic fragment, while we found overexpression of the anti-apoptotic gene *BCL2A1*, both at transcriptional and protein level. Moreover, microarray analysis revealed a highly significant overrepresentation of GO processes related to the negative regulation of apoptosis in sphere cells compared to adherent cells. Recent evidence supports the hypothesis of a protective effect of c-Myc down-regulation against stressful conditions. Wong and colleagues (2013) demonstrated that low O_2 tension reduced c-Myc protein levels in colorectal cancer cell lines by increasing its ubiquitinilation and proteasomal degradation, in order to allow cell survival under hypoxic conditions. The decrease in Nucleostemin and Notch levels could also take part in restraining cellular proliferation or apoptosis in non-optimal growth conditions, given their positive activity in cell growth and apoptosis induction in some tumors (Tsai, 2014; Wael et al. 2014). Thus, we are tempted to speculate that the down-regulation of c-Myc, Notch1 and Nucleostemin and the up-regulation of miR-34a contribute to the activation of a survival mechanism that prevents sphere cell death; i*n vivo* this mechanism might contribute to protect cells that detach from the extracellular matrix from apoptosis, allowing them to grow in suspension and disseminate

To get a better insight into the molecular changes characterizing cen3tel 600 and 1000 tumorspheres and their possible relationship with the CSC phenotype, we determined genome-wide gene expression profiles of these cells compared to their parental adherent cells. By microarray analysis we found that sphere cells showed profound changes in the transcriptional program compared to their adherent counterparts, greater in cen3tel 600 sphere cells than in cen3tel 1000 sphere cells. As mentioned above, during transformation, cen3tel cells showed a progressive increase in the number of genes deregulated compared to parental fibroblasts and a particularly elevated increase was observed during the transition between cen3tel 600 and cen3tel 1000 cells, which also corresponds to the transition from non-metastatic to metastatic cells (Ostano et al. 2012). Cen3tel 600 sphere global transcription profiling was actually more similar to that of cen3tel 1000 adherent and sphere cells than to that of their adherent counterparts, suggesting that sphere cells tend to acquire features linked to more advanced stages of transformation.

In the analysis of the microarray results, we focused on the common transcriptional changes between cen3tel 600 and cen3tel 1000 sphere cells *vs* their corresponding adherent counterparts. Cen3tel 600 and 1000 sphere cells showed about 650 genes commonly up-regulated and about 150 commonly down-regulated.

A common feature of spheres derived from both cen3tel 600 and cen3tel 1000 cells was the up-regulation of several *MMP* genes and *Rnd3*, suggesting a transition towards a more mesenchymal phenotype in sphere cells compared to adherent cells. This observation is in agreement with several data of the literature indicating that, on one hand, CSCs frequently show the acquisition of mesenchymal traits and, on the other hand the induction of the epithelial-mesenchymal transition makes cells acquire a CSC phenotype (Mani et al. 2008). The knowledge of the transcriptional changes occurring during cen3tel transformation allowed us to show that the increase in *MMP* and *Rnd3* expression is actually a reversion towards a pattern of expression more similar to that of untransformed cells. This confirms once more the high plasticity of transformed

cells that can switch from one phenotype to the other, making it difficult to eliminate them by hitting specific targets.

Functional annotation on the lists of commonly deregulated genes in cen3tel 600 and 1000 tumorsphere cells identified several biological processes. The up-regulated genes identified significantly processes related to chromatin organization, cholesterol metabolism, negative regulation of apoptosis, immunity and inflammation.

Up-regulation of mevalonate/cholesterol metabolism genes is a main feature of cen3tel tumorspheres. A large body of evidence indicates that cholesterol metabolism is up-regulated in cancer (Kuzu et al. 2016), moreover, a peculiar up-regulation of these pathway was shown in cancer stem cells derived from different tumors. In particular, mevalonate metabolism appears to regulate cancer stem cells in basal breast cancer (Ginestier et al. 2012) and to play a role in the survival of pancreatic cancer CSCs (Brandi et al. 2016). Moreover, a meta-analysis on gene expression profiles from several studies that utilized tumorspheres to investigate tumor stem-like breast cancer cells showed up-regulation of *HMGCS1*, one of the first enzyme of the mevalonate/cholesterol biosynthetic pathways, as one of the main signatures for the identification of breast cancer stem cells (Lee et al. 2016b). As reported by Ginestier and coworkers (2012), we found that inhibition of the HMGCR enzyme led to a decrease in cen3tel sphere formation, rescued by the addition of mevalonate but not of cholesterol. This suggests that the activity of this enzyme is important for CSC generation, in particular through the generation of intermediates involved in branch metabolic pathways starting from mevalonate. In breast cancer, the protein geranylgeranylation pathway seems to be critical for CSC maintenance (Ginestier et al. 2012), further experiments have to be done to find out whether this holds true in cen3tel cells.

GO analysis on the up-regulated genes in tumorsphere cells using the Panther bioinformatics tool highlighted the overrepresentation of cytokine and chemokine mediated signaling pathway, suggesting a link between tumorsphere formation and inflammation/immune response. Although inflammation can have both a promoting and a restraining role in cancer, a large body of evidence indicates that chronic inflammation plays crucial roles at different phases of tumor development and is a hallmark of cancer (Grivennikov et al. 2010; Hanahan and Weinberg, 2011). Moreover, genes acting in this process are also involved in cancer stem cell induction and maintenance (Iliopoulos et al. 2011; Oh et al. 2016; Wang et al. 2016). Within this pathway, there are two genes among the most up-regulated in spheres, *IL13RA2* and *IL1B*, and *IL6*. The overexpression of *IL13RA2* is strongly associated with an increase in the metastatic potential of several cancers (Barderas et al. 2012; Zhao et al. 2015; Papageorgis et al. 2015), IL-6 has been shown to promote the conversion of bulk tumor cells into CSCs in *in vitro* transformed mammary cells, breast and prostate cancer cell lines (Iliopoulus et al. 2011; Kim et al. 2015), and regulate growth of lung cancer CSCs (Malanga et al. 2015). We found a significant increase in sphere formation in cen3tel 600 cells exposed to exogenous IL-6, while in cen3tel 1000 cells the increase was not significant. This indicates that *in vitro* transformed fibroblasts can respond to IL-6 increasing sphere formation capacity and IL-6 could be involved in the maintenance of CSC traits in cen3tel tumorspheres.

The *IL1B* gene is one of the most overexpressed genes in cen3tel 600 and 1000 sphere cells and, at the protein level, IL-1β is undetectable in adherent cells and highly expressed in sphere cells. However, this protein does not appear to be processed and secreted in sphere cells. In addition, when cen3tel 600 and cen3tel 1000 cells were seeded in sphere formation medium in the presence of recombinant mature IL-1β, the frequency of sphere formation was highly reduced. Despite the paradox of the overexpression of the IL-1β precursor form in spheres, on one hand, and the negative effect of mature IL-1β on sphere formation, on the other hand, the observation that the effect of IL-1β was much greater on sphere formation than on the viability of the bulk of the population opens up the possibility, to be further evaluated, that this cytokine could specifically interfere with the viability of cells with CSC features.

A strong transcriptional signature of tumorspheres is the overexpression of several genes related to the interferon response pathway, among which *ISG15* and *STAT1*. Although interferon-mediated responses have been classically associated with antiviral defense and tumor-suppressive functions, recent evidence indicates that interferon signaling could play an important role in promoting tumor cell survival and mediating tumor growth; furthermore, a link has been shown between deregulation of the expression of interferon pathway related genes, neoplastic transformation and cancer stem cells. For example, in glioblastoma multiforme, overexpression of eight genes belonging to the IFN pathway, including *ISG15* and *STAT1*, has been found predictive of poor prognosis (Duarte et al. 2012). In mouse embryonic fibroblasts, inactivation of p53 and ARF leads to cellular transformation and to the activation of a gene signature strongly associated with innate immune response, in particular to the overexpression of Stat1, which in turn up-regulates ISG15 (Forys et al. 2014). *ISG15* has recently been shown deregulated in several solid tumors (Andersen et al. 2006; Bektas et al. 2008; Li et al. 2014; Zuo et al. 2016). Moreover, pancreas ductal carcinoma stem cells, enriched through the tumorsphere technique, show an increase in ISG15 expression and protein ISGylation and respond to ISG15 secreted by tumor associated macrophages enhancing the CSC phenotype (Sainz et al. 2014). It is also worth mentioning that ISG15 is overexpressed in human fibroblasts undergoing reprogramming by ectopic transfection of Oct4, Sox2, Klf4 and c-Myc (Cai et al. 2015) and, in the stem cell fraction of mammospheres produced by normal human mammary glands, an increased ISG15 expression was found compared to their more differentiated progenitor cells, indicating a further link between ISG15 and stemness (Pece et al. 2010).

ISG15 is one of the most up-regulated IFN pathway genes in cen3tel 600 and 1000 spheres. At the protein level ISG15 was undetectable in adherent cells and its expression was generally higher in cen3tel 600 sphere samples than in spheres derived from cen3tel 1000 cells. The same type of signal distribution was found for ISGylated proteins, higher in cen3tel 600 spheres than in cen3tel 1000 ones. This difference might be due to a different percentage of ISG15 expressing cells in cen3tel 1000 spheres compared to cen3tel 600 ones. We also found that ISG15 was secreted by sphere cells; we detected the protein in the culture medium of cen3tel 600 spheres; in cen3tel 1000 sphere culture medium, ISG15 was not observed,

probably because it was under the limit of sensitivity of the technique we applied. Given the lower levels of ISG15 observed in cen3tel 1000 sphere cell extracts compared to cen3tel 600 sphere cells, it is plausible that ISG15 secretion also occurs in cen3tel 1000 sphere cells although at a lower extent than in cen3tel 600 sphere cells. We then showed that exogenous ISG15 increases sphere formation in both cen3tel cell populations. Thus, our observations confirm an involvement of ISG15 in CSC generation, as observed in pancreas ductal carcinomas and in nasopharyngeal carcinomas (Sainz et al. 2014; Chen et al. 2016), and suggest that ISG15 plays a crucial role in the maintenance of stemness properties of cen3tel tumorspheres.

A preliminary analysis of the down-regulated genes highlighted by microarray analysis revealed a decrease in the expression of *ID1* and *ID3* in sphere cells compared to adherent cells. This was a surprising observation since these genes encode two transcription factors involved in the inhibition of cellular differentiation programs and promotion of self-renewal in normal and cancer stem cells (Romero-Lanman et al. 2011; Lasorella et al. 2014). However, other works showed down-regulation of *ID1* and *ID3* in tumorspheres derived from different types of tumors, as for example breast and ovarian cancer (Kok et al. 2009; Wang et al. 2013c), lung cancer (Dubrovska et al. 2009) and prostate cancer (Duhagon et al. 2010), suggesting that, in particular genetic background, *ID1* and *ID3* can be dispensable for sphere cells self-renewal.

Finally, running GSEA (Gene Set Enrichment Analysis; see Materials and Methods) on the cen3tel sphere up-regulated gene list, we found a statistically significant enrichment in two genesets containing all the genes deregulated in ovarian and breast cancer tumorspheres (geneset "GSE43657", Wang et al. 2013c) and in prostate cancer tumorspheres (geneset "GSE10832", Dubrovska et al, 2009). Among the genes commonly up-regulated in these genesets and in cen3tel sphere cells there were genes involved in mevalonate/cholesterol metabolism, chromatin organization and interferon pathway, including *STAT1* and *ISG15*, indicating that the de-regulation of these genes is likely related to the CSC phenotype.

Taken together, the results presented so far indicate that cen3tel spheres are characterized by gene expression changes related to stemness and tumorigenesis. However, despite this molecular signature of sphere cells, the *in vivo* tumorigenicity experiments performed so far on cen3tel 600 sphere cells have shown only a modest increase in the tumorigenic capacity of these cells compared to their adherent counterparts. In particular, injecting a relatively small number of cells ($2.5x10^4$ or $5x10^4$), tumors induced by sphere cells appeared earlier than those induced by adherent cells, but afterwards both types of tumors developed with a similar growth rate. This observation might be explained by the heterogeneity of sphere cells, by the segregation of the CSC phenotype during sphere cell proliferation in mice and also by a possible negative interaction of sphere cells with the mouse microenvironment. However, it is also plausible that other subpopulations, besides those selected by the tumorsphere approach, can support tumorigenicity in *in vitro* transformed cell lines.

6. Conclusions and perspectives

In this study we have shown that *in vitro* transformed cen3tel cells are heterogeneous and plastic populations, containing a subset of cells endowed with the capacity to grow in suspension as spherical aggregates in the absence of serum and in the presence of specific growth factors, a peculiar feature of CSCs derived from several tumors. Tumorspheres derived from cen3tel cells express stemness traits, as self-renewal, and are characterized by profound changes in gene expression compared to cells grown in adhesion. Several genes deregulated in cen3tel sphere cells have been found involved in CSC genesis and maintenance in different tumors, suggesting that this cellular system can be a useful tool to investigate the CSC phenotype. Further studies could help to unravel the possible function of the genes and pathways deregulated in cen3tel sphere cells in CSC biology. In particular, further investigations on the cholesterol/mevalonate pathway could highlight pathway branches relevant to the CSC phenotype. Moreover, the analysis of spheres grown in the presence of ISG15 could allow the identification of pathways strengthening the CSC phenotype. In addition, the possible role of mature IL-1β in suppressing tumorsphere formation could be deepened analyzing its effects on different tumor cells. Finally, to get insights into the role of the biological processes associated with the list of the down-regulated genes in cen3tel sphere cells could give additional information on pathways linked to the CSC phenotype. Our results have also shown that cen3tel sphere cells are only moderately more tumorigenic than the bulk of the population, suggesting that different subpopulations of cen3tel cells could support tumor development *in vivo*, thus adding a further layer of complexity to tumor heterogeneity. Interestingly, the results obtained by microarray analysis indicate that cen3tel 600 spheres show gene expression profiles closer to the metastatic cen3tel 1000 cells than to their adherent counterpart, suggesting that cen3tel 600 sphere cells could express metastatic ability. In this regard, it will be interesting to test the metastatic potential of cen3tel 600 sphere cells *in vivo*. In conclusion, our results indicate that differentiated cells undergoing oncogenic transformation can acquire CSC properties, supporting the hypothesis that bulk tumor cells are plastic entities able to switch between different phenotypes. However, the "CSC phenotype" is not necessarily linked to a clear increase in tumorigenicity, indicating the possibility that different tumor subpopulations must be identified and hit to defeat tumors.

References

Abel EV, Kim EJ, Wu J, Hynes M, Bednar F, Proctor E, et al. The Notch pathway is important in maintaining the cancer stem cell population in pancreatic cancer. PLoS One. 2014;9:e91983.

d'Adda di Fagagna F. Living on a break: cellular senescence as a DNA-damage response. Nat Rev Cancer. 2008 Jul;8:512-522.

Al-Hajj M, Wicha MS, Benito-Hernandez A, Morrison SJ and Clarke MF. Prospective identification of tumorigenic breast cancer cells. Proc Natl Acad Sci U S A. 2003 Apr 1;100(7):3983-3988.

Amsterdam A, Raanan C, Schreiber L, Freyhan O, Schechtman L and Givol D. Localization of the stem cell markers LGR5 and Nanog in the normal and the cancerous human ovary and their inter-relationship. Acta Histochem. 2013;115:330-338.

Andersen JB, Aaboe M, Borden EC, Goloubeva OG, Hassel BA and Orntoft TF. Stage-associated overexpression of the ubiquitin-like protein, ISG15, in bladder cancer. Br J Cancer. 2006;94:1465-1471.

Artavanis-Tsakonas S, Rand MD and Lake RJ. Notch signaling: cell fate control and signal integration in development. Science. 1999;284:770-776.

Atlasi Y, Mowla SJ, Ziaee SA and Bahrami AR. OCT-4, an embryonic stem cell marker, is highly expressed in bladder cancer. Int J Cancer. 2007;120:1598-1602.

Baker AM, Cereser B, Melton S, Fletcher AG, Rodriguez-Justo M, tadrous PJ, et al. Quantification of crypt and stem cell evolution in the normal and neoplastic human colon. Cell Rep. 2014;8:940–947

Balbous A, Cortes U, Guilloteau K, Villalva C, Flamant S, Gaillard A, et al. A mesenchymal glioma stem cell profile is related to clinical outcome. Oncogenesis. 2014;3:e91.

Balkwill F and Mantovani A. Inflammation and cancer: back to Virchow? Lancet. 2001;357:539-545.

Bapat SA, Mali AM, Koppikar CB and Kurrey NK. Stem and progenitor-like cells contribute to the aggressive behavior of human epithelial ovarian cancer. Cancer Res. 2005;65:3025-3029.

Bao S, Wu Q, McLendon RE, Hao Y, Shi Q, Hjelmeland AB, et al. Glioma stem cells promote radioresistance by preferential activation of the DNA damage response. Nature. 2006;444:756–60.

Bao L, Cardiff RD, Steinbach P, Messer KS, Ellies LG. Multipotent luminal mammary cancer stem cells model tumor heterogeneity. Breast Cancer Res. 2015;17:137.

Barderas R, Bartolomé RA, Fernandez-Aceñero MJ, Torres S and Casal JI. High expression of IL-13 receptor α2 in colorectal cancer is associated with invasion, liver metastasis, and poor prognosis. Cancer Res. 2012;72:2780-2790.

Barker N, Ridgway RA, van Es JH, van de Wetering M, Begthel H, van den Born M, et al. Crypt stem cells as the cells-of-origin of intestinal cancer. Nature. 2009;457:608-611.

Barriere G, Fici P, Gallerani G, Fabbri F, Zoli W, Riqaud M. Circulating tumor cells and epithelial, mesenchymal and stemness markers: characterization of cell subpopulations. Ann Transl Med. 2014;2:109.

Basu-Roy U, Seo E, Ramanathapuram L, Rapp TB, Perry JA, Orkin SH, et al. Sox2 maintains self-renewal of tumor-initiating cells in osteosarcomas. Oncogene. 2012;31:2270-2282.

Beier D, Hau P, Proescholdt M, Lohmeier A, Wischhusen J, Oefner PJ, et al. CD133(+) and CD133(−) glioblastoma-derived cancer stem cells show differential growth characteristics and molecular profiles. Cancer Res. 2007;67:4010-4015.

Bektas N, Noetzel E, Veeck J, Press MF, Kristiansen G, Naami A, et al. The ubiquitin-like molecule interferon-stimulated gene 15 (ISG15) is a potential prognostic marker in human breast cancer. Breast Cancer Res. 2008;10:R58.

Belgiovine C, Frapolli R, Bonezzi K, Chiodi I, Favero F, Mello-Grand M, et al. Reduced expression of the ROCK inhibitor Rnd3 is associated with increased invasiveness and metastatic potential in mesenchymal tumor cells. PLoS One. 2010;5:e14154.

Beltran AS, Rivenbark AG, Richardson BT, Yuan X, Quian H, Hunt JP, et al. Generation of tumor-initiating cells by exogenous delivery of OCT4 transcription factor. Breast Cancer Res. 2011;13:R94.

Ben-Porath I, Thomson MW, Carey VJ, Ge R, Bell GW, Regev A et al. An embryonic stem cell-like gene expression signature in poorly differentiated aggressive human tumors. Nat Genet. 2008;40:499-507.

Benjamini Y and Hochberg Y. Controlling the false discovery rate: a practical and powerful approach to multiple testing. J R Stat Soc B. 1995;57:289–300.

Bhagwandin VJ, Bishop JM, Wright WE and Shay JW. The metastatic potential and chemoresistance of human pancreatic cancer stem cells. PLoS ONE. 2016;11:e0148807.

Blaylock RL. Cancer microenvironment, inflammation and cancer stem cells: A hypothesis for a paradigm change and new targets in cancer control. Surg Neurol Int. 2015;6:92.

Bonnet D and Dick JE. Human acute myeloid leukemia is organized as a hierarchy that originates from a primitive hematopoietic cell. Nat Med. 1997;3:730-737.

Borah A, Raveendran S, Rochani A, Maekawa T and Kumar DS. Targeting self-renewal pathways in cancer stem cells: clinical implications for cancer therapy. Oncogenesis. 2015;4:e177.

Bourillot PY and Savatier P. Krüppel-like transcription factors and control of pluripotency. BMC Biol. 2010;8:125.

Boyer LA, Lee TI, Cole MF, Johnstone SE, Levine SS, Zucker JP, et al. Core transcriptional regulatory circuitry in human embryonic stem cells. Cell. 2005; 122:947-956.

Boyer LA, Plath K, Zeitlinger J, Brambrink T, Medeiros LA, Lee TI, et al. Polycomb complexes repress developmental regulators in murine embryonic stem cells. Nature. 2006; 441:349-353.

Brabletz T. EMT and MET in metastasis: where are the cancer stem cells? Cancer Cell. 2012;22:699-701.

Brandi J, Dando I, Pozza ED, Biondani G, Jenkins R, Elliott V, et al. Proteomic analysis of pancreatic cancer stem cells: Functional role of fatty acid synthesis and mevalonate pathways. J Proteomics. 2016.pii: S1874-3919:30441-30449.

Bretones G, Delgado MD, León J. Myc and cell cycle control. Biochim Biophys Acta. 2015;1849:506-516.

Brocks D, Assenov Y, Minner S, Bogatyrova O, Simon R, Koop C, et al. Intratumor DNA methylation heterogeneity reflects clonal evolution in aggressive prostate cancer. Cell Rep. 2014;8:798-806.

Brugarolas J. Molecular genetics of clear-cell renal cell carcinoma. J Clin Oncol. 2014;32:1968-1976.

Bu P, Chen KY, Chen JH, Wang L, Walters J, Shin YJ, et al. A microRNA miR-34a-regulated bimodal switch targets Notch in colon cancer stem cells. Cell Stem Cell. 2013;12:602-615.

Burkhart DL and Sage J. Cellular mechanisms of tumour suppression by the retinoblastoma gene. Nat. Rev. Cancer 2008;8:671–682.

Burrell RA, McGranahan N, Bartek J and Swanton C. The causes and consequences of genetic heterogeneity in cancer evolution. Nature. 2013;501:338-345.

Bussolati B, Bruno S, Grange C, Ferrando U and Camussi G. Identification of a tumor-initiating stem cell population in human renal carcinomas. FASEB J. 2008;22:3696–3705.

Cabarcas SM, Mathews LA ans Farrar WL. The cancer stem cell niche—there goes the neighborhood? Int J Cancer. 2011;129:2315–2327.

Cabrera MC, Hollingsworth RE and Hurt EM. Cancer stem cell plasticity and tumor hierarchy. World J Stem Cells. 2015;7:27-36.

Cai Y, Dai X, Zhang Q and Dai Z. Gene expression of OCT4, SOX2, KLF4 and MYC (OSKM) induced pluripotent stem cells: identification for potential mechanisms. Diagn Pathol. 2015;10:35.

Campbell PJ, Yachida S, Mudie LJ, Stephens PJ, Pleasance ED, Stebbings LA, et al. The patterns and dynamics of genomic instability in metastatic pancre- atic cancer. Nature 2010;467:1109–1113.

Campisi J. Aging, cellular senescence, and cancer. Annu Rev Physiol. 2013;75:685–705.

Camussi G, Deregibus MC and Tetta C. Tumor-derived microvesicles and the cancer microenvironment. Curr Mol Med. 2013;13:58-67.

Cao L, Zhou Y, Zhai B, Liao J, Xu W, Zhang R, et al. Sphere-forming cell subpopulations with cancer stem cell properties in human hepatoma cell lines. BMC Gastroenterol. 2011;11:71.

Cao H, Zhang J, Liu H, Wan L, Zhang H, Huang Q, et al. IL-13/STAT6 signaling plays a critical role in the epithelial-mesenchymal transition of colorectal cancer cells. Oncotarget. 2016 Aug 13.

Chaffer C, Brueckmann I, Scheel C, Kaestli A, Wiggins P, Rodrigues L, et al. Normal and neoplastic nonstem cells can spontaneously convert to a stem-like state. Proc. Natl. Acad. Sci. U.S.A., 2011;108:7950–7955.

Chang T-CC, Yu D, Lee Y-SS, Wentzel EA, Arking DE, West KM, et al. Widespread microRNA repression by Myc contributes to tumorigenesis. Nat. Genet. 2008;40:43–50.

Charafe-Jauffret E, Ginestier C, Iovino F, Tarpin C, Diebel M, Esterni B, et al. Aldehyde dehydrogenase 1-positive cancer stem cells mediate metastasis and poor clinical outcome in inflammatory breast cancer. Clin Cancer Res. 2010;16:45-55.

Charles N and Holland EC. The perivascular niche microenvironment in brain tumor progression. Cell Cycle. 2010;9:3012–3021.

Chen J, Li Y, Yu TS, McKay RM, Burns DK, Kernie SG, et al. A restricted cell population propagates glioblastoma growth after chemotherapy. Nature. 2012; 488:522-526.

Chen X, Xu H, Yuan P, Fang F, Huss M, Vega VB, et al. Integration of external signaling pathways with the core transcriptional network in embryonic stem cells. Cell. 2008a;133:1106-1117.

Chen YC, Hsu HS, Chen YW, Tsai TH, How CK, Wang CY, et al. Oct-4 expression maintained cancer stem-like properties in lung cancer-derived CD133-positive cells. PLoS One. 2008b;3:e2637.

Chen F, Zhuang X, Lin L, Yu P, Wang Y, Shi Y, et al. New horizons in tumor microenvironment biology: challenges and opportunities. BMC Med. 2015;13:45.

Chen RH, Du Y, Han P, Wang HB, Liang FY, Feng GK, et al. ISG15 predicts poor prognosis and promotes cancer stem cell phenotype in nasopharyngeal carcinoma. Oncotarget. 2016 Mar 29;7:16910-16922.

Cheng N, Chytil A, Shyr Y, Joly A and Moses HL. Transforming growth factor-beta signaling-deficient fibroblasts enhance hepatocyte growth factor signaling in mammary carcinoma cells to promote scattering and invasion. Mol Cancer Res. 2008;6:1521-1533.

Cheng Y, Cheung AK, Ko JM, Phoon YP, Chiu PM, Lo PH, et al. Physiological β-catenin signaling controls self-renewal networks and generation of stem-like cells from nasopharyngeal carcinoma. BMC Cell Biol. 2013;14:44.

Chiba T, Kita K, Zheng YW et al. Side population purified from hepatocellular carcinoma cells harbors cancer stem cell- like properties. Hepatology. 2006;44:240-251.

Chiba T, Zheng YW, Kita K, Yokosuka O, Saisho H, Onodera M, et al. Enhanced self-renewal capability in hepatic stem/progenitor cells drives cancer initiation. Gastroenterology 2007;133:937-950.

Chiodi I, Belgiovine C, Zongaro S, Ricotti R, Horard B, Lossani A, et al. Super-telomeres in transformed human fibroblasts. Biochim. Biophys. Acta. 2013;1833:1885–1893.

Chiou SH, Yu CC, Huang CY, Lin SC, Liu CJ, Tsai TH, et al. Positive correlations of Oct-4 and Nanog in oral cancer stem-like cells and high-grade oral squamous cell carcinoma. Clin Cancer Res. 2008;14:4085-4095.

Chiou SH, Wang ML, Chou YT, Chen CJ, Hong CF, Hsieh WJ, et al. Coexpression of Oct4 and Nanog enhances malignancy in lung adenocarcinoma by inducing cancer stem cell-like properties and epithelial-mesenchymal transdifferentiation. Cancer Res. 2010;70:10433–10444.

Christoffersen NR, Shalgi R, Frankel LB, Leucci E, Lees M, Klausen M, et al. p53-independent upregulation of miR-34a during oncogene-induced senescence represses MYC. *Cell Death Differ*.2010;17:236–45.

Civenni G, Malek A, Albino D, Garcia-Escudero R, Napoli S, Di Marco S, et al. RNAi-mediated silencing of Myc transcription inhibits stem-like cell maintenance and tumorigenicity in prostate cancer. Cancer Res. 2013;73:6816-6827.

Clement V, Sanchez P, de Tribolet N, Radovanovic I and Ruiz i Altaba A. HEDGEHOG-GLI1 signaling regulates human glioma growth, cancer stem cell self-renewal, and tumorigenicity. Curr Biol. 2007;17:165-172.

Clevers H. The cancer stem cell: premises, promises and challenges. Nature Medicine. 2011;17:313-319.

Cole MD and Henriksson M. 25 years of the c-Myc oncogene. Semin Cancer Biol. 2006;16:241.

Collins AT, Berry PA, Hyde C, Stower MJ and Maitland NJ. Prospective identification of tumorigenic prostate cancer stem cells. Cancer Res. 2005;65:10946-10951.

Cooper GM. Elements of Human Cancer. Jones and Bartlett Publishers, Boston. 1992.

Coussens LM and Werb Z. Inflammation and cancer. Nature. 2002;420:860-867.

Croce CM. Oncogenes and cancer. N Engl J Med. 2008;358:502-511.

Croker AK and Allan AL. Inhibition of aldehyde dehydrogenase (ALDH) activity reduces chemotherapy and radiation resistance of stem-like ALDHhiCD44+ human breast cancer cells. Breast Cancer Res Treat. 2012;133:75-87.

Cuiffo BG, Campagne A, Bell GW, Lembo A, Orso F, Lien EC, et al. MSC-regulated microRNAs converge on the transcription factor FOXP2 and promote breast cancer metastasis. Cell Stem Cell. 2014;15:762-774.

Dalerba P, Dylla SJ, Park IK, Liu R, Wang X, Cho RW, et al. Phenotypic characterization of human colorectal cancer stem cells. Proc Natl Acad Sci U S A. 2007;104:10158-10163.

Dando I, Dalla Pozza E, Biondani G, Cordani M, Palmieri M and Donadelli M. The metabolic landscape of cancer stem cells. IUBMB Life. 2015;67(9):6.

Davies MA and Samuels Y. Analysis of the genome to personalize therapy for melanoma. Oncogene 2010;29:5545–5555.

Deaglio S, Vaisitti T, Aydin S, Bergui L, D'Arena G, Bonello L, et al. CD38 and ZAP-70 are functionally linked and mark CLL cells with high migratory potential. Blood. 2007;110:4012-4021.

Decker T, Müller M and Stockinger S. The yin and yang of type I interferon activity in bacterial infection. Nat. Rev. Immunol. 2005;5:675–687.

DeNardo DG, Andreu P and Coussens LM. Interactions between lymphocytes and myeloid cells regulate pro- versus anti-tumor immunity. Cancer Metastasis Rev. 2010;29:309–316.

DI C and Zhao Y. Multiple drug resistance due to resistance to stem cells and stem cell treatment progress in cancer (Review). Exp Ther Med. 2015;9:289-293.

Dick JE. Stem cell concepts renew cancer research. Blood. 2008;112:4793-4807.

Diehn M, Cho RW, Lobo NA, Kalisky T, Dorie MJ, Kulp AN, et al. Association of reactive oxygen species levels and radioresistance in cancer stem cells. Nature. 2009;458:780-783.

Dierks C, Beigi R, Guo GR, Zirlik K, Stegert MR, Manley P, et al. Expansion of Bcr-Abl-positive leukemic stem cells is dependent on Hedgehog pathway activation. Cancer Cell. 2008;14:238-249.

Ding DC, Liu HW and Chu TY. Interleukin-6 from Ovarian Mesenchymal Stem Cells Promotes Proliferation, Sphere and Colony Formation and Tumorigenesis of an Ovarian Cancer Cell Line SKOV3. J Cancer. 2016;7:1815-1823.

Dirks PB. Cancer: stem cells and brain tumours. Nature. 2006;444:687-688.

Donà F, Chiodi I, Belgiovine C, Raineri T, Ricotti R, Mondello C, et al. Poly(ADP-ribosylation) and neoplastic transformation: effect of PARP inhibitors. Curr Pharm Biotechnol. 2013;14:524-536.

Dreesen O and Brivanlou AH. Signaling pathways in cancer and embryonic stem cells. Stem Cell Rev. 2007;3:7–17.

Du L, Wang H, He L, Zhang J, Ni B, Wang X, et al. CD44 is of functional importance for colorectal cancer stem cells. Clin Cancer Res. 2008;14:6751-6760.

Duarte CW, Willey CD, Zhi D, Cui X, Harris JJ, Vaughan LK, et al. Expression signature of IFN/STAT1 signaling genes predicts poor survival outcome in glioblastoma multiforme in a subtype-specific manner. PLoS One. 2012;7:e29653.

Dubrovska A, Kim S, Salamone RJ, Walker JR, Maira SM, García-Echeverría C, et al. The role of PTEN/Akt/PI3K signaling in the maintenance and viability of prostate cancer stem-like cell populations. Proc Natl Acad Sci U S A. 2009;106:268-273.

Duhagon MA, Hurt EM, Sotelo-Silveira JR, Zhang X and Farrar WL. Genomic profiling of tumor initiating prostatospheres. BMC Genomics. 2010;11:324.

Easwaran H, Tsai HC and Baylin SB. Cancer epigenetics: tumor heterogeneity, plasticity of stem-like states, and drug resistance. Mol Cell. 2014;54:716-727.

Emlet DR, Gupta P, Holgado-Madruga M, Del Vecchio CA, Mitra SS, Han SY, et al. Targeting a glioblastoma cancer stem-cell population defined by EGF receptor variant III. Cancer Res. 2014;74:1238-1249.

Eppert K, Takenaka K, Lechman ER, Waldron L, Nilsson B, van Galen P, et al. Stem cell gene expression programs influence clinical outcome in human leukemia. Nat Med. 2011;17:1086–1093.

Eramo A, Lotti F, Sette G, Pilozzi E, Biffoni M, Di Virgilio A, et al. Identification and expansion of the tumorigenic lung cancer stem cell population. Cell Death Differ. 2008;15:504–514.

Evan GI, Wyllie AH, Gilbert CS, Littlewood TD, Land H, Brooks M, et al. Induction of apoptosis in fibroblasts by c-myc protein. Cell. 1992;69:119-128.

Fang D, Nguyen TK, Leishear K, Finko R, Kulp AN, Hotz S, et al. A tumorigenic sub- population with stem cell properties in melanomas. Cancer Res 2005;65:9328–9337.

Farnie G, Clarke RB, Spence K, Pinnock N, Brennan K, Anderson NG, et al. Novel cell culture technique for primary ductal carcinoma in situ: Role of Notch and

EGF receptor signaling pathways. Journal of the National Cancer Institute, 2007;99:616–627.

Farnie G, Sotgia F and Lisanti MP. High mitochondrial mass identifies a sub-population of stem-like cancer cells that are chemo-resistant. Oncotarget. 2015;6:30472–30486.

Feldmann G, Dhara S, Fendrich V, Bedja D, Beaty R, Mullendore M, et al. Blockade of hedgehog signaling inhibits pancreatic cancer invasion and metastases: a new paradigm for combination therapy in solid cancers. Cancer Res. 2007; 67:2187-2196.

Fernald K and Kurokawa M. Evading apoptosis in cancer. Trands Cell Biol. 2013;23:620:633.

Fessler E, Borovski T and Medema JP. Endothelial cells induce cancer stem cell features in differentiated glioblastoma cells via bFGF. Mol Cancer. 2015;14:157.

Fialkow PJ, Denman AM, Jacobson RJ, Lowenthal MN. Chronic myelocytic leukemia. Origin of some lymphocytes from leukemic stem cells. J Clin Invest. 1978;62:815-823.

Forys JT, Kuzmicki CE, Saporita AJ, Winkeler CL, Maggi LB Jr and Weber JD. ARF and p53 coordinate tumor suppression of an oncogenic IFN-β-STAT1-ISG15 signaling axis. Cell Rep. 2014;7:514-526.

Friedmann-Morvinski D, Bushong EA, Ke E, Soda Y, Marumoto T, Singer O, et al. Dedifferentiation of neurons and astrocytes by oncogenes can induce gliomas in mice. Science. 2012;338:1080-1084.

Friedmann-Morvinski D and Verma IM. Dedifferentiation and reprogramming: origins of cancer stem cells. EMBO Rep. 2014;15:244-253.

Gajewski TF, Schreiber H and Fu YX. Innate and adaptive immune cells in the tumor microenvironment. Nat Immunol. 2013;14:1014-1022.

Galli R, Binda E, Orfanelli U, Cipelletti B, Gritti A, De Vitis S, et al. Isolation and characterization of tumorigenic, stem-like neural precursors from human glioblastoma. Cancer Res. 2004;64:7011-7021.

Garzia L, Andolfo I, Cusanelli E, Marino N, Petrosino G, De Martino D, et al. MicroRNA-199b-5p impairs cancer stem cells through negative regulation of HES1 in medulloblastoma. PLoS One. 2009;4:e4998.

Gatenby RA and Gillies RJ. A microenvironmental model of carcinogenesis. Nat Rev Cancer. 2008;8:56-61.

Gatto F, Nookaew I and Nielsen J. Chromosome 3p loss of heterozygosity is associated with a unique metabolic network in clear cell renal carcinoma. Proc Natl Acad Sci U S A. 2014;111:E866-E875.

Gauthaman K, Fong CY and Bongso A. Statins, stem cells, and cancer. J Cell Biochem. 2009 ;106:975-983.

Gedye C, Davidson AJ, Elmes MR, Cebon J, Bolton D and Davis ID. Cancer stem cells in urologic cancers. Urol Oncol. 2010;28:585-590.

Gedye C, Sirskyj D, Lobo NC, Meens J, Hyatt E, Robinette M, et al. Cancer stem cells are underestimated by standard experimental methods in clear cell renal cell carcinoma. Sci Rep. 2016;6:25220.

Gentleman RC, Carey VJ, Bates DM, Bolstad B, Dettling M, Dudoit S, et al. Bioconductor: open software development for computational biology and bioinformatics. Genome Biol. 2004;5:R80.

Gerlinger M, Rowan AJ, Horswell S, Larkin J, Endesfelder D, Gronroos E, et al. Intratumor heterogeneity and branched evolution revealed by multiregion sequencing. N Engl J Med. 2012;366:883-892.

Gerlinger M, Horswell S, Larkin J, Rowan AJ, Salm MP, Varela I, et al. Genomic architecture and evolution of clear cell renal cell carcinomas defined by multiregion sequencing. Nat Genet. 2014 ;46:225-233.

Gibbs CP1, Kukekov VG, Reith JD, Tchigrinova O, Suslov ON, Scott EW, et al. Stem-Like Cells in Bone Sarcomas: Implications for Tumorigenesis. Neoplasia. 2005;7:967-976.

Gillies RJ, Flowers CI, Drukteinis JS and Gatenby RA. A unifying theory of carcinogenesis, and why targeted therapy doesn't work. Eur J Radiol. 2012;81 Suppl 1:S48-50.

Ginestier C, Wicinski J, Cervera N, Monville F, Finetti P, Bertucci F,et al. Retinoid signaling regulates breast cancer stem cell differentiation. Cell cycle (Georgetown, Tex.). 2009;8:3297–3302.

Ginestier C, Monville F, Wicinski J, Cabaud O, Cervera N, Josselin E, et al. Mevalonate metabolism regulates Basal breast cancer stem cells and is a potential therapeutic target. Stem Cells. 2012;30:1327-1337.

Goardon N, Marchi E, Atzberger A, Quek L, Schuh A, Soneji S, et al. Coexistence of LMPP-like and GMP-like leukemia stem cells in acute myeloid leukemia. Cancer Cell. 2011;19:138–152.

Goldstein AS, Huang J, Guo C, Garraway IP and Witte ON. Identification of a cell of origin for human prostate cancer. Science. 2010;329:568-571.

Golebiewska A, Brons NHC, Bjerkvig R and Niclou SP. Critical appraisal of the side population assay in stemcell and cancer stem cell research. Cell Stem Cell. 2011;8:136–147.

Greaves M and Maley CC. Clonal evolution in cancer. Nature. 2012;481:306-313.

Greve B, Kelsch R, Spaniol K, Eich HT and Götte M. Flow cytometry in cancer stem cell analysis and separation. Cytometry Part A. 2012;81:284–293.

Grimshaw MJ, Cooper L, Papazisis K, Coleman JA, Bohnenkamp HR, Chiapero-Stanke L, et al. Mammosphere culture of metastatic breast cancer cells enriches for tumorigenic breast cancer cells. Breast Cancer Res. 2008;10:R52.

Grivennikov SI, Greten FR and Karin M. Immunity, inflammation, and cancer. Cell. 2010;140:883-899.

Gunther HS, Schmidt NO, Phillips HS, Kemming D, Kharbanda S, Soriano R, et al. Glioblastoma-derived stem cell-enriched cultures form distinct subgroups according to molecular and phenotypic criteria. Oncogene. 2007.

Gupta R, Forloni M, Bisserier M, Dogra SK, Yang Q and Wajapeyee N. Interferon alpha-inducible protein 6 regulates NRASQ61K-induced melanomagenesis and growth. Elife. 2016;5.pii:e16432.

Hadjimichael C, Chanoumidou K, Papadopoulou N, Arampatzi P, Papamatheakis J and Kretsovali A. Common stemness regulators of embryonic and cancer stem cells. World J Stem Cells. 2015;7:1150–1184.

Hahn WC. Immortalization and transformation of human cells. Mol Cells. 2002;13:351-361.

Hanahan D and Weinberg RA. Hallmarks of cancer: the next generation. Cell. 2011;144:646-674.

Hanahan D and Folkman J. Patterns and emerging mechanisms of the angiogenic switch during tumorigenesis. Cell. 1996;86:353-364.

Hayes J, Peruzzi PP and Lawler S. MicroRNAs in cancer: biomarkers, functions and therapy. Trends Mol Med. 2014;20:460-469.

He A, Qi W, Huang Y, Feng T, Chen J, Sun Y, et al. CD133 expression predicts lung metastasis and poor prognosis in osteosarcoma patients: A clinical and experimental study. Exp Ther Med. 2012;4:435–441.

Held MA, Curley DP, Dankort D, McMahon M, Muthusamy V, Bosenberg MW. Characterization of melanoma cells capable of propagating tumors from a single cell. Cancer Res. 2010;70:388-397.

Hermann PC, Huber SL, Herrler T, Aicher A, Ellwart JW, Guba M, et al. Distinct populations of cancer stem cells determine tumor growth and metastatic activity in human pancreatic cancer. Cell Stem Cell. 2007;1:313–323.

Herreros-Villanueva M, Zhang JS, Koenig A, Abel EV, Smyrk TC, Bamlet WR, et al. SOX2 promotes dedifferentiation and imparts stem cell-like features to pancreatic cancer cells. Oncogenesis. 2013 2:e61.

Hirschhaeuser F, Menne H, Dittfeld C, West J, Mueller-Klieser W and Kunz-Schughart LA. Multicellular tumor spheroids: an underestimated tool is catching up again. J Biotechnol. 2010;148:3-15.

Hjelmeland AB and Rich JN. The quest for self-identity: not all cancer stem cells are the same. Clin Cancer Res. 2012;18:3495-3498.

Ho MM, Ng AV, Lam S and Hung JY. Side population in human lung cancer cell lines and tumors is enriched with stem-like cancer cells. Cancer Res. 2007;67:4827-4833.

Hoffman B and Liebermann DA. Apoptotic signaling by c-MYC. Oncogene. 2008;27:6462-6472.

Hu T, Liu S, Breiter DR, Wang F, Tang Y and Sun S. Octamer 4 small interfering RNA results in cancer stem cell-like cell apoptosis. Cancer Res. 2008;68:6533-6540.

Hwang-Verslues WW, Kuo WH, Chang PH, Pan CC, Wang HH, Tsai ST, et al. Multiple lineages of human breast cancer stem/progenitor cells identified by profiling with stem cell markers. PLoS One. 2009;4:e8377.

Ibrahim EE, Babaei-Jadidi R, Saadeddin A, Spencer-Dene B, Hossaini S, Abuzinadah M, et al. Embryonic NANOG activity defines colorectal cancer stem cells and modulates through AP1- and TCF-dependent mechanisms. Stem Cells. 2012;30:2076–2087.

Ignatova TN, Kukekov VG, Laywell ED, Suslov ON, Vrionis FD and Steindler DA. Human cortical glial tumors contain neural stem-like cells expressing astroglial and neuronal markers in vitro. Glia. 2002;39:193-206.

Iliopoulos D, Lindahl-Allen M, Polytarchou C, Hirsch HA, Tsichlis PN and Struhl K. Loss of miR-200 inhibition of Suz12 leads to polycomb-mediated repression required for the formation and maintenance of cancer stem cells. Mol Cell. 2010;39:761-772.

Iliopoulos D, Hirsch HA, Wang G and Struhl K. Inducible formation of breast cancer stem cells and their dynamic equilibrium with non-stem cancer cells via IL6 secretion. Proc Natl Acad Sci U S A. 2011;108:1397-1402.

Inoue A, Takahashi H, Harada H, Kohno S, Ohue S, Kobayashi K, et al. Cancer stem-like cells of glioblastoma characteristically express MMP-13 and display highly invasive activity. Int J Oncol. 2010;37:1121-1131.

Ishikawa F, Yoshida S, Saito Y, Hijikata A, Kitamura H, Tanaka S, et al. Chemotherapy-resistant human AML stem cells home to and engraft within the bone-marrow endosteal region. Nat Biotechnol. 2007;25:1315–1321

Ivashkiv LB and Donlin LT. Regulation of type I interferon responses. Nat Rev Immunol. 2014;14:36-49.

Iwamoto FM, Abrey LE, Beal K, Gutin PH, Rosenblum MK, Reuter VE, et al. Patterns of relapse and prognosis after bevacizumab failure in recurrent glioblastoma. Neurology. 2009;73:1200-1206.

Jaenisch R and Young R. Stem cells, the molecular circuitry of pluripotency and nuclear reprogramming. Cell. 2008; 132:567-582.

Jaiswal S, Traver D, Miyamoto T, Akashi K, Lagasse E and Weissman IL. Expression of BCR/ABL and BCL-2 in myeloid progenitors leads to myeloid leukemias. Proc Natl Acad Sci U S A. 2003;100:10002–10007.

Jamieson CH1, Ailles LE, Dylla SJ, Muijtjens M, Jones C, Zehnder JL, et al. Granulocyte-macrophage progenitors as candidate leukemic stem cells in blast-crisis CML. N Engl J Med. 2004;351:657-667

Jansson MD and Lund AH. MicroRNA and cancer. Mol Oncol. 2012;6:590-610.

Jeter CR, Liu B, Liu X, Chen X, Liu C, Calhoun-et al. NANOG promotes cancer stem cell characteristics and prostate cancer resistance to androgen deprivation. Oncogene. 2011;30:3833-3845.

Ji Q, Hao X, Zhang M, Tang W, Yang M, Li L, et al. MicroRNA miR-34 inhibits human pancreatic cancer tumor-initiating cells. PLoS One. 2009;4:e6816.

Jiang F, Qiu Q, Khanna A, Todd NW, Deepak J, Xing L, et al. Aldehyde dehydrogenase 1 is a tumor stem cell-associated marker in lung cancer. Mol Cancer Res. 2009;7:330-338.

Junttila MR and de Sauvage FJ. Influence of tumour micro-environment heterogeneity on therapeutic response. Nature. 2013;501:346-354.

Justilien V, Regala RP, Tseng IC, Walsh MP, Batra J, Radisky ES, et al. Matrix metalloproteinase-10 is required for lung cancer stem cell maintenance, tumor initiation and metastatic potential. PLoS One. 2012;7:e35040.

Kang L, Mao J, Tao Y, Song B, Ma W, Lu Y, et al. MicroRNA-34a suppresses the breast cancer stem cell-like characteristics by downregulating Notch1 pathway. Cancer Sci. 2015;106:700-708.

Kim J, Woo AJ, Chu J, Snow JW, Fujiwara Y, Kim CG, et al. A Myc network accounts for similarities between embryonic stem and cancer cell transcription programs. Cell. 2010a;143:313-324.

Kim YS, Hwan JD, Bae S, Bae DH and Shick WA. Identification of differentially expressed genes using an annealing control primer system in stage III serous ovarian carcinoma. BMC Cancer. 2010b;10:576.

Kim MP, Fleming JB, Wang H, Abbruzzese JL, Choi W, Kopetz S, et al. ALDH activity selectively defines an enhanced tumor-initiating cell population

relative to CD133 expression in human pancreatic adenocarcinoma. PLoS One. 2011;6:e20636.

Kim T, Yang SJ, Hwang D, Song J, Kim M, Kyum Kim S, et al. A basal-like breast cancer-specific role for SRF-IL6 in YAP-induced cancer stemness. Nat Commun. 2015;6:10186.

Kok M, Koornstra RH, Margarido TC, Fles R, Armstrong NJ, Linn SC, et al. Mammosphere-derived gene set predicts outcome in patients with ER-positive breast cancer. J Pathol. 2009;218:316-326.

Koo BS, Lee SH, Kim JM, Huang S, Kim SH, Rho YS, et al. Oct4 is a critical regulator of stemness in head and neck squamous carcinoma cells. Oncogene. 2015;34:2317-2324.

Kozar S, Morrissey E, Nicholson AM, van der Heijden M, Zecchini HI, Kemp R, et al. Continuous clonal labeling reveals small numbers of functional stem cells in intestinal crypts and adenomas. Cell Stem Cell. 2013;13:626–633.

Kreso A and Dick JE. Evolution of the cancer stem cell model. Cell Stem Cell. 2014;14:275-291.

Krivtsov AV, Twomey D, Feng Z, Stubbs MC, Wang Y, Faber J, et al. Transformation from committed progenitor to leukaemia stem cell initiated by MLL-AF9. Nature. 2006;442:818-822.

Kryczek I, Lin Y, Nagarsheth N, Peng D, Zhao L, Zhao E, et al. IL-22(+)CD4(+) T cells promote colorectal cancer stemness via STAT3 transcription factor activation and induction of the methyltransferase DOT1L. Immunity. 2014;40:772-784.

Kuperwasser C, Chavarria T, Wu M, Magrane G, Gray JW, Carey L, et al. Reconstruction of functionally normal and malignant human breast tissues in mice. Proc Natl Acad Sci U S A. 2004;101:4966-4971.

Kuzu OF, Noory MA and Robertson GP. The Role of Cholesterol in Cancer. Cancer Res. 2016;76:2063-2070.

Lamouille S, Xu J and Derynck R. Molecular mechanisms of epithelial-mesenchymal transition. Nat Rev Mol Cell Biol. 2014;15:178-196.

Lapidot T, Sirard C, Vormoor J, Murdoch B, Hoang T, Caceres-Cortes J, et al. A cell initiating human acute myeloid leukaemia after transplantation into SCID mice. Nature. 1994;367:645-648.

Lasorella A, Benezra R and Iavarone A. The ID proteins: master regulators of cancer stem cells and tumour aggressiveness. Nat Rev Cancer. 2014;14:77-91.

Lasry A, Zinger A and Ben-Neriah Y. Inflammatory networks underlying colorectal cancer. Nat Immunol. 2016;17:230-240.

Laurenti E, Wilson A and Trumpp A. Myc's other life: stem cells and beyond. Curr Opin Cell Biol. 2009;21:844–854.

Lawrence MS, Stojanov P, Polak P, Kryukov GV, Cibulskis K, Sivachenko A, et al. Mutational heterogeneity in cancer and the search for new cancer-associated genes. Nature. 2013;499:214-218.

Leal JA and Lleonart ME. MicroRNAs and cancer stem cells: therapeutic approaches and future perspectives. Cancer Lett. 2013;338:174-183.

Lee M, Nam EJ, Kim SW, Kim S, Kim JH and Kim YT. Prognostic impact of the cancer stem cell-related marker NANOG in ovarian serous carcinoma. Int J Gynecol Cancer. 2012;22:1489–1496.

Lee SH, Koo BS, Kim JM, Huang S, Rho YS, Bae WJ, et al. Wnt/β-catenin signalling maintains self-renewal and tumourigenicity of head and neck squamous cell carcinoma stem-like cells by activating Oct4. J. Pathol. 2014;234:99–107.

Lee E, Wang J, Yumoto K, Jung Y, Cackowski FC, Decker AM, et al. DNMT1 Regulates Epithelial-Mesenchymal Transition and Cancer Stem Cells, Which Promotes Prostate Cancer Metastasis. Neoplasia. 2016a;18:553-566.

Lee WJ, Kim SC, Yoon JH, Yoon SJ, Lim J, Kim YS et al. Meta-Analysis of Tumor Stem-Like Breast Cancer Cells Using Gene Set and Network Analysis. PLoS One. 2016b ;11:e0148818.

Lemmon MA and Schlessinger J. Cell signaling by receptor tyrosine kinases. Cell. 2010;141:1117-11134.

Lessard J and Sauvageau G. Polycomb group genes as epigenetic regulators of normal and leukemic hemopoiesis. Exp. Hematol. 2003;31:567–585.

Leung EL, Fiscus RR, Tung JW, Tin VP, Cheng LC, Sihoe AD, et al. Non-small cell lung cancer cells expressing CD44 are enriched for stem cell-like properties. PLoS One. 2010;5:e14062.

Levings PP, SV McGarry, TP Currie, DM Nickerson, S McClellan, SC Ghivizzani, et al. Expression of an exogenous human Oct-4 promoter identifies tumor-initiating cells in osteosarcoma. Cancer Res. 2009;69:5648–5655.

Li C, Heidt DG, Dalerba P, Burant CF, Zhang L, Adsay V, et al. Identification of pancreatic cancer stem cells. Cancer Res. 2007;67:1030-1037.

Li SC, Vu LT, Ho HW, Yin HZ, Keschrumrus V, Lu Q, et al. Cancer stem cells from a rare form of glioblastoma multiforme involving the neurogenic ventricular wall. Cancer Cell Int. 2012;12:41.

Li X, Lewis MT, Huang J, Gutierrez C, Osborne CK, Wu MF, et al. Intrinsic resistance of tumorigenic breast cancer cells to chemotherapy. J Natl Cancer Inst. 2008;100:672-679.

Li Y, Guessous F, Zhang Y, Dipierro C, Kefas B, Johnson E, et al. MicroRNA-34a inhibits glioblastoma growth by targeting multiple oncogenes. Cancer Res. 2009a;69:7569–7576.

Li Z, Bao S, Wu Q, Wang H, Eyler C, Sathornsumetee S, et al. Hypoxia-inducible factors regulate tumorigenic capacity of glioma stem cells. Cancer Cell. 2009b;15:501-513.

Li S, Xie Y, Zhang W, Gao J, Wang M, Zheng G, et al. Interferon alpha-inducible protein 27 promotes epithelial-mesenchymal transition and induces ovarian tumorigenicity and stemness. J Surg Res. 2015a;193:255-264.

Li D, Fu Z, Chen R, Zhao X, Zhou Y, Zeng B, et al. Inhibition of glutamine metabolism counteracts pancreatic cancer stem cell features and sensitizes cells to radiotherapy. Oncotarget. 2015b;6:31151–31163.

Li C, Wang J, Zhang H, Zhu M, Chen F, Hu Y, et al. Interferon-stimulated gene 15 (ISG15) is a trigger for tumorigenesis and metastasis of hepatocellular carcinoma. Oncotarget. 2014;5:8429-8441.

Liao S, Xia J, Chen Z, Zhang S, Ahmad A, Miele L, et al. Inhibitory effect of curcumin on oral carcinoma CAL-27 cells via suppression of Notch-1 and NF-κB signaling pathways. J Cell Biochem. 2011;112:1055-1065.

Lin T, Meng L, Li Y and Tsai RY. Tumor-initiating function of nucleostemin-enriched mammary tumor cells. Cancer Res. 2010;70:9444-9452.

Lin T, Ding YQ and Li JM. Overexpression of Nanog protein is associated with poor prognosis in gastric adenocarcinoma. Med Oncol. 2012;29:878-885.

Little SE, Popov S, Jury A, Bax DA, Doey L, Al-Sarraj S, et al. Receptor tyrosine kinase genes amplified in glioblastoma exhibit a mutual exclusivity in variable proportions reflective of individual tumor heterogeneity. Cancer Res. 2012;72:1614-1620.

Liu S, Dontu G, Mantle ID, Patel S, Ahn NS, Jackson KW, et al. Hedgehog signaling and Bmi-1 regulate self-renewal of normal and malignant human mammary stem cells. Cancer Res. 2006;66:6063-6071.

Liu CG, Lu Y, Wang BB, Zhang YJ, Zhang RS, Lu Y, et al. Clinical implications of stem cell gene Oct-4 expression in breast cancer. Ann Surg. 2011a;253:1165-1171.

Liu C, Kelnar K, Liu B, Chen X, Calhoun-Davis T, Li H, et al. The microRNA miR-34a inhibits prostate cancer stem cells and metastasis by directly repressing CD44. Nat Med. 2011b;17:211-215.

Liu S, Ginestier C, Ou SJ, Clouthier SG, Patel SH, Monville F, et al. Breast cancer stem cells are regulated by mesenchymal stem cells through cytokine networks. Cancer Res. 2011c;71:614-624.

Liu C and Tang DG. MicroRNA regulation of cancer stem cells. Cancer Res. 2011;71:5950-5954.

Liu H, Lv L and Yang K. Chemotherapy targeting cancer stem cells. American Journal of Cancer Research. 2015a;5:880–893.

Liu J, Chi N, Zhang JY, Zhu W, Bian YS and Chen HG. Isolation and characterization of cancer stem cells from medulloblastoma. Genetics and Molecular Research. 2015b;14:3355–3361.

Liu CC, Lin JH, Hsu TW, Su K, Li AF, Hsu HS and Hung SC. IL-6 enriched lung cancer stem-like cell population by inhibition of cell cycle regulators via DNMT1 upregulation. Int J Cancer. 2015c;136:547-559.

Liu S, Liu C, Min X, Ji Y, Wang N, Liu D, Cai J, Li K. Prognostic value of cancer stem cell marker aldehyde dehydrogenase in ovarian cancer: a meta-analysis. PLoS One. 2013;8:e81050.

Liu PP, Liao J, Tang ZJ, Wu WJ, Yang J, Zeng ZL, et al. Metabolic regulation of cancer cell side population by glucose through activation of the Akt pathway. Cell Death Differ. 2012;21:124–135.

Lobry C, Oh P, Mansour MR, Look AT and Aifantis I. Notch signaling: switching an oncogene to a tumor suppressor. Blood. 2014;123:2451–2459.

Loh YH, Wu Q, Chew JL, Vega VB, Zhang W, Chen X, et al. The Oct4 and Nanog transcription network regulates pluripotency in mouse embryonic stem cells. Nat Genet. 2006;38:431-440.

Lonardo E, Frias-Aldeguer J, Hermann PC and Heeschen C. Pancreatic stellate cells form a niche for cancer stem cells and promote their self-renewal and invasiveness. Cell Cycle. 2012;11:1282-90.

Lu X, Mazur SJ, Lin T, Appella E and Xu Y. The pluripotency factor nanog promotes breast cancer tumorigenesis and metastasis. Oncogene. 2014;33:2655–2664.

Magee JA, Piskounova E, Morrison SJ. Cancer stem cells: impact, heterogeneity, and uncertainty. Cancer Cell. 2012;21:283-296.

Malanchi I, Peinado H, Kassen D, Hussenet T, Metzger D, Chambon P, et al. Cutaneous cancer stem cell maintenance is dependent on beta-catenin signalling. Nature. 2008;452:650-653.

Malanchi I, Santamaria-Martínez A, Susanto E, Peng H, Lehr HA, Delaloye JF, et al. Interactions between cancer stem cells and their niche govern metastatic colonization. Nature. 2011;481:85-89.

Malanga D, De Marco C, Guerriero I, Colelli F, Rinaldo N, Scrima M, et al. The Akt1/IL-6/STAT3 pathway regulates growth of lung tumor initiating cells. Oncotarget. 2015;6:42667-42686.

Man SM and Kanneganti TD. Converging roles of caspases in inflammasome activation, cell death and innate immunity. Nat Rev Immunol. 2016;16:7-21.

Mani SA, Guo W, Liao MJ, Eaton EN, Ayyanan A, Zhou AY, et al. The epithelial-mesenchymal transition generates cells with properties of stem cells. Cell. 2008;133:704-715.

Manz MG. Human-hemato-lymphoid-system mice: opportunities and challenges. Immunity. 2007;26:537–541.

Martinez-Cruzado L, Tornin J, Santos L, Rodriguez A, García-Castro J, Morís F, et al. Aldh1 Expression and Activity Increase During Tumor Evolution in Sarcoma Cancer Stem Cell Populations. Sci Rep. 2016;6:27878.

Martins VR, Dias MS and Hainaut P. Tumor-cell-derived microvesicles as carriers of molecular information in cancer. Curr Opin Oncol. 2013;25:66-75.

Marusyk A and Polyak K. Tumor heterogeneity: causes and consequences. Biochim Biophys Acta. 2010;1805:105-117.

Medema JP. Cancer stem cells: the challenges ahead. Nature Cell Biology. 2013;15:338–344.

Menendez JA and Alarcon T. Metabostemness: a new cancer hall-mark. Front. Oncol. 2014;4:262.

Merlo LM, Pepper JW, Reid BJ, and Maley CC. . Cancer as an evolutionary and ecological process. Nat Rev Cancer 2006;6: 924–935.

Meyer N, Kim SS and Penn LZ. The Oscar-worthy role of Myc in apoptosis. Semin Cancer Biol. 2006;16:275-287.

Minn A. Interferons and the immunogenic effects of cancer therapy. Trends Immunol. 2015 Nov;36:725-737.

Mitchem JB, Brennan DJ, Knolhoff BL, Belt BA, Zhu Y, Sanford DE, et al. Targeting tumor-infiltrating macrophages decreases tumor-initiating cells, relieves immunosuppression, and improves chemotherapeutic responses. Cancer Res. 2013;73:1128–1141.

Miyamoto Y, Maitra A, Ghosh B, Zechner U, Argani P, Iacobuzio-Donahue CA, et al. Notch mediates TGF alpha-induced changes in epithelial differentiation during pancreatic tumorigenesis. Cancer Cell. 2003;3:565-576.

Molofsky AV, Pardal R, Iwashita T, Park IK, Clarke MF and Morrison SJ. Bmi-1 dependence distinguishes neural stem cell self-renewal from progenitor proliferation. Nature. 2003;425:962–967

Mondello C, Chiesa M, Rebuzzini P, Zongaro S, Verri A, Colombo T, et al. Karyotype instability and anchorage-independent growth in telomerase-

immortalized fibroblasts from two centenarian individuals. Biochem Biophys Res Commun. 2003;308:914-921.

Monzani E, Facchetti F, Galmozzi E, Corsini E, Benetti A, Cavazzin C, et al. Melanoma contains CD133 and ABCG2 positive cells with enhanced tumourigenic potential. Eur J Cancer. 2007;43:935-946.

Morin PJ, Sparks AB, Korinek V, Barker N, Clevers H, Vogelstein B et al. Activation of beta-catenin-Tcf signaling in colon cancer by mutations in beta-catenin or APC. Science. 1997;275:1787-1790.

Morel AP, Hinkal GW, Thomas C, Fauvet F, Courtois-Cox S, Wierinckx A, et al. EMT inducers catalyze malignant transformation of mammary epithelial cells and drive tumorigenesis towards claudin-low tumors in transgenic mice. PLoS Genet. 2012;8:e1002723.

Muñoz P, Iliou MS and Esteller M. Epigenetic alterations involved in cancer stem cell reprogramming. Mol Oncol. 2012;6:620-636.

Muthurajan UM, Hepler MR, Hieb AR, Clark NJ, Kramer M, Yao T, et al. Automodification switches PARP-1 function from chromatin architectural protein to histone chaperone. Proc Natl Acad Sci U S A. 2014;111:12752-12757.

Nassar D and Blanpain C. Cancer Stem Cells: Basic Concepts and Therapeutic Implications. Annu Rev Pathol. 2016;11:47-76.

Negrini S, Gorgoulis, VG and Halazonetis TD. Genomic instability - an evolving hallmark of cancer. Nat. Rev. Mol. Cell Biol. 2010;11:220–228.

Nickerson ML, Jaeger E, Shi Y, Durocher JA, Mahurkar S, Zaridze D, et al. Improved identification of von Hippel-Lindau gene alterations in clear cell renal tumors. Clin Cancer Res. 2008 ;14:4726-4734.

Nik-Zainal S, Van Loo P, Wedge DC, Alexandrov LB, Greenman CD, Lau KW, et al. The life history of 21 breast cancers. Cell. 2012;149:994-1007.

Nishida S, Hirohashi Y, Torigoe T, Kitamura H, Takahashi A, Masumori N, et al. Gene expression profiles of prostate cancer stem cells isolated by aldehyde dehydrogenase activity assay. J Urol. 2012;188:294-299.

Norton N, Advani PP, Serie DJ, Geiger XJ, Necela BM, Axenfeld BC, et al. Assessment of Tumor Heterogeneity, as Evidenced by Gene Expression Profiles, Pathway Activation, and Gene Copy Number, in Patients with Multifocal Invasive Lobular Breast Tumors. PLoS One. 2016;11:e0153411.

Notta F, Mullighan CG, Wang JC, Poeppl A, Doulatov S, Phillips LA, et al. Evolution of human BCR-ABL1 lymphoblastic leukaemia-initiating cells. Nature 2011;469:362–367.

Nowell PC. The clonal evolution of tumor cell populations. Science. 1976;194:23-28.

O'Brien CA, Pollett A, Gallinger S and Dick JE. A human colon cancer cell capable of initiating tumour growth in immunodeficient mice. Nature. 2007;445:106-110.

Ocaña OH1, Córcoles R, Fabra A, Moreno-Bueno G, Acloque H, Vega S, et al. Metastatic Colonization Requires the Repression of the Epithelial-Mesenchymal Transition Inducer Prrx1. Cancer Cell. 2012 Dec 11;22(6):709-724.

Oh K, Lee OY, Park Y, Seo MW and Lee DS. IL-1β induces IL-6 production and increases invasiveness and estrogen-independent growth in a TG2-dependent manner in human breast cancer cells. BMC Cancer. 2016;16:724.

Oliveira LR. Stem cells and cancer stem cells. In: Shostak S, editor. Cancer Stem Cells - The Cutting Edge. Rijeka: InTech; 2011. pp. 3–28.

Olmez I, Shen W, McDonald H and Ozpolat B. Dedifferentiation of patient-derived glioblastoma multiforme cell lines results in a cancer stem cell-like state with mitogen-independent growth. J Cell Mol Med. 2015;19:1262-1272.

Orkin SH, Wang J, Kim J, Chu J, Rao S, Theunissen TW, et al. The transcriptional network controlling pluripotency in ES cells. Cold Spring Harb Symp Quant Biol. 2008;73:195-202.

Orkin SH and Hochedlinger K. Chromatin connections to pluripotency and cellular reprogramming. Cell. 2011;145:835-850.

Ostano P, Bione S, Belgiovine C, Chiodi I, Ghimenti C, Scovassi AI, et al. Cross-analysis of gene and miRNA genome-wide expression profiles in human fibroblasts at different stages of transformation. OMICS. 2012;16:24-36.

Ostyn P, El Machhour R, Begard S, Kotecki N, Vandomme J, Flamenco P, et al. Transient TNF regulates the self-renewing capacity of stem-like label-retaining cells in sphere and skin equivalent models of melanoma. Cell Commun Signal. 2014;12:52.

Papageorgis P, Ozturk S, Lambert AW, Neophytou CM, Tzatsos A, Wong CK, et al. Targeting IL13Ralpha2 activates STAT6-TP63 pathway to suppress breast cancer lung metastasis. Breast Cancer Res. 2015 Jul 25;17:98.

Park IK, Qian D, Kiel M, Becker MW, Pihalja M, Weissman IL, et al. Bmi-1 is required for maintenance of adult self-renewing haematopoietic stem cells. Nature. 2003;423:302–305.

Parker BS, Rautela J and Hertzog PJ. Antitumour actions of interferons: implications for cancer therapy. Nat Rev Cancer. 2016;16:131-144.

Pastò A, Bellio C, Pilotto G, Ciminale V, Silic-Benussi M, et al. Cancer stem cells from epithelial ovarian cancer patients privilege oxidative phosphorylation, and resist glucose deprivation. Oncotarget. 2014;5:4305-4319.

Patel AP, Tirosh I, Trombetta JJ, Shalek AK, Gillespie SM, Wakimoto H, et al. Single-cell RNA-seq highlights intratumoral heterogeneity in primary glioblastoma. Science. 2014;344:1396-1401.

Pavlova NN and Thompson CB. The Emerging Hallmarks of Cancer Metabolism. Cell Metab. 2016;23:27-47.

Peacock CD, Wang Q, Gesell GS, Corcoran-Schwartz IM, Jones E, et al. Hedgehog signaling maintains a tumor stem cell compartment in multiple myeloma. Proc Natl Acad Sci U S A. 2007;104:4048-4053.

Pece S, Tosoni D, Confalonieri S, Mazzarol G, Vecchi M, Ronzoni S, et al. Biological and molecular heterogeneity of breast cancers correlates with their cancer stem cell content. Cell 2010;140:62–73.

Peiris-Pagès M, Martinez-Outschoorn UE, Pestell RG, Sotgia F and Lisanti MP. Cancer stem cell metabolism. Breast Cancer Res. 2016;18:55.

Pelosi E, Castelli G and Testa U. Targeting LSCs through membrane antigens selectively or preferentially expressed on these cells. Blood Cells Mol Dis. 2015;55:336-346.

Pérez-Caro M, Cobaleda C, González-Herrero I, Vicente-Dueñas C, Bermejo-Rodríguez C, Sánchez-Beato M, et al. Cancer induction by restriction of oncogene expression to the stem cell compartment. EMBO J. 2009;28:8-20.

Pietras A, Katz AM, Ekstrom EJ, Wee B, Halliday JJ, Pitter KL, et al. Osteopontin-CD44 signaling in the glioma perivascular niche enhances cancer stem cell phenotypes and promotes aggressive tumor growth. Cell Stem Cell 2014;14:357–369.

Pizon M, Schott D, Pachmann U and Pachmann K. The number of tumorspheres cultured from peripheral blood is a predictor for presence of metastasis in patients with breast cancer. Oncotarget. 2016;7:48143-48154.

Ponti D, Costa A, Zaffaroni N, Pratesi G, Petrangolini G, Coradini D, et al. Isolation and in vitro propagation of tumorigenic breast cancer cells with stem/progenitor cell properties. Cancer Res. 2005;65:5506-5511

Prince ME, Sivanandan R, Kaczorowski A, Wolf GT, Kaplan MJ, Dalerba P, et al. Identification of a subpopulation of cells with cancer stem cell properties in head and neck squamous cell carcinoma. Proc Natl Acad Sci U S A. 2007;104:973-978.

Qian BZ and Pollard JW. Macrophage Diversity Enhances Tumor Progression and Metastasis. Cell. 2010;141:39-51.

Qin J, Liu X, LaffinB, ChenX, ChoyG, Jeter CR, et al. The PSA(-/lo) prostate cancer cell population harbors self-renewing long-term tumor-propagating cells that resist castration. Cell Stem Cell. 2012;10:556–569

Quintana E, Shackleton M, Sabel MS, Fullen DR, Johnson TM and Morrison SJ. Efficient tumour formation by single human melanoma cells. Nature. 2008;456:593–598.

Quintana E, Shackleton M, Foster HR, Fullen DR, Sabel MS, Johnson TM et al. Phenotypic heterogeneity among tumorigenic melanoma cells from patients that is reversible and not hierarchically organized. Cancer cell. 2010;18:510–523.

Rainusso N, Man TK, Lau CC, Hicks J, Shen JJ, Yu A, et al. Identification and gene expression profiling of tumor-initiating cells isolated from human osteosarcoma cell lines in an orthotopic mouse model. Cancer Biol Ther. 2011;12:278-287.

Reedijk M, Odorcic S, Chang L, Zhang H, Miller N, McCready DR, et al High-level coexpression of JAG1 and NOTCH1 is observed in human breast cancer and is associated with poor overall survival. Cancer Res. 2005;65:8530-8537.

Reya T, Morrison S, Clarke M and Weissman I. Stem cells, cancer, and cancer stem cells. Nature, 2001;414:105–111.

Reynolds BA and Weiss S. Generation of neurons and astrocytes from isolated cells of the adult mammalian central nervous system. Science. 1992;255:1707-1710.

Ricci-Vitiani L, Lombardi DG, Pilozzi E, Biffoni M, Todaro M, Peschle C et al. Identification and expansion of human colon-cancer-initiating cells. Nature 2007;445: 111–115

Romero-Lanman EE, Pavlovic S, Amlani B, Chin Y and Benezra R. Id1 maintains embryonic stem cell self-renewal by up-regulation of Nanog and repression of Brachyury expression. Stem Cells Dev. 2012;21:384-393.

Rongvaux A, Takizawa H, Strowig T, Willinger T, Eynon EE, Flavell RA et al. Human hemato-lymphoid system mice: current use and future potential for medicine. Annu. Rev. Immunol. 2013;31:635–674.

Roy M, Pear WS and Aster JC. The multifaceted role of Notch in cancer. Curr Opin Genet Dev. 2007;17:52-59.

Ruiz i Altaba A, Sánchez P and Dahmane N. Gli and hedgehog in cancer: tumours, embryos and stem cells. Nat Rev Cancer. 2002;2:361-372.

Rybak AP and Tang D. SOX2 plays a critical role in EGFR-mediated self-renewal of human prostate cancer stem-like cells. Cell Signal. 2013;25:2734-2742.

Rybak AP, He L, Kapoor A, Cutz JC and Tang D. Characterization of sphere propagating cells with stem-like properties from DU145prostate cancer cells. Biochim. Biophys. Acta. 2011;1813:683–694.

Rycaj K and Tang DG. Cell-of-Origin of Cancer versus Cancer Stem Cells: Assays and Interpretations. Cancer Res. 2015;75:4003-4011.

Saeed AI, Bhagabati NK, Braisted JC, Liang W, Sharov V, Howe EA, et al. TM4 microarray software suite. Methods Enzymol 2006;411:134–193.

Sainz B Jr, Martín B, Tatari M, Heeschen C and Guerra S. ISG15 is a critical microenvironmental factor for pancreatic cancer stem cells. Cancer Res. 2014;74:7309-7320.

Salerno M, Avnet S, Bonuccelli G, Eramo A, De Maria R, Gambarotti M, et al. Sphere-forming cell subsets with cancer stem cell properties in human musculoskeletal sarcomas. Int J Oncol. 2013;43:95-102.

Sanguinetti A, Santini D, Bonafè M, Taffurelli M and Avenia N. Interleukin-6 and pro inflammatory status in the breast tumor microenvironment. World J Surg Oncol. 2015;13:129.

Santagata S, Demichelis F, Riva A, Varambally S, Hofer MD, Kutok JL, et al. JAGGED1 expression is associated with prostate cancer metastasis and recurrence. Cancer Res. 2004;64:6854-6857.

Santini R, Pietrobono S, Pandolfi S, Montagnani V, D'Amico M, Penachioni JY, et al. SOX2 regulates self-renewal and tumorigenicity of human melanoma-initiating cells. Oncogene. 2014;33:4697-4708.

Sarry JE, Murphy K, Perry R, Sanchez PV, Secreto A, Keefer C, et al. Human acute myelogenous leukemia stem cells are rare and heterogeneous when assayed in NOD/SCID/IL2Rgammac-deficient mice. J Clin Invest. 2011;121:384–395

Satoh Y, Matsumura I, Tanaka H, Ezoe S, Sugahara H, Mizuki M, et al. Roles for c-Myc in self-renewal of hematopoietic stem cells. J. Biol. Chem. 2004;279:24986–24993.

Scaffidi P and Misteli T. In vitro generation of human cells with cancer stem cell properties. Nat. Cell Biol. 2011;13;1051–1061.

Schatton T and Frank MH Cancer stem cells and human malignant melanoma. Pigment Cell Melanoma Res. 2008;21:39–55.

Schepers AG, Snippert HJ, Stange DE, van den Born M, van Es JH, van de Wetering M, et al. Lineage tracing reveals Lgr5+ stem cell activity in mouse intestinal adenomas. Science. 2012; 337:730-735.

Schroder K, Hertzog PJ, Ravasi T and Hume DA. Interferon-gamma: an overview of signals, mechanisms and functions. J Leukoc Biol 2004;75:163–189.

Schwitalla S, Fingerle AA, Cammareri P, Nebelsiek T, Göktuna SI, Ziegler PK, et al. Intestinal tumorigenesis initiated by dedifferentiation and acquisition of stem-cell-like properties. Cell. 2013;152:25-38.

Schraivogel D, Weinmann L, Beier D, Tabatabai G, Eichner A, Zhu JY, et al. CAMTA1 is a novel tumour suppressor regulated by miR-9/9* in glioblastoma stem cells. EMBO J. 2011;30:4309-4322.

Seluanov A, Hine C, Azpurua J, Feigenson M, Bozzella M, Mao Z, et al. Hypersensitivity to contact inhibition provides a clue to cancer resistance of naked mole-rat. Proc Natl Acad Sci U S A. 2009;106:19352-19357.

Sgorbissa A and Brancolini C. IFNs, ISGylation and cancer: Cui prodest? Cytokine Growth Factor Rev. 2012;23:307-314.

Shackleton M, Quintana E, Fearon ER and Morrison SJ. Heterogeneity in cancer: cancer stem cells versus clonal evolution. Cell. 2009;138:822–829.

Shah SP, Morin RD, Khattra J, Prentice L, Pugh T, Burleigh A, et al. Mutational evolution in a lobular breast tumour profiled at single nucleotide resolution. Nature. 2009;461:809-813.

Shay JW and Roninson IB. Hallmarks of senescence in carcinogenesis and cancer therapy. Oncogene. 2004;23:2919–2933.

Shay JW and Wright WE. Telomeres and telomerase in normal and cancer stem cells. FEBS Lett. 2010;584:3819–3825.

Sheng X, Li Z, Wang DL, Li WB, Luo Z, Chen KH, et al. Isolation and enrichment of PC-3 prostate cancer stem-like cells using MACS and serum-free medium. Oncol Lett. 2013;5:787-792.

Sherr CJ. Principles of tumor suppression. Cell. 2004;116:235-246.

Singh SK, Clarke ID, Terasaki M, Bonn VE, Hawkins C, Squire J et al. Identification of a cancer stem cell in human brain tumors. Cancer Res. 2003;63:5821–5828

Singh SK, Hawkins C, Clarke ID, Squire JA, Bayani J, Hide T et al. Identification of human brain tumour initiating cells. Nature. 2004;432: 396–401.

Shi Y, Liu C, Liu X, Tang DG and Wang J. The microRNA miR-34a inhibits non-small cell lung cancer (NSCLC) growth and the CD44hi stem-like NSCLC cells. PLoS One. 2014;9:e90022.

Shimono Y, Zabala M, Cho RW, Lobo N, Dalerba P, Qian D, et al. Downregulation of miRNA-200c links breast cancer stem cells with normal stem cells. Cell. 2009;138:592-603.

Shlush LI, Zandi S, Mitchell A, Chen WC, Brandwein JM, Gupta V, et al. Identification of pre-leukaemic haematopoietic stem cells in acute leukaemia. Nature. 2014 Feb 20;506(7488):328-333.

Smyth GK. Linear models and empirical bayes methods for assessing differential expression in microarray experiments. Stat Appl Genet Mol Biol. 2004;3 Article3.

Stratton MR, Campbell PJ and Futreal PA. The cancer genome. Nature. 2009;458:719-724.

Subramanian A, Tamayo P, Mootha VK, Mukherjee S, Ebert BL, Gillette MA, et al. Gene set enrichment analysis: a knowledge-based approach for interpreting genome-wide expression profiles. Proc Natl Acad Sci USA. 2005;102:15545–15550.

Sun X, Jiao X, Pestell TG, Fan C, Qin S, Mirabelli E, et al. MicroRNAs and cancer stem cells: the sword and the shield. Oncogene. 2014 Oct 16;33(42):4967-4977.

Sun XX and Yu Q. Intra-tumor heterogeneity of cancer cells and its implications for cancer treatment. Acta Pharmacol Sin. 2015;36:1219-1227.

Suomela S, Cao L, Bowcock A and Saarialho-Kere U. Interferon alpha-inducible protein 27 (IFI27) is upregulated in psoriatic skin and certain epithelial cancers. J Invest Dermatol. 2004;122:717-721.

Suvà ML, Riggi N, Stehle JC, Baumer K, Tercier S, Joseph JM, et al. Identification of cancer stem cells in Ewing's sarcoma. Cancer Res. 2009;69:1776–1781

Swanton C. Intratumor heterogeneity: evolution through space and time. Cancer Res. 2012;72:4875-4882.

Swartling FJ, Savov V, Persson AI, Chen J, Hackett CS, Northcott PA, et al. Distinct neural stem cell populations give rise to disparate brain tumors in response to N-MYC. Cancer Cell. 2012;21:601-613.

Szerlip NJ, Pedraza A, Chakravarty D, Azim M, McGuire J, Fang Y, et al. Intratumoral heterogeneity of receptor tyrosine kinases EGFR and PDGFRA amplification in glioblastoma defines subpopulations with distinct growth factor response. Proc Natl Acad Sci U S A. 2012;109:3041-3046.

Takahashi K and Yamanaka S. Induction of pluripotent stem cells from mouse embryonic and adult fibroblast cultures by defined factors. Cell. 2006; 126:663-676.

Takahashi K, Tanabe K, Ohnuki M, Narita M, Ichisaka T, Tomoda K, et al. Induction of pluripotent stem cells from adult human fibroblasts by defined factors. Cell. 2007;131: 861–872.

Takaishi S, Okumura T, Tu S, Wang SS, Shibata W, Vigneshwaran R, et al. Identification of gastric cancer stem cells using the cell surface marker CD44. Stem Cells. 2009;27:1006-1020.

Talmadge JE and Fidler IJ. AACR centennial series: the biology of cancer metastasis: historical perspective. Cancer Res. 2010;70:5649–5669.

Tamase A, Muraguchi T, Naka K, Tanaka S, Kinoshita M, Hoshii T, et al. Identification of tumor-initiating cells in a highly aggressive brain tumor using promoter activity of nucleostemin. Proc Natl Acad Sci U S A. 2009;106:17163-17168.

Tata PR, Mou H, Pardo-Saganta A, Zhao R, Prabhu M, Law BM, et al. Dedifferentiation of committed epithelial cells into stem cells in vivo. Nature. 2013;503:218-223.

Taussig DC, Vargaftig J, Miraki-Moud F, Griessinger E, Sharrock K, Luke T, et al. Leukemia-initiating cells from some acute myeloid leukemia patients with mutated nucleophosmin reside in the CD34(-) fraction. Blood. 2010;115:1976-1984.

Terry J and Nielsen T. Expression of CD133 in synovial sarcoma. Appl Immunohistochem Mol Morphol. 2010;18:159-165.

Thiery JP, Acloque H, Huang RY and Nieto MA. Epithelial-mesenchymal transitions in development and disease. Cell 2009;139:871–890.

Tin AS, Park AH, Sundar SN and Firestone GL. Essential role of the cancer stem/progenitor cell marker nucleostemin for indole-3-carbinol anti-

proliferative responsiveness in human breast cancer cells. BMC Biol. 2014;12:72.

Tian T, Zhang Y, Wang S, Zhou J and Xu S. Sox2 enhances the tumorigenicity and chemoresistance of cancer stem-like cells derived from gastric cancer. J Biomed Res. 2012;26:336-345.

Tirino V, Camerlingo R, Franco R, Malanga D, La Rocca A, Viglietto G, et al. The role of CD133 in the identification and characterization of tumor-initiating cells in non-small-cell lung cancer. Eur. J. Cardiothorac. Surg. 2009;36:446–453.

Tirino V, Desiderio V, Paino F, De Rosa A, Papaccio F, Fazioli F,et al. Human primary bone sarcomas contain CD133+ cancer stem cells displaying high tumorigenicity in vivo. FASEB J. 2011;25:2022–2030.

Tirosh I, Izar B, Prakadan SM, Wadsworth MH, Treacy D, Trombetta JJ, et al. Dissecting the multicellular ecosystem of metastatic melanoma by single-cell RNA-seq. Science. 2016;352:189-196.

Trowbridge JJ, Sinha AU, Zhu N, Li M, Armstrong SA and Orkin SH. Haploinsufficiency of Dnmt1 impairs leukemia stem cell function through derepression of bivalent chromatin domains. Genes Dev. 2012;26:344-349.

Tsai RY and McKay RD. A nucleolar mechanism controlling cell proliferation in stem cells and cancer cells. Genes Dev. 2002;16:2991-3003.

Tsai RY. Turning a new page on nucleostemin and self-renewal. J Cell Sci. 2014;127:3885-3891.

van Es JH, Sato T, van de Wetering M, Lyubimova A, Nee AN, Gregorieff A, et al. Dll1+ secretory progenitor cells revert to stem cells upon crypt damage. Nat Cell Biol. 2012;14:1099-1104.

Vermeulen L, De Sousa E Melo F, van der Heijden M, Cameron K, de Jong JH, et al. Wnt activity defines colon cancer stem cells and is regulated by the microenvironment. Nat Cell Biol. 2010;12:468-476.

Viale A, Pettazzoni P, Lyssiotis CA, Ying H, Sanchez N, Marchesini M, et al. Oncogene ablation-resistant pancreatic cancer cells depend on mitochondrial function. Nature. 2014;514:628–632.

Visvader JE and Lindeman GJ. Cancer stem cells: current status and evolving complexities. Cell Stem Cell. 2012;10:717-728.

Wael H, Yoshida R, Kudoh S, Hasegawa K, Niimori-Kita K et al. Notch1 signaling controls cell proliferation, apoptosis and differentiation in lung carcinoma. Lung Cancer. 2014;85:131–140.

Wang J, Sakariassen PØ, Tsinkalovsky O, Immervoll H, Bøe SO, Svendsen A, et al. CD133 negative glioma cells form tumors in nude rats and give rise to CD133 positive cells. Int. J. Cancer. 2008a;122:761–768.

Wang Y, Krivtsov AV, Sinha AU, North TE, Goessling W, Feng Z, et al. The Wnt/beta-catenin pathway is required for the development of leukemia stem cells in AML. Science. 2010;327:1650-1653.

Wang M, Xue L, Cao Q, Lin Y, Ding Y, Yang P, et al. Expression of Notch1, Jagged1 and beta-catenin and their clinicopathological significance in hepatocellular carcinoma. Neoplasma. 2009;56:533-541.

Wang YD, Cai N, Wu XL, Cao HZ, Xie LL and Zheng PS. OCT4 promotes tumorigenesis and inhibits apoptosis of cervical cancer cells by miR-125b/BAK1 pathway. Cell Death Dis. 2013a;4:e760.

Wang ML, Chiou SH and Wu CW. Targeting cancer stem cells: emerging role of Nanog transcription factor. Onco Targets Ther. 2013b;6:1207–1220.

Wang H, Zhang Y and Du Y. Ovarian and breast cancer spheres are similar in transcriptomic features and sensitive to fenretinide. Biomed Res Int. 2013c;2013:510905.

Wang J, Wang H, Li Z, Wu Q, Lathia JD, McLendon RE, et al. c-Myc is required for maintenance of glioma cancer stem cells. PLoS One. 2008b;3:e3769.

Wang CQ, Sun HT, Gao XM, Ren N, Sheng YY, Wang Z, et al. Interleukin-6 enhances cancer stemness and promotes metastasis of hepatocellular carcinoma via up-regulating osteopontin expression. Am J Cancer Res. 2016;6:1873-1889.

Warburg OH. The Metabolism of Tumours: Investigations from the Kaiser Wilhelm Institute for Biology, Berlin-Dahlem (London, UK: Arnold Constable). 1930.

Watanabe Y, Yoshimura K, Yoshikawa K, Tsunedomi R, Shindo Y, Matsukuma S, et al. A stem cell medium containing neural stimulating factor induces a pancreatic cancer stem-like cell-enriched population. Int J Oncol. 2014;45:1857-1866.

Wellner U, Schubert J, Burk UC, Schmalhofer O, Zhu F, Sonntag A, et al. The EMT-activator ZEB1 promotes tumorigenicity by repressing stemness-inhibiting microRNAs. Nat Cell Biol. 2009;11:1487-1495.

Welte Y, Adjaye J, Lehrach HR and Regenbrecht CR. Cancer stem cells in solid tumors: elusive or illusive? Cell Commun Signal. 2010;8:6.

Wenzel J, Tomiuk S, Zahn S, Küsters D, Vahsen A, Wiechert A, et al. Transcriptional profiling identifies an interferon-associated host immune response in invasive squamous cell carcinoma of the skin. Int J Cancer 2008;123:2605.

Wicha MS. Migratory gene expression signature predicts poor patient outcome: are cancer stem cells to blame? Breast Cancer Res. 2012;14:114.

Widera D, Mikenberg I, Elvers M, Kaltschmidt C and Kaltschmidt B. Tumor necrosis factor alpha triggers proliferation of adult neural stem cells via IKK/NF-kappaB signaling. BMC Neurosci. 2006;7:64.

Witsch E, Sela M and Yarden Y. Roles for growth factors in cancer progression. Physiology (Bethesda). 2010;25:85-101.

Wong W, Qiu B, Nakazawa M, Qing G and Simon M. MYC Degradation Under Low O2 Tension Promotes Survival by Evading Hypoxia-Induced Cell Death. Mol. Cell. Biol. 2013;33:3494–3504.

Woodward WA, Chen MS, Behbod F, Alfaro MP, Buchholz TA, Rosen JM, et al. WNT/beta-catenin mediates radiation resistance of mouse mammary progenitor cells. Proc Natl Acad Sci U S A. 2007;104:618-623.

Wu F, J Zhang, P Wang, X Ye, K Jung, KM Bone, et al. Identification of two novel phenotypically distinct breast cancer cell subsets based on Sox2 transcription activity. Cell Signal. 2012;24:1989–1998.

Yamamura S, Saini S, Majid S, Hirata H, Ueno K, Chang I, et al. MicroRNA-34a suppresses malignant transformation by targeting c-Myc transcriptional complexes in human renal cell carcinoma. Carcinogenesis. 2012a;33:294–300.

Yamamura S, Saini S, Majid S, Hirata H, Ueno K, Deng G et al. MicroRNA-34a modulates c-Myc transcriptional complexes to suppress malignancy in human prostate cancer cells. PLoS ONE. 2012b;7:e29722.

Yan Y, Zuo X and Wei D. Concise Review: Emerging Role of CD44 in Cancer Stem Cells: A Promising Biomarker and Therapeutic Target. Stem Cells Transl Med. 2015;4:1033-1043.

Yang ZF, Ngai P, Ho DW, Yu WC, Ng MN, Lau CK, et al. Identification of local and circulating cancer stem cells in human liver cancer. Hepatology. 2008 Mar;47(3):919-928.

Yang MH, Imrali A and Heeschen C. Circulating cancer stem cells: the importance to select. Chin J Cancer Res. 2015;27:437-449

Yang YP, Chien Y, Chiou GY, Cherng JY, Wang ML, Lo WL, et al. Inhibition of cancer stem cell-like properties and reduced chemoradioresistance of glioblastoma using microRNA145 with cationic polyurethane-short branch PEI. Biomaterials. 2012;33:1462-1476.

Yang MH, Hsu DS, Wang HW, Wang HJ, Lan HY, Yang WH, et al. Bmi1 is essential in Twist1-induced epithelial-mesenchymal transition. Nat Cell Biol. 2010;12:982-992.

Yashiro-Ohtani Y, Wang H, Zang C, Arnett KL, Bailis W, Ho Y, et al. Long-range enhancer activity determines Myc sensitivity to Notch inhibitors in T cell leukemia. Proc Natl Acad Sci U S A. 2014;111:E4946-4953.

Yates LR, Gerstung M, Knappskog S, Desmedt C, Gundem G, Van Loo P, et al. Subclonal diversification of primary breast cancer revealed by multiregion sequencing. Nat Med. 2015;21:751-759.

Ye XZ, Xu SL, Xin YH, Yu SC, Ping YF, Chen L, et al. Tumor-associated microglia/macrophages enhance the invasion of glioma stem-like cells via TGF-β1 signaling pathway. J Immunol. 2012;189:444–453.

Ye J, Wu D, Wu P, Chen Z and Huang J. The cancer stem cell niche: cross talk between cancer stem cells and their microenvironment. Tumour Biol. 2014;35:3945-3951.

Yin S, Li J, Hu C, Chen X, Yao M, Yan M, et al. CD133 positive hepatocellular carcinoma cells possess high capacity for tumorigenicity. Int J Cancer. 2007;120:1444-1450.

Yoshida GJ. Metabolic reprogramming: the emerging concept and associated therapeutic strategies. J Exp Clin Cancer Res. 2015;34:111.

Yoshida A, Hsu LC and Davé V. Retinal oxidation activity and biological role of human cytosolic aldehyde dehydrogenase. Enzyme. 1992; 46:239-244.

Young RA. Control of the embryonic stem cell state. Cell. 2011;144:940-954.

Yuan X, Curtin J, Xiong Y, Liu G, Waschsmann-Hogiu S, Farkas DL, et al. Isolation of cancer stem cells from adult glioblastoma multiforme. Oncogene. 2004;23:9392-9400.

Yu F, Yao H, Zhu P, Zhang X, Pan Q, Gong C, et al. let-7 regulates self renewal and tumorigenicity of breast cancer cells. Cell. 2007;131:1109-1123.

Yu F, Deng H, Yao H, Liu Q, Su F and Song E. Mir-30 reduction maintains self-renewal and inhibits apoptosis in breast tumor-initiating cells. Oncogene. 2010;29:4194-4204.

Xiang T, Long H, He L, Han X, Lin K, Liang Z, et al. Interleukin-17 produced by tumor microenvironment promotes self-renewal of CD133+ cancer stem-like cells in ovarian cancer. Oncogene. 2015;34:165-176.

Zagorac S, Alcala S, Fernandez Bayon G, Bou Kheir T, Schoenhals M, González-Neira A, et al. DNMT1 Inhibition Reprograms Pancreatic Cancer Stem Cells via Upregulation of the miR-17-92 Cluster. Cancer Res. 2016;76:4546-4558.

Zbinden M, A Duquet, A Lorente-Trigos, SN Ngwabyt, I Borges et al. NANOG regulates glioma stem cells and is essential in vivo acting in a cross-functional network with GLI1 and p53. Embo J. 2010;29:2659– 2674.

Zetter BR. Angiogenesis and tumor metastasis. Annu Rev Med. 1998;49:407-424.

Zhang S, Balch C, Chan MW, Lai HC, Matei D, Schilder JM, et al. Identification and characterization of ovarian cancer-initiating cells from primary human tumors. Cancer Res. 2008;68:4311-4320.

Zhang J, Fujimoto J, Zhang J, Wedge DC, Song X, Zhang J, et al. Intra-tumor heterogeneity in localized lung adenocarcinomas delineated by multiregion sequencing. Science 2014;346:256–259.

Zhang M, Biswas S, Qin X, Gong W, Deng W and Yu H. Does Notch play a tumor suppressor role across diverse squamous cell carcinomas? Cancer Med. 2016a;5:2048-2060.

Zhang H, Li N, Zhang J, Jin F, Shan M, Qin J et al. The influence of miR-34a expression on stemness and cytotoxic susceptibility of breast cancer stem cells. Cancer Biol Ther. 2016b;17:614-624.

Zhao C, Chen A, Jamieson CH, Fereshteh M, Abrahamsson A, Blum J, et al. Hedgehog signalling is essential for maintenance of cancer stem cells in myeloid leukaemia. Nature. 2009a; 458:776-779.

Zhao H, Boije H, Granberg F, Pettersson U and Svensson C. Activation of the interferon-induced STAT pathway during an adenovirus type 12 infection. Virology. 2009b;392:186-195.

Zhao A, Yang L, Ma K, Sun M, Li L, Huang J, et al. Overexpression of cyclin D1 induces the reprogramming of differentiated epidermal cells into stem cell-like cells. Cell Cycle. 2016;15:644-653.

Zhao Z, Wang L and Xu W. IL-13Rα2 mediates PNR-induced migration and metastasis in ERα-negative breast cancer. Oncogene. 2015;34:1596-1607.

Zhou Y, Zhou Y, Shingu T, Feng L, Chen Z, Ogasawara M, et al. Metabolic alterations in highly tumorigenic glioblastoma cells: preference for hypoxia and high dependency on glycolysis. J Biol Chem. 2011;286:32843-32853.

Zinin N, Adameyko I, Wilhelm M, Fritz N, Uhlén P, Ernfors P et al. MYC proteins promote neuronal differentiation by controlling the mode of progenitor cell division. EMBO Rep. 2014;15:383-391.

Zomer A, Ellenbroek SI, Ritsma L, Beerling E, Vrisekoop N and Van Rheenen J. Intravital imaging of cancer stem cell plasticity in mammary tumors. Stem Cells. 2013;31:602–606.

Zona S, Bella L, Burton MJ, Nestal de Moraes G and Lam EW. FOXM1: An emerging master regulator of DNA damage response and genotoxic agent resistance. Biochim Biophys Acta. 2014;1839:1316-1322.

Zongaro S, de Stanchina E, Colombo T, D'Incalci M, Giulotto E, Mondello C. Stepwise neoplastic transformation of a telomerase immortalized fibroblast cell line. Cancer Res. 2005;65:11411-11418.

Zou W and Wicha MS. Chemokines and cellular plasticity of ovarian cancer stem cells. Oncoscience. 2015;2:615–616.

Zuo C, Sheng X, Ma M, Xia M and Ouyang L. ISG15 in the tumorigenesis and treatment of cancer: An emerging role in malignancies of the digestive system. Oncotarget. 2016;1–17.

Zwolinska A, Whiting A, Beekman C, Sedivy J and Marine JC. Suppression of Myc oncogenic activity by Nucleostemin haploinsufficiency. Oncogene. 2012; 29:997–1003.

Supplementary Information

Supplementary Table S1. List of the genes commonly up-regulated in cen3tel 600 and 1000 sphere cells. Gene expression in sphere cells is expressed as Log_2FC relative to the corresponding adherent cells. Genes with $Log_2FC > 0.58$ and adjusted *p*-value < 0.05 are reported.

		Cen3tel 600 spheres		Cen3tel 1000 spheres	
Probe Name	**Gene Symbol**	**Log_2FC**	**AdjPvalue**	**Log_2FC**	**AdjPvalue**
A_23_P251002	0	0.59	4.14E-02	1.70	2.50E-03
A_23_P170719	0	0.62	5.25E-03	0.93	7.07E-03
A_23_P205500	0	0.81	5.87E-04	0.72	1.19E-02
A_23_P147404	0	1.31	8.85E-05	1.50	7.96E-04
A_23_P113716	HLA-C	1.44	8.88E-05	0.99	9.09E-03
A_23_P170713	0	1.57	3.79E-05	1.43	1.18E-03
A_24_P585004	0	1.60	8.85E-05	0.84	3.00E-02
A_24_P936272	HLA-C	1.66	1.25E-06	0.71	1.87E-03
A_24_P912382	HLA-A	1.86	4.78E-05	0.84	3.71E-02
A_32_P49164	0	2.11	1.59E-07	0.67	7.34E-04
A_23_P314024	0	2.11	2.59E-05	0.88	3.17E-02
A_23_P125109	0	2.64	1.60E-05	1.16	1.81E-02
A_24_P101771	0	3.17	6.72E-07	1.17	1.96E-03
A_23_P95917	HLA-C	3.34	8.86E-06	1.04	4.99E-02
A_23_P384355	0	3.35	8.04E-07	2.17	1.41E-04
A_32_P144281	LOC101928228	0.68	3.66E-03	0.80	1.46E-02
A_23_P56898	KYNU	3.30	2.19E-07	2.32	2.41E-05
A_24_P11506	KYNU	3.57	1.18E-06	2.06	4.25E-04
A_24_P305938	RAB9BP1	1.11	2.40E-04	0.69	2.91E-02
A_24_P310756	FBXO28	0.71	2.13E-03	0.59	4.40E-02
A_24_P456944	LOC441124	0.81	8.23E-04	0.82	8.86E-03
A_24_P453793	LOC441124	1.08	2.59E-05	0.92	1.16E-03
A_23_P412515	CLDN12	0.64	1.43E-03	0.69	1.03E-02
A_23_P31453	STEAP1	0.65	2.19E-02	0.97	2.55E-02
A_32_P69149	STEAP1	1.50	3.04E-05	1.10	2.78E-03
A_24_P406334	STEAP1	1.64	3.71E-05	1.14	4.17E-03
A_23_P428260	STEAP2	2.03	3.02E-06	1.01	2.21E-03
A_24_P29401	PIK3R1	1.80	5.68E-06	0.59	2.71E-02
A_24_P174924	HIST1H3B	0.60	6.66E-03	0.89	8.18E-03
A_24_P217834	HIST1H3D	0.74	6.26E-04	1.23	6.65E-04
A_23_P59045	HIST1H2AE	0.90	4.67E-04	1.06	2.65E-03
A_23_P133814	HIST1H3C	1.09	7.76E-05	0.61	2.03E-02
A_23_P167983	HIST1H2AC	1.17	1.40E-04	1.13	2.65E-03
A_23_P122443	HIST1H1C	1.25	4.47E-04	1.50	2.42E-03
A_23_P7976	HIST1H1E	1.28	1.78E-03	1.59	6.66E-03
A_23_P42198	HIST1H3G	1.54	5.35E-05	0.91	1.23E-02
A_23_P111054	HIST1H2BB	1.56	4.64E-04	1.25	1.65E-02
A_23_P428184	HIST1H2AD	1.74	6.48E-04	1.65	9.93E-03
A_23_P366216	HIST1H2BH	1.77	5.18E-05	1.48	2.43E-03
A_23_P42178	HIST1H2BF	1.89	4.37E-06	1.31	6.65E-04
A_23_P30776	HIST1H2BE	1.96	1.68E-05	1.33	2.44E-03
A_23_P111041	HIST1H2BI	2.19	8.70E-06	1.22	3.59E-03
A_23_P167997	HIST1H2BG	2.24	4.30E-05	1.43	7.25E-03
A_24_P146211	HIST1H2BD	2.27	1.19E-04	1.38	2.04E-02
A_23_P93180	HIST1H2BC	2.36	1.45E-04	1.49	1.96E-02
A_23_P40470	HIST1H2BE	2.74	1.92E-06	1.28	1.92E-03
A_24_P316965	RSAD2	3.58	1.58E-07	1.88	7.04E-05
A_24_P28722	RSAD2	3.63	5.49E-06	2.63	6.62E-04
A_23_P134366	ETV1	1.54	9.44E-06	0.80	5.42E-03
A_32_P78491	ETV1	2.00	2.45E-05	0.79	3.78E-02

Supplementary Table S1. (continued)

		Cen3tel 600 spheres		Cen3tel 1000 spheres	
Probe Name	**Gene Symbol**	**Log_2FC**	**AdjPvalue**	**Log_2FC**	**AdjPvalue**
A_23_P11685	PLA2G4A	1.95	1.92E-06	1.29	3.75E-04
A_24_P77008	PTGS2	1.96	4.53E-06	0.59	3.19E-02
A_24_P250922	PTGS2	2.90	2.53E-07	1.39	1.58E-04
A_23_P87560	BTG1	1.38	2.62E-04	0.85	3.21E-02
A_23_P128319	ATP2B1	1.74	1.86E-05	0.70	2.95E-02
A_23_P139704	DUSP6	1.95	3.80E-04	2.06	3.84E-03
A_23_P64873	DCN	3.39	2.17E-06	1.47	3.08E-03
A_23_P145874	SAMD9L	0.85	1.48E-03	0.64	4.99E-02
A_23_P355244	SAMD9	1.37	9.97E-05	1.03	6.66E-03
A_24_P175188	SAMD9	1.53	4.59E-05	0.88	1.25E-02
A_24_P130041	CYP51A1	1.57	4.54E-06	1.55	1.07E-04
A_24_P175187	SAMD9	1.58	8.03E-05	1.01	1.13E-02
A_23_P257716	CYP51A1	2.66	1.65E-05	1.81	2.43E-03
A_23_P396858	FZD8	1.04	1.30E-04	0.83	6.40E-03
A_24_P171075	CREM	1.22	9.81E-05	0.90	7.38E-03
A_24_P278393	CREM	1.68	1.11E-05	0.88	6.22E-03
A_32_P172848	GK	1.10	3.92E-04	0.74	2.96E-02
A_23_P96556	GK	2.28	4.03E-07	1.41	9.16E-05
A_24_P100387	GK	2.39	6.19E-07	1.22	3.84E-04
A_32_P33304	ANK3	1.06	1.18E-03	1.03	1.41E-02
A_32_P214758	0	1.57	6.05E-05	1.52	1.27E-03
A_32_P117186	0	2.06	1.55E-05	1.77	7.22E-04
A_23_P301530	ANK3	2.08	1.30E-06	1.73	8.59E-05
A_23_P202269	ANK3	2.34	6.40E-07	1.77	7.04E-05
A_23_P212482	SLC9A9	0.89	4.77E-05	0.89	8.98E-04
A_24_P371399	C3orf58	1.37	1.31E-05	0.71	7.22E-03
A_23_P69109	PLSCR1	1.53	3.60E-05	0.92	7.92E-03
A_23_P40847	CHST2	2.23	6.26E-06	1.78	4.43E-04
A_32_P46214	SLC9A9	2.69	6.12E-06	1.87	8.29E-04
A_23_P218086	TPCN1	0.87	5.91E-04	0.69	2.04E-02
A_24_P343929	OAS2	1.30	6.25E-06	0.68	3.59E-03
A_24_P335305	OAS3	1.51	1.57E-05	0.97	3.08E-03
A_24_P244575	TPCN1	1.56	6.11E-06	0.63	1.13E-02
A_23_P47955	OAS3	1.65	3.41E-04	1.18	2.12E-02
A_23_P204087	OAS2	2.07	2.14E-06	1.15	9.01E-04
A_23_P64828	OAS1	3.22	5.86E-06	1.92	1.70E-03
A_23_P4561	SERPINB8	0.91	7.23E-05	0.78	2.67E-03
A_24_P365180	DSEL	1.79	4.95E-06	0.64	1.66E-02
A_23_P170733	ANTXR2	0.67	1.85E-04	0.95	5.64E-04
A_24_P377144	ANTXR2	0.70	4.11E-04	0.64	8.09E-03
A_24_P345846	ANTXR2	0.70	3.34E-04	0.65	6.57E-03
A_32_P107876	FRAS1	1.16	7.43E-05	0.82	7.05E-03
A_23_P168014	HIST1H2AJ	0.85	1.52E-03	1.12	4.15E-03
A_23_P81859	HIST1H2AH	1.02	1.53E-03	0.86	3.19E-02
A_23_P145238	HIST1H2BK	1.20	2.73E-03	1.36	1.37E-02
A_24_P311926	HLA-G	1.39	2.57E-05	0.96	3.25E-03
A_24_P394510	HIST1H2AJ	1.40	1.71E-05	1.00	1.92E-03
A_24_P55148	HIST1H2BJ	1.41	5.33E-05	1.47	8.17E-04
A_24_P86389	HIST1H2AM	1.49	1.56E-05	1.44	4.18E-04
A_23_P59069	HIST1H2BO	1.53	3.06E-04	1.47	5.24E-03
A_23_P338113	0	1.55	2.09E-05	0.70	1.92E-02
A_23_P145264	HLA-F	1.85	8.44E-06	0.86	8.11E-03
A_23_P8013	HIST1H2BL	1.93	2.84E-06	1.23	6.62E-04
A_23_P408353	HLA-A	1.97	1.34E-05	0.85	1.71E-02
A_24_P3783	HIST1H2BM	2.16	4.34E-06	1.37	9.51E-04
A_24_P418044	HLA-J	2.25	2.45E-06	0.93	4.36E-03

Supplementary Table S1. (Continued)

		Cen3tel 600 spheres		Cen3tel 1000 spheres	
Probe Name	**Gene Symbol**	**Log_2FC**	**AdjPvalue**	**Log_2FC**	**AdjPvalue**
A_24_P263767	HLA-J	2.71	3.16E-06	1.11	6.18E-03
A_23_P402081	HIST1H2BN	2.76	1.36E-06	1.44	7.86E-04
A_24_P376483	HLA-A	3.34	1.30E-07	1.14	2.89E-04
A_32_P234459	HLA-H	3.90	5.86E-06	1.23	3.21E-02
A_32_P193080	FMNL2	1.92	8.15E-06	0.80	1.27E-02
A_23_P142849	RND3	2.52	4.03E-07	1.50	9.71E-05
A_23_P165624	TNFAIP6	2.71	4.40E-06	1.30	3.81E-03
A_24_P52882	HRK	1.12	4.41E-04	0.70	4.38E-02
A_32_P156786	HRK	1.51	5.12E-05	0.70	3.28E-02
A_24_P324465	HIST2H3D	1.20	2.35E-05	0.68	7.68E-03
A_23_P436281	HIST2H4B	0.61	1.53E-03	0.91	2.44E-03
A_23_P149545	HIST2H2BE	0.65	1.60E-04	0.93	4.27E-04
A_24_P68631	HIST2H2AB	0.87	2.07E-03	1.52	1.43E-03
A_24_P8721	HIST2H2AC	1.09	9.42E-04	1.47	2.58E-03
A_23_P103981	HIST2H2AA4	1.37	1.06E-03	1.89	2.58E-03
A_24_P544661	HIST2H2BC	2.04	1.73E-06	1.21	5.64E-04
A_24_P156911	HIST2H2BE	2.67	3.24E-06	1.35	2.29E-03
A_23_P309381	HIST2H2AA4	3.02	1.44E-05	1.84	3.67E-03
A_23_P374782	SH3KBP1	1.29	6.35E-06	0.83	1.27E-03
A_23_P417331	RPS6KA3	1.56	7.93E-06	0.60	1.84E-02
A_32_P61684	PAG1	0.64	7.05E-03	0.76	2.57E-02
A_23_P8812	0	0.83	1.34E-02	1.49	7.10E-03
A_23_P347070	PAG1	1.21	1.97E-04	1.03	6.56E-03
A_23_P8820	FABP4	1.21	2.98E-05	1.31	4.27E-04
A_23_P52761	MMP7	0.78	2.12E-03	1.53	8.17E-04
A_23_P1691	MMP1	5.11	2.81E-07	4.69	1.59E-05
A_23_P83007	LURAP1L	1.89	5.86E-06	0.80	8.51E-03
A_24_P36944	CEP170	1.07	2.47E-05	0.58	9.64E-03
A_23_P348857	CEP170	1.52	8.54E-05	0.74	4.06E-02
A_23_P97181	GREM2	1.69	6.15E-06	0.73	8.62E-03
A_23_P23151	CEP170	2.35	1.30E-06	0.78	6.64E-03
A_24_P40626	GREM2	2.75	2.82E-06	1.37	2.03E-03
A_23_P138541	AKR1C3	1.21	3.11E-03	1.25	2.35E-02
A_23_P257971	AKR1C1	1.98	9.57E-04	1.84	1.47E-02
A_24_P220947	AKR1C1	2.44	2.41E-03	2.14	3.81E-02
A_24_P152968	AKR1C1	2.99	4.14E-04	2.22	2.10E-02
A_32_P42684	SLC7A11	1.17	2.94E-04	0.74	3.22E-02
A_24_P334361	DDX60	0.66	4.82E-03	0.72	2.64E-02
A_23_P41470	DDX60	1.18	2.75E-05	0.89	2.27E-03
A_23_P110184	MSMO1	3.46	4.61E-05	2.50	4.26E-03
A_23_P371495	TMTC1	0.64	1.55E-02	0.83	3.28E-02
A_32_P2452	TMTC1	0.84	3.83E-03	0.80	3.94E-02
A_24_P80532	CCNG2	0.85	8.64E-05	0.63	6.63E-03
A_24_P303091	CXCL10	1.96	7.50E-07	0.63	4.51E-03
A_24_P20607	CXCL11	2.05	1.81E-06	0.86	2.94E-03
A_23_P125278	CXCL11	2.34	2.18E-06	1.01	3.08E-03
A_23_P35912	CASP4	0.80	2.10E-04	0.59	1.32E-02
A_23_P47304	CASP5	0.84	1.39E-04	0.66	7.10E-03
A_23_P388993	ZC3H12C	1.47	2.32E-05	0.97	3.70E-03
A_23_P64173	CARD16	1.49	7.20E-05	1.49	1.27E-03
A_23_P202978	CASP1	1.83	2.31E-04	1.93	2.62E-03
A_23_P377957	KCTD12	1.80	2.22E-06	0.98	1.02E-03
A_23_P129133	OCA2	1.05	1.90E-03	0.83	4.99E-02
A_24_P316059	0	1.30	3.82E-05	0.82	7.09E-03
A_23_P218858	ABI3BP	1.43	1.66E-04	1.18	6.56E-03
A_24_P666795	XLOC_l2_013823	1.10	3.47E-06	0.76	5.64E-04

Supplementary Table S1. (Continued)

		Cen3tel 600 spheres		Cen3tel 1000 spheres	
Probe Name	**Gene Symbol**	**Log_2FC**	**AdjPvalue**	**Log_2FC**	**AdjPvalue**
A_23_P321703	BCL2A1	2.35	2.37E-05	1.77	1.94E-03
A_23_P129221	FAH	2.48	3.55E-06	0.88	1.24E-02
A_23_P152002	BCL2A1	3.40	9.31E-07	2.64	8.59E-05
A_23_P324754	CEMIP	3.81	1.57E-07	2.59	1.68E-05
A_32_P161855	CEMIP	4.19	1.30E-07	2.65	1.68E-05
A_23_P52266	IFIT1	1.00	1.92E-03	1.52	2.65E-03
A_23_P150053	ACTA2	1.11	1.49E-03	0.97	2.79E-02
A_23_P35412	IFIT3	2.64	6.21E-04	1.81	3.89E-02
A_23_P29769	WWTR1	0.83	2.44E-04	0.83	3.44E-03
A_24_P944383	WWTR1	1.06	6.97E-04	0.72	4.49E-02
A_32_P231617	TM4SF1	1.40	2.46E-04	1.34	4.33E-03
A_24_P944390	WWTR1	1.64	1.33E-05	0.84	7.68E-03
A_23_P102060	SSFA2	0.72	4.55E-04	0.70	6.66E-03
A_24_P345837	MSX1	1.44	2.89E-06	0.84	1.00E-03
A_23_P76450	PHLDA1	1.49	6.50E-04	1.53	7.05E-03
A_23_P338912	PHLDA1	1.51	2.01E-05	0.89	5.75E-03
A_24_P943597	PHLDA1	2.54	2.45E-05	1.05	3.17E-02
A_23_P140146	IFI27L2	0.85	3.91E-04	0.75	9.18E-03
A_24_P364591	FBLN5	1.27	2.02E-05	0.60	1.53E-02
A_24_P270460	IFI27	3.30	3.68E-05	1.79	1.32E-02
A_23_P48513	IFI27	3.42	1.52E-06	1.83	7.61E-04
A_32_P177953	GCLM	1.13	7.14E-03	1.73	7.79E-03
A_23_P103996	GCLM	1.44	2.68E-05	1.81	1.61E-04
A_23_P160940	ABCA4	2.12	6.15E-05	1.93	1.76E-03
A_23_P213766	ANKH	1.18	3.31E-05	0.74	6.40E-03
A_24_P243278	DAP	2.03	8.97E-06	1.13	3.79E-03
A_23_P92687	DAP	2.44	1.08E-06	0.93	2.89E-03
A_23_P214789	SNX9	1.09	2.84E-04	0.74	2.36E-02
A_23_P383835	ACAT2	1.32	3.47E-04	1.76	1.16E-03
A_23_P31135	ACAT2	1.55	4.29E-05	1.66	6.25E-04
A_23_P134176	SOD2	2.01	1.53E-04	1.20	2.57E-02
A_24_P179044	SNX9	2.56	4.51E-06	0.82	2.47E-02
A_23_P23074	IFI44	1.01	3.44E-03	1.21	1.33E-02
A_23_P114662	CRYZ	1.05	7.83E-05	0.60	1.97E-02
A_24_P342632	AK5	1.44	1.26E-05	0.75	6.87E-03
A_23_P62741	ELTD1	1.47	2.51E-05	0.84	7.68E-03
A_23_P200015	AK5	1.59	4.51E-06	1.24	3.91E-04
A_23_P45871	IFI44L	2.98	1.00E-05	1.55	5.68E-03
A_23_P212061	MME	1.64	1.07E-04	0.85	3.70E-02
A_23_P364324	ABCA13	0.95	1.13E-04	0.65	1.16E-02
A_24_P346431	TNS3	1.71	1.10E-04	1.63	2.42E-03
A_24_P709377	PAX8-AS1	0.81	2.00E-04	0.89	1.85E-03
A_23_P91076	TMEM87B	1.46	1.23E-05	0.63	1.60E-02
A_23_P165657	SLC20A1	1.85	3.40E-04	1.53	1.09E-02
A_23_P209995	IL1RN	2.88	9.37E-07	2.26	8.59E-05
A_24_P103004	SLC20A1	3.46	5.86E-07	1.69	4.18E-04
A_23_P79518	IL1B	4.30	5.62E-08	3.16	8.55E-07
A_23_P70161	ITGA2	0.96	4.24E-04	0.89	7.74E-03
A_23_P92730	HSPB3	1.17	4.82E-05	0.71	9.57E-03
A_32_P178800	ITGA2	1.87	3.86E-06	1.39	4.18E-04
A_32_P208076	ITGA2	1.96	8.86E-06	1.62	5.64E-04
A_24_P243329	ITGA2	2.34	3.24E-06	1.58	5.64E-04
A_24_P269432	BET1	1.45	3.20E-04	0.93	3.16E-02
A_23_P59700	BET1	1.80	2.64E-05	0.87	1.75E-02
A_23_P111701	GNG11	2.47	5.59E-05	1.83	4.34E-03
A_32_P146764	GNG11	2.50	4.97E-06	1.54	1.27E-03

Supplementary Table S1. (Continued)

		Cen3tel 600 spheres		Cen3tel 1000 spheres	
Probe Name	**Gene Symbol**	**Log_2FC**	**AdjPvalue**	**Log_2FC**	**AdjPvalue**
A_23_P30666	TNFRSF21	1.56	1.37E-04	0.82	4.01E-02
A_23_P42065	TNFRSF21	1.94	1.74E-06	0.61	1.09E-02
A_24_P127051	0	2.55	2.46E-05	1.10	2.69E-02
A_24_P399680	FAM210B	2.21	1.20E-06	1.31	3.84E-04
A_23_P68486	FAM210B	2.98	4.24E-06	1.92	8.61E-04
A_24_P582889	TPBG	1.11	2.82E-05	0.74	4.13E-03
A_23_P59261	TPBG	1.90	1.11E-04	1.95	1.61E-03
A_24_P349648	0	2.29	2.53E-06	0.70	1.81E-02
A_23_P35349	SVIL	1.68	4.47E-05	0.92	1.48E-02
A_23_P54144	BMP4	0.82	1.37E-03	0.94	7.68E-03
A_23_P252106	RIPK2	0.92	7.61E-05	0.64	7.94E-03
A_23_P422083	TMEM55A	0.93	3.28E-04	0.84	7.38E-03
A_23_P146146	ATP6V0D2	0.94	4.73E-05	0.61	7.25E-03
A_23_P94533	CTSL	2.50	1.85E-05	1.04	2.51E-02
A_23_P83134	GAS1	2.70	2.17E-06	1.34	1.57E-03
A_23_P112846	MTHFD2L	0.65	5.82E-04	0.71	4.62E-03
A_24_P183150	CXCL3	1.10	2.01E-03	1.00	2.84E-02
A_32_P87013	CXCL8	1.51	3.47E-06	1.38	1.25E-04
A_23_P7144	CXCL1	2.23	4.53E-05	1.39	8.18E-03
A_24_P257416	CXCL2	2.55	8.81E-06	1.09	1.23E-02
A_24_P37264	RNF144A	1.31	3.15E-06	0.99	3.04E-04
A_32_P52609	LPIN1	1.78	3.37E-05	1.55	1.31E-03
A_23_P320371	LPIN1	1.87	3.08E-06	1.04	1.31E-03
A_23_P5831	HPCAL1	2.56	1.30E-07	1.40	2.41E-05
A_23_P29248	TST	0.71	9.73E-04	0.75	8.29E-03
A_23_P29237	APOL3	0.73	4.12E-03	0.94	1.07E-02
A_24_P7594	APOL6	1.02	1.42E-03	0.79	4.38E-02
A_23_P120883	HMOX1	1.18	8.64E-04	1.83	1.21E-03
A_23_P103084	TOM1	1.60	4.65E-06	0.66	8.14E-03
A_24_P406986	SLC43A3	1.44	5.88E-05	0.94	8.11E-03
A_23_P87150	LPXN	1.86	7.90E-06	0.62	3.19E-02
A_23_P358548	SLC43A3	2.28	9.27E-06	1.11	7.27E-03
A_23_P139104	RTN4RL2	2.83	2.41E-05	1.46	1.18E-02
A_23_P75741	UBE2L6	3.19	4.57E-06	1.01	2.72E-02
A_23_P90696	TRIB2	0.80	3.56E-03	0.82	2.70E-02
A_23_P79155	GPR39	0.99	7.16E-05	0.58	1.58E-02
A_23_P250800	ST3GAL6	1.30	1.39E-04	1.03	7.13E-03
A_24_P541483	0	1.48	9.06E-06	0.71	7.51E-03
A_24_P162211	LSS	0.59	3.79E-03	0.64	2.16E-02
A_23_P211252	LSS	0.65	1.99E-03	0.60	2.58E-02
A_23_P154894	CSTB	0.89	3.57E-04	0.67	1.81E-02
A_32_P32254	COL6A1	1.00	1.25E-02	1.16	4.38E-02
A_24_P110799	LSS	1.29	1.47E-05	1.04	9.35E-04
A_24_P117294	MX2	1.74	8.32E-06	0.88	5.46E-03
A_23_P310956	COL6A2	1.78	7.16E-06	1.47	4.42E-04
A_23_P6263	MX2	2.19	1.27E-05	1.10	7.79E-03
A_23_P17663	MX1	2.36	1.59E-06	0.77	8.74E-03
A_23_P211233	COL6A2	2.98	5.69E-07	0.98	2.67E-03
A_24_P201702	CLEC2B	0.58	9.80E-03	0.88	1.13E-02
A_23_P61466	CD163L1	0.81	5.69E-05	0.69	2.44E-03
A_23_P125423	C1R	1.02	6.45E-03	1.06	4.08E-02
A_23_P87742	IFFO1	1.08	5.22E-04	0.74	3.36E-02
A_23_P363968	C1RL	1.20	1.39E-05	0.70	4.43E-03
A_23_P2492	C1S	2.51	6.74E-05	2.01	3.67E-03
A_23_P76364	CD9	2.98	2.41E-05	1.24	3.10E-02
A_24_P201739	SH2B3	1.52	1.77E-06	1.36	8.59E-05

Supplementary Table S1. (Continued)

		Cen3tel 600 spheres		Cen3tel 1000 spheres	
Probe Name	**Gene Symbol**	**Log_2FC**	**AdjPvalue**	**Log_2FC**	**AdjPvalue**
A_23_P79199	DBI	1.15	1.73E-04	0.96	6.40E-03
A_23_P16733	RALB	1.29	2.15E-05	0.62	1.47E-02
A_24_P63522	HMGCS1	2.52	1.04E-05	2.56	2.17E-04
A_23_P133263	HMGCS1	2.70	1.17E-06	2.32	7.08E-05
A_32_P164246	FOXQ1	2.12	4.85E-06	1.31	1.26E-03
A_32_P74983	MICB	0.64	3.30E-04	0.80	1.58E-03
A_23_P257516	MICA	1.22	4.32E-05	0.79	7.10E-03
A_24_P298409	HLA-C	1.29	5.14E-04	1.01	2.03E-02
A_24_P394533	NEU1	1.56	7.02E-06	0.85	3.23E-03
A_32_P460973	HLA-E	1.66	4.91E-06	0.67	9.77E-03
A_24_P161933	HLA-B	3.20	2.61E-07	1.08	1.01E-03
A_23_P30848	HLA-E	3.36	1.76E-07	0.98	1.26E-03
A_23_P70539	HLA-C	3.64	6.54E-08	1.20	9.71E-05
A_32_P204218	FAM180A	0.67	1.60E-04	0.61	3.80E-03
A_23_P31177	TMEM140	1.50	4.40E-06	0.77	2.65E-03
A_23_P258190	AKR1B1	3.61	4.51E-06	1.75	3.80E-03
A_24_P931636	TBRG1	0.58	1.67E-02	0.75	3.60E-02
A_23_P98463	TBRG1	1.22	3.56E-06	0.73	1.08E-03
A_24_P135769	VWA5A	1.35	3.13E-05	0.81	7.45E-03
A_24_P181055	ST3GAL4	2.42	9.37E-07	0.64	1.44E-02
A_23_P128698	SPRY2	2.89	1.18E-06	1.98	1.61E-04
A_23_P108835	YPEL5	1.23	6.84E-05	0.64	2.71E-02
A_23_P301855	LSAMP	1.62	1.30E-05	0.73	1.35E-02
A_24_P152345	0	2.19	1.01E-04	1.45	1.21E-02
A_23_P377115	MCC	0.72	2.02E-04	0.61	6.66E-03
A_32_P187704	SNTG1	2.38	1.09E-05	1.04	1.35E-02
A_32_P166031	0	0.60	6.05E-04	0.68	4.16E-03
A_23_P54460	SPRED1	0.83	4.27E-05	0.72	1.58E-03
A_24_P107859	SPRED1	1.13	5.00E-05	0.85	3.81E-03
A_23_P86012	LAMB3	0.64	1.98E-03	0.59	2.59E-02
A_23_P35230	CD46	0.81	4.40E-04	0.78	7.27E-03
A_23_P201758	CD46	1.45	8.96E-05	0.72	3.82E-02
A_23_P74290	GBP5	0.71	1.11E-04	0.88	6.62E-04
A_23_P85693	GBP2	1.46	5.26E-05	0.83	1.47E-02
A_23_P93739	EPDR1	0.95	1.39E-04	0.63	1.51E-02
A_23_P436336	LINC00265	1.34	1.67E-05	0.72	7.34E-03
A_23_P413193	SFR1	0.59	7.66E-04	0.70	4.08E-03
A_23_P202939	APLP2	2.27	6.19E-07	1.49	1.02E-04
A_24_P300952	APLP2	3.21	1.36E-06	1.47	1.49E-03
A_32_P35047	LINC00944	1.06	3.48E-05	1.07	6.75E-04
A_23_P114947	RGS2	1.83	1.00E-05	1.45	7.30E-04
A_24_P298179	0	2.06	8.22E-05	1.16	2.11E-02
A_23_P351270	PAPPA	1.83	1.63E-05	0.80	1.89E-02
A_24_P799048	LINC01540	0.85	5.74E-03	1.17	1.04E-02
A_23_P153197	TGIF1	1.84	7.80E-05	0.86	4.51E-02
A_23_P139500	BHLHE41	1.22	2.82E-04	0.85	2.07E-02
A_24_P913561	RASSF8	2.27	9.58E-07	1.12	7.30E-04
A_24_P407224	RASSF8	2.28	4.69E-07	1.32	1.26E-04
A_23_P204277	H2AFJ	1.32	1.19E-05	0.72	5.46E-03
A_24_P236003	H2AFJ	1.99	1.17E-05	0.86	1.53E-02
A_32_P189781	LINC00520	0.96	2.23E-04	1.70	1.86E-04
A_23_P128919	LGALS3	1.45	8.19E-04	1.34	1.32E-02
A_23_P113245	RBPJ	1.11	2.29E-05	0.62	8.06E-03
A_23_P254741	SOD3	2.00	4.82E-04	1.52	2.14E-02
A_32_P53183	HSD17B7	0.68	9.61E-03	0.84	2.71E-02

Supplementary Table S1. (Continued)

		Cen3tel 600 spheres		Cen3tel 1000 spheres	
Probe Name	**Gene Symbol**	**Log_2FC**	**AdjPvalue**	**Log_2FC**	**AdjPvalue**
A_32_P52282	HSD17B7	1.26	9.26E-04	1.22	1.18E-02
A_23_P11859	HSD17B7	1.45	4.09E-05	1.27	1.51E-03
A_24_P248345	OLFML2B	1.48	4.28E-05	1.28	1.61E-03
A_23_P137689	OLFML2B	1.86	3.55E-05	1.47	2.29E-03
A_24_P89457	CDKN1A	1.15	2.37E-04	1.21	2.75E-03
A_23_P351888	KIF6	1.38	1.17E-05	0.72	6.56E-03
A_23_P59210	CDKN1A	2.23	3.95E-05	1.60	3.82E-03
A_23_P149345	PTPN22	0.70	3.46E-04	0.61	8.67E-03
A_23_P201181	PTPN22	1.12	6.81E-05	0.72	1.02E-02
A_32_P24832	OLFML3	3.21	8.79E-07	1.66	5.64E-04
A_24_P11315	OLFML3	3.39	1.08E-06	1.47	1.49E-03
A_23_P105592	MVK	1.54	4.57E-05	1.03	6.40E-03
A_24_P372901	MVK	1.60	1.87E-05	1.03	3.49E-03
A_24_P364381	MMAB	2.67	2.53E-05	1.26	1.85E-02
A_23_P55616	SLC14A1	3.03	1.77E-06	1.63	8.61E-04
A_23_P211957	TGFBR2	1.30	1.48E-05	0.60	1.32E-02
A_24_P285768	EDEM1	2.15	1.20E-06	0.78	3.95E-03
A_23_P82088	NRN1	0.88	8.54E-05	1.03	7.01E-04
A_23_P22027	INSIG1	1.94	7.45E-05	1.72	2.44E-03
A_23_P73096	0	2.46	1.34E-05	1.57	2.75E-03
A_23_P52451	HKDC1	0.71	4.62E-04	0.61	1.19E-02
A_23_P202427	HKDC1	0.87	2.09E-04	0.94	2.20E-03
A_23_P12680	PSAP	3.23	3.41E-07	0.74	8.73E-03
A_24_P309317	PSAP	3.54	1.58E-07	0.85	2.64E-03
A_23_P153185	SERPINB2	2.68	7.47E-05	1.71	1.12E-02
A_24_P245379	SERPINB2	3.81	1.77E-06	1.66	2.44E-03
A_24_P67268	0	2.28	9.92E-05	1.43	1.50E-02
A_23_P328511	HSBP1	0.61	2.00E-03	0.61	2.00E-02
A_23_P207999	PMAIP1	0.70	6.93E-04	0.77	5.57E-03
A_24_P11900	MYH15	1.37	2.51E-06	1.20	1.07E-04
A_24_P157926	TNFAIP3	1.25	1.55E-05	0.71	5.50E-03
A_23_P19691	HEBP2	1.27	9.88E-06	0.70	4.23E-03
A_32_P164758	0	1.30	4.75E-06	0.74	1.78E-03
A_24_P659122	0	1.46	4.67E-05	0.78	1.72E-02
A_32_P191895	0	2.46	2.08E-06	0.96	4.94E-03
A_23_P203475	PRKCDBP	0.91	8.08E-04	0.72	2.59E-02
A_24_P304154	AMPD3	1.27	6.34E-05	0.84	8.53E-03
A_23_P127868	SLC22A18	1.36	9.30E-05	0.78	2.06E-02
A_24_P172481	TRIM22	1.79	2.58E-05	1.16	4.36E-03
A_23_P116286	AMPD3	1.80	5.31E-05	1.13	9.18E-03
A_23_P203498	TRIM22	1.85	2.12E-04	1.27	1.80E-02
A_23_P47614	PHLDA2	2.18	2.77E-06	1.79	1.61E-04
A_24_P215352	PRKCDBP	2.93	3.92E-07	0.68	8.66E-03
A_23_P156431	MAN1A1	0.78	1.88E-04	0.66	6.57E-03
A_23_P156425	MAN1A1	1.02	1.09E-04	0.67	1.31E-02
A_23_P156861	RGS17	1.36	6.57E-05	0.88	9.45E-03
A_24_P149036	DPYSL3	0.59	4.88E-02	1.03	2.92E-02
A_23_P7528	DPYSL3	0.99	1.29E-04	0.64	1.64E-02
A_23_P214079	SPINK1	1.38	2.37E-05	1.43	4.18E-04
A_24_P818010	LOC729737	0.74	2.82E-03	0.68	3.61E-02
A_24_P720185	LOC100132287	0.94	1.53E-04	1.09	1.14E-03
A_24_P761130	LOC729737	0.99	3.40E-04	0.77	1.47E-02
A_24_P586390	LOC100133331	1.71	2.03E-06	1.23	2.32E-04
A_23_P819	ISG15	3.54	8.49E-07	2.16	2.17E-04
A_32_P170736	CCDC71L	1.06	9.40E-05	0.60	2.34E-02

Supplementary Table S1. (Continued)

		Cen3tel 600 spheres		Cen3tel 1000 spheres	
Probe Name	**Gene Symbol**	**Log_2FC**	**AdjPvalue**	**Log_2FC**	**AdjPvalue**
A_23_P305060	NAMPT	1.47	6.02E-06	0.68	6.34E-03
A_23_P62642	CFAP45	0.98	1.65E-05	0.73	1.56E-03
A_23_P200138	SLAMF8	1.87	1.56E-05	1.17	3.49E-03
A_24_P898915	LOC729218	1.19	3.06E-05	0.89	2.58E-03
A_32_P12183	LOC729218	1.27	7.34E-06	1.30	1.41E-04
A_32_P11372	KGFLP1	1.71	3.08E-05	0.77	2.67E-02
A_24_P50543	LOC100419583	1.43	1.58E-05	0.94	2.61E-03
A_23_P3221	SQRDL	1.75	2.06E-05	1.28	2.08E-03
A_23_P37441	B2M	2.23	1.87E-05	1.07	1.38E-02
A_23_P372234	CA12	0.90	4.06E-04	0.97	3.81E-03
A_23_P420209	GCNT3	0.99	4.73E-05	0.74	3.81E-03
A_23_P151915	GCNT3	1.48	3.02E-05	1.00	4.08E-03
A_32_P192842	0	1.06	4.58E-03	1.72	3.99E-03
A_23_P314755	STC1	1.87	1.90E-05	1.25	2.92E-03
A_23_P96985	PSEN2	1.32	4.96E-06	0.67	3.34E-03
A_23_P149301	HIST3H2A	1.98	2.93E-04	1.45	1.71E-02
A_23_P332992	HIST3H2BB	2.13	2.36E-04	1.21	4.40E-02
A_24_P103886	IDI1	1.79	3.75E-04	1.84	4.36E-03
A_23_P86390	NRP1	0.77	1.11E-03	0.60	3.52E-02
A_23_P13701	TMBIM4	2.23	3.05E-06	0.80	1.04E-02
A_23_P46149	GPR137B	0.74	4.53E-04	0.59	1.64E-02
A_24_P252497	TRIB1	0.78	5.94E-03	0.93	2.06E-02
A_23_P146284	SQLE	1.32	3.55E-05	1.63	2.40E-04
A_23_P9416	ACO1	1.26	2.26E-05	0.72	7.27E-03
A_23_P411296	CEBPB	1.86	6.71E-07	1.26	1.01E-04
A_23_P143242	CEBPB	1.95	1.41E-06	0.88	1.58E-03
A_23_P1962	RARRES3	0.67	1.85E-03	0.97	3.34E-03
A_32_P820503	FTH1	3.31	1.10E-05	1.08	4.78E-02
A_24_P919330	FTH1	3.39	1.23E-06	1.02	9.78E-03
A_23_P115608	ARHGAP21	1.21	2.55E-04	0.69	4.55E-02
A_24_P7330	0	1.97	2.41E-06	1.24	5.64E-04
A_23_P29939	SNCA	1.39	8.44E-06	1.09	6.65E-04
A_23_P250353	HERC6	1.57	3.25E-05	0.92	8.46E-03
A_23_P71037	IL6	1.15	4.49E-04	0.78	3.17E-02
A_23_P82449	DFNA5	2.21	5.86E-06	0.83	1.52E-02
A_23_P168556	STX1A	0.70	1.91E-03	0.75	1.32E-02
A_23_P82420	STX1A	0.83	1.86E-03	0.78	2.39E-02
A_23_P8561	RHBDD2	1.97	2.09E-06	0.66	9.54E-03
A_24_P29723	POR	2.89	1.99E-06	0.85	1.67E-02
A_32_P95223	FDPSP2	3.01	1.25E-04	1.53	4.52E-02
A_23_P157283	TMEM243	0.88	1.00E-04	0.59	1.13E-02
A_23_P145485	ULBP2	1.31	4.54E-06	0.63	4.00E-03
A_24_P149314	ULBP2	1.69	2.14E-06	0.80	1.97E-03
A_32_P12372	0	0.95	6.72E-05	0.82	2.58E-03
A_32_P134056	DOCK4	1.07	6.59E-06	0.74	9.31E-04
A_32_P223256	ZFPM2-AS1	1.48	5.84E-06	1.14	5.10E-04
A_23_P114929	MPC2	0.99	6.02E-06	0.86	2.93E-04
A_23_P502731	PRRX1	2.97	2.29E-07	1.02	7.47E-04
A_32_P149174	C6orf226	1.39	2.61E-05	0.59	3.06E-02
A_24_P12401	VEGFA	1.54	9.07E-05	0.89	2.04E-02
A_23_P70398	VEGFA	1.69	5.12E-05	0.77	3.72E-02
A_32_P148058	RUNX2	1.72	2.56E-05	0.85	1.54E-02
A_23_P81805	VEGFA	2.42	4.48E-06	0.81	2.08E-02
A_23_P209726	SP140	1.02	2.63E-04	0.64	3.17E-02
A_23_P120002	SP110	1.04	1.53E-03	0.80	4.67E-02
A_23_P317620	ARL4C	2.84	8.70E-06	0.93	3.80E-02

Supplementary Table S1. (Continued)

		Cen3tel 600 spheres		Cen3tel 1000 spheres	
Probe Name	**Gene Symbol**	**Log_2FC**	**AdjPvalue**	**Log_2FC**	**AdjPvalue**
A_23_P166797	RTP4	1.36	4.31E-05	1.02	3.39E-03
A_23_P69908	GLRX	1.03	8.58E-05	1.76	1.07E-04
A_24_P212481	MCTP1	1.04	2.36E-04	0.65	2.97E-02
A_24_P92771	0	2.11	8.21E-05	1.11	2.83E-02
A_32_P132206	USP18	1.65	1.36E-04	1.18	1.06E-02
A_23_P120776	SLC25A1	2.09	2.24E-06	0.86	3.94E-03
A_32_P54553	USP41	2.10	2.01E-05	0.94	1.96E-02
A_23_P132159	USP18	2.32	1.23E-05	1.44	2.89E-03
A_23_P126159	HPCA	1.49	1.01E-06	1.13	9.71E-05
A_23_P34510	PHC2	1.81	6.49E-06	0.65	2.05E-02
A_23_P64617	FZD4	1.42	2.25E-05	0.82	6.66E-03
A_23_P76488	EMP1	1.29	1.61E-05	1.11	7.61E-04
A_24_P233786	FAM129A	0.64	1.06E-02	1.02	9.64E-03
A_23_P126803	ARPC5	0.67	2.26E-04	0.65	3.79E-03
A_23_P21485	PID1	1.88	5.03E-06	1.13	1.43E-03
A_23_P85164	DNASE1L1	0.65	3.46E-04	0.79	1.87E-03
A_24_P917384	LOC158960	0.82	2.43E-04	0.65	1.07E-02
A_23_P73493	CETN2	0.99	8.79E-05	0.81	4.17E-03
A_23_P34093	G6PD	1.47	7.19E-06	0.77	4.08E-03
A_23_P171034	NSDHL	2.86	9.06E-06	1.12	1.87E-02
A_23_P204581	TXNRD1	2.70	6.55E-06	0.99	1.88E-02
A_23_P76267	TMEM119	2.71	3.78E-06	0.89	1.97E-02
A_32_P41026	SC5D	1.11	4.34E-06	0.86	3.91E-04
A_23_P372888	SC5D	1.36	4.82E-04	1.36	6.40E-03
A_23_P98446	SC5D	1.45	9.90E-06	1.50	1.86E-04
A_24_P281683	0	2.43	1.51E-05	0.97	2.51E-02
A_23_P14612	FGF7	0.87	8.50E-04	0.60	4.65E-02
A_24_P99244	FGF7	1.79	2.37E-06	0.88	1.86E-03
A_23_P150018	DUSP5	0.96	1.19E-04	0.65	1.24E-02
A_23_P151133	TSPAN9	1.68	4.72E-06	0.59	1.78E-02
A_24_P931443	GPR68	1.61	1.52E-04	1.25	7.79E-03
A_23_P164451	TBX2	1.16	5.11E-04	0.75	4.50E-02
A_24_P236799	RAB31	1.84	2.70E-06	0.77	4.53E-03
A_24_P212539	GALM	1.22	3.31E-05	0.62	1.60E-02
A_24_P126741	0	0.67	3.12E-03	1.12	2.58E-03
A_24_P921086	CAPN8	0.67	2.69E-04	0.85	1.16E-03
A_24_P182494	DUSP10	1.14	1.33E-05	0.71	3.01E-03
A_23_P372874	S100A13	1.16	4.61E-05	1.07	1.27E-03
A_23_P145863	S100A11	1.16	3.16E-04	0.87	1.67E-02
A_23_P126593	S100A11	1.17	1.84E-03	1.02	3.17E-02
A_23_P201711	S100A6	1.66	2.74E-05	0.96	7.68E-03
A_23_P34744	CTSK	2.22	3.15E-05	1.90	1.35E-03
A_23_P46141	CTSS	2.70	4.53E-07	2.05	5.13E-05
A_24_P344087	REC8	0.66	2.29E-03	0.59	3.31E-02
A_23_P65442	IRF9	2.44	2.24E-06	1.17	1.94E-03
A_23_P67529	KCNN4	1.83	6.25E-06	0.86	6.23E-03
A_23_P16469	PLAUR	3.19	3.14E-06	0.84	4.28E-02
A_23_P68155	IFIH1	1.41	1.11E-03	1.01	4.96E-02
A_24_P798431	SMIM14	0.76	4.70E-05	0.64	2.08E-03
A_23_P112634	SMIM14	2.48	4.78E-06	1.72	7.06E-04
A_23_P332536	PDGFRA	1.12	7.92E-06	0.77	1.16E-03
A_23_P300033	PDGFRA	2.50	2.22E-05	2.09	1.14E-03
A_23_P21618	PDZRN3	1.11	1.30E-04	0.74	1.42E-02
A_23_P110571	MAST4	0.87	2.48E-04	1.02	1.61E-03
A_24_P246591	0	1.95	1.36E-04	1.13	2.68E-02
A_32_P103955	LOC101929484	1.11	1.38E-04	0.97	4.21E-03

Supplementary Table S1. (Continued)

		Cen3tel 600 spheres		Cen3tel 1000 spheres	
Probe Name	**Gene Symbol**	**Log_2FC**	**AdjPvalue**	**Log_2FC**	**AdjPvalue**
A_23_P62021	THBS2	1.37	1.69E-05	0.90	2.91E-03
A_24_P759477	ITGB8	0.76	1.33E-03	1.08	2.61E-03
A_32_P45009	IDH1	1.56	7.95E-04	1.11	4.11E-02
A_23_P94501	ANXA1	1.14	1.02E-04	0.80	9.18E-03
A_24_P557479	XAF1	1.01	4.35E-05	0.77	3.13E-03
A_23_P15394	CD68	1.40	3.97E-05	0.64	2.98E-02
A_23_P4283	XAF1	1.83	3.70E-05	1.04	1.09E-02
A_23_P4286	XAF1	2.26	1.34E-05	1.12	8.97E-03
A_23_P128706	DYNC1H1	1.50	7.92E-06	0.68	8.33E-03
A_24_P117954	INO80C	1.54	5.31E-05	0.71	3.67E-02
A_23_P94230	LY96	0.87	1.06E-04	1.08	6.25E-04
A_23_P77731	CRYM	0.97	9.16E-03	1.76	4.56E-03
A_24_P112984	METTL9	1.61	1.83E-04	1.08	1.80E-02
A_24_P451992	0	1.63	6.58E-07	1.11	9.71E-05
A_24_P274270	STAT1	2.88	7.88E-06	1.42	5.91E-03
A_23_P214144	COL10A1	1.27	1.12E-04	1.34	1.43E-03
A_23_P116280	WT1	1.23	3.17E-05	0.67	1.18E-02
A_23_P127911	PAMR1	2.29	6.02E-07	0.93	1.03E-03
A_23_P148194	ADI1	0.86	1.61E-04	0.62	1.14E-02
A_23_P18939	RASA1	1.15	7.40E-05	0.62	2.35E-02
A_23_P152838	CCL5	2.15	1.76E-06	1.82	9.71E-05
A_23_P321920	CCL3L3	2.40	5.38E-07	0.64	7.05E-03
A_24_P228130	CCL3L3	2.43	9.37E-07	0.72	8.14E-03
A_23_P373017	CCL3	2.68	1.23E-06	1.05	2.85E-03
A_23_P164650	APOE	0.73	1.09E-04	1.00	4.18E-04
A_23_P55706	RELB	1.21	1.07E-03	0.92	3.75E-02
A_23_P107701	ERCC1	1.77	1.11E-05	0.61	3.90E-02
A_24_P114183	FDPS	1.54	6.37E-06	1.45	1.91E-04
A_32_P512061	GBAP1	1.63	8.66E-06	0.64	1.75E-02
A_23_P126908	TNFRSF14	0.71	1.83E-03	0.61	3.35E-02
A_23_P68851	KREMEN1	1.40	5.70E-05	0.63	4.27E-02
A_23_P30495	HMGCR	1.14	9.09E-04	1.23	7.40E-03
A_23_P145965	TPST1	1.00	1.30E-04	0.68	1.24E-02
A_23_P111797	LOC84214	1.10	7.37E-05	0.81	6.04E-03
A_23_P217379	COL4A6	0.69	3.06E-03	0.73	2.16E-02
A_23_P32404	ISG20	1.80	1.46E-05	1.36	1.27E-03
A_23_P88626	ANPEP	3.31	4.33E-06	1.37	7.56E-03
A_23_P141394	WIPI1	1.14	1.66E-05	0.96	8.17E-04
A_23_P168882	TP53INP1	1.64	2.50E-05	0.89	9.65E-03
A_24_P321184	0	1.33	3.85E-05	0.86	6.48E-03
A_32_P116957	0	1.41	1.06E-04	0.94	1.23E-02
A_23_P397248	CLCA2	1.77	1.52E-06	0.64	4.99E-03
A_23_P85209	IL13RA2	3.01	1.69E-06	3.03	5.34E-05
A_23_P200252	NTPCR	1.07	4.32E-05	0.67	7.88E-03
A_23_P144054	PRKCD	1.62	1.42E-06	0.61	4.00E-03
A_23_P15357	LGALS3BP	1.00	6.15E-05	0.71	6.12E-03
A_23_P10591	METRNL	1.38	8.04E-07	0.65	7.61E-04
A_24_P404245	PCYT2	1.96	7.82E-07	0.87	9.38E-04
A_24_P48204	SECTM1	2.75	8.73E-06	1.87	1.33E-03
A_23_P65174	PHF11	0.75	1.65E-03	0.74	1.78E-02
A_23_P121265	TWF2	3.04	5.30E-07	0.67	1.57E-02
A_23_P75786	SLC15A3	1.15	2.80E-05	0.79	3.59E-03
A_23_P88381	NUMB	1.19	9.67E-05	0.74	1.53E-02
A_23_P10182	ACOX2	1.46	1.04E-04	1.74	7.38E-04
A_32_P466514	IRF2BPL	0.72	2.25E-04	0.70	3.81E-03
A_23_P25935	C14orf1	2.35	7.37E-07	1.21	4.32E-04

Supplementary Table S1. (Continued)

		Cen3tel 600 spheres		Cen3tel 1000 spheres	
Probe Name	**Gene Symbol**	**Log_2FC**	**AdjPvalue**	**Log_2FC**	**AdjPvalue**
A_23_P153745	IFI30	0.65	2.46E-03	0.74	1.24E-02
A_23_P16523	GDF15	1.46	9.58E-05	1.58	1.14E-03
A_23_P39465	BST2	3.37	2.08E-06	0.96	2.04E-02
A_23_P379475	DHCR24	0.69	4.08E-04	0.80	2.58E-03
A_23_P34325	LRP8	0.97	2.47E-04	0.72	1.44E-02
A_23_P127150	TUBGCP2	2.57	5.32E-07	0.88	2.10E-03
A_23_P47924	PTPRR	0.67	1.05E-03	0.73	7.38E-03
A_23_P162739	TSC22D1	3.39	1.81E-06	1.29	4.70E-03
A_23_P112026	IDO1	0.70	2.76E-03	1.21	1.92E-03
A_23_P107587	NPC1	2.47	6.71E-05	1.23	3.03E-02
A_24_P201171	STXBP1	0.95	6.81E-05	0.66	7.10E-03
A_23_P112531	FAM102A	1.07	1.83E-03	1.07	1.72E-02
A_23_P148297	SH3BGRL	1.11	6.01E-04	0.83	2.71E-02
A_23_P27724	SEPW1	1.26	2.94E-05	0.84	4.18E-03
A_23_P502520	IL4I1	1.54	3.10E-05	0.70	2.59E-02
A_23_P78762	HSD17B14	1.94	6.03E-06	0.83	8.66E-03
A_24_P492562	YWHAZ	2.19	1.49E-05	0.83	3.21E-02
A_24_P393312	KIRREL	1.34	7.50E-06	0.58	9.82E-03
A_23_P259506	CYSTM1	1.47	8.04E-05	0.93	1.23E-02
A_24_P269062	SPRY4	1.62	6.32E-06	0.85	3.44E-03
A_23_P420196	SOCS1	0.95	2.01E-04	0.84	5.66E-03
A_23_P219197	RGS3	3.29	3.14E-06	1.37	5.61E-03
A_23_P117506	DHRS7	1.67	2.02E-05	1.32	1.33E-03
A_24_P530977	XLOC_l2_007656	1.28	1.91E-03	1.05	4.28E-02
A_23_P209564	CYBRD1	1.48	6.90E-05	0.84	1.85E-02
A_23_P144916	GFPT2	1.17	5.41E-04	1.38	3.08E-03
A_23_P81399	SQSTM1	2.46	2.09E-05	0.93	4.17E-02
A_23_P24104	PLAU	1.85	8.61E-06	1.14	2.20E-03
A_24_P378019	IRF7	1.26	9.25E-06	0.91	1.04E-03
A_23_P72737	IFITM1	2.87	4.23E-05	1.98	4.99E-03
A_23_P210900	ACSS2	2.16	1.34E-06	1.21	5.64E-04
A_23_P164179	TOB1	1.36	3.06E-05	0.68	1.70E-02
A_23_P16976	ANXA4	0.67	1.62E-03	0.82	6.36E-03
A_23_P252471	PECAM1	0.76	9.81E-05	0.90	7.43E-04
A_24_P177795	0	2.15	9.93E-05	1.29	1.88E-02
A_24_P218814	RDH5	1.27	1.57E-05	0.70	6.40E-03
A_24_P868905	0	1.85	2.11E-05	0.72	3.61E-02
A_23_P201459	IFI6	3.54	2.65E-07	2.31	5.79E-05
A_23_P318115	SMAGP	1.11	1.01E-04	0.71	1.37E-02
A_23_P64837	SMAGP	1.38	7.02E-06	0.63	7.68E-03
A_23_P109143	PRNP	0.75	1.08E-03	1.89	1.26E-04
A_23_P166051	RBCK1	1.55	4.81E-06	0.71	5.36E-03
A_32_P2050	lnc-RP1-239B22.1.1-1	0.85	2.37E-05	0.59	3.04E-03
A_23_P45389	RAB9A	0.59	1.68E-04	0.67	1.43E-03
A_24_P148717	CCR1	1.73	1.68E-05	0.92	7.68E-03
A_23_P144113	GNAI2	2.31	6.58E-07	0.60	1.02E-02
A_32_P222450	TMEM158	2.41	2.43E-06	0.78	1.37E-02
A_24_P190168	TMEM97	0.83	6.69E-04	0.79	9.91E-03
A_24_P151920	TMEM97	0.88	5.94E-04	0.65	2.87E-02
A_23_P126623	PGD	3.40	2.64E-06	1.37	5.52E-03
A_24_P184295	EHD1	1.17	3.13E-05	0.72	6.64E-03
A_23_P52647	EHD1	1.30	1.61E-05	1.05	1.01E-03
A_23_P53623	P2RX4	1.39	4.71E-05	0.72	2.02E-02
A_23_P139786	OASL	2.22	6.60E-06	1.87	3.84E-04
A_23_P152125	MVD	1.33	2.47E-04	0.89	2.19E-02
A_23_P49708	GRN	1.17	6.13E-04	1.11	9.44E-03

Supplementary Table S1. (Continued)

		Cen3tel 600 spheres		Cen3tel 1000 spheres	
Probe Name	**Gene Symbol**	**Log_2FC**	**AdjPvalue**	**Log_2FC**	**AdjPvalue**
A_23_P152782	IFI35	3.20	2.75E-06	1.05	1.42E-02
A_23_P11800	CAMK2N1	2.11	7.16E-06	0.68	3.57E-02
A_23_P89941	CDKN2D	0.66	2.63E-03	0.61	3.24E-02
A_23_P142075	ACP5	1.34	4.99E-05	1.19	1.61E-03
A_23_P208595	LDLR	1.99	1.31E-06	0.85	2.00E-03
A_23_P415021	METTL7A	1.36	6.19E-05	0.75	1.94E-02
A_23_P1782	CD82	1.70	3.70E-05	1.46	1.52E-03
A_24_P365571	MRPS6	1.56	5.06E-05	0.78	2.51E-02
A_23_P59005	TAP1	1.62	9.21E-05	0.99	1.65E-02
A_24_P63950	AP1S1	3.15	1.58E-07	0.62	6.62E-03
A_23_P20196	ARPC1B	3.17	1.30E-07	0.82	9.40E-04
A_24_P122137	LIF	1.40	4.91E-06	0.75	2.55E-03
A_23_P171077	EBP	0.67	3.31E-03	0.94	6.62E-03
A_23_P24444	DHCR7	0.85	6.19E-05	1.16	2.33E-04
A_24_P349196	CCDC30	0.67	1.85E-04	0.67	2.85E-03
A_23_P434710	PPP1CA	3.24	4.21E-07	0.65	2.02E-02
A_23_P166502	SREBF2	0.97	8.52E-05	0.62	1.23E-02
A_23_P106898	ORAI3	1.00	4.82E-05	0.65	7.30E-03
A_23_P88819	MVP	1.54	7.13E-05	0.75	3.48E-02
A_23_P133656	LAMA4	1.54	1.29E-04	1.00	1.65E-02
A_23_P41765	IRF1	1.29	1.12E-05	0.64	7.74E-03
A_24_P341938	ZC3HAV1	0.98	3.84E-04	0.60	4.40E-02
A_23_P71319	FDFT1	1.66	9.25E-06	2.00	9.71E-05
A_23_P17855	TRIOBP	1.53	2.27E-05	0.69	2.03E-02
A_23_P5903	SLCO4A1	0.95	4.13E-04	0.80	1.19E-02
A_23_P259490	MXD4	2.07	2.44E-06	0.59	2.47E-02
A_24_P148521	TMBIM1	1.71	5.49E-05	0.77	3.95E-02
A_23_P210465	PI3	0.67	1.83E-03	0.81	7.79E-03
A_23_P38346	DHX58	0.82	1.82E-03	0.89	1.20E-02
A_24_P82106	MMP14	2.64	4.31E-06	1.30	3.40E-03
A_23_P207911	TRPV2	1.19	5.49E-05	0.84	5.72E-03
A_23_P319520	TSNARE1	1.02	1.33E-04	0.62	2.16E-02
A_32_P19135	RAB4B	1.48	4.59E-06	0.68	5.15E-03
A_24_P48162	MPG	2.61	2.15E-07	0.60	4.99E-03
A_23_P101407	C3	2.84	1.07E-06	2.08	1.07E-04

Supplementary Table S2. List of the genes commonly down-regulated in cen3tel 600 and 1000 sphere cells. Gene expression in sphere cells is expressed as Log_2FC relative to the corresponding adherent cells. Genes with $Log_2FC < -0.58$ and adjusted *p*-value < 0.05 are reported.

		Cen3tel 600 spheres		Cen3tel 1000 spheres	
Probe Name	**Gene Symbol**	**Log_2FC**	**AdjPvalue**	**Log_2FC**	**AdjPvalue**
A_24_P254833	0	-0.76	4.50E-02	-1.15	4.80E-02
A_23_P132763	VGLL3	-2.13	9.09E-07	-0.93	1.26E-03
A_23_P41227	ALCAM	-1.60	1.55E-04	-0.91	3.18E-02
A_32_P228618	RBMS3	-2.48	2.19E-05	-1.42	7.00E-03
A_32_P74477	RBMS3	-1.98	3.30E-07	-1.15	9.71E-05
A_24_P359942	RBMS3	-1.32	1.19E-04	-0.77	2.35E-02
A_23_P110598	WDR36	-1.53	1.23E-06	-0.61	2.62E-03
A_24_P149124	NREP	-1.01	5.51E-04	-0.84	1.64E-02
A_23_P166686	AMOTL2	-3.00	2.47E-05	-1.66	8.90E-03
A_23_P19102	0	-1.45	5.78E-05	-0.78	2.03E-02
A_24_P234871	0	-1.41	4.16E-05	-1.05	3.46E-03
A_24_P937405	PRSS23	-2.74	1.30E-07	-1.71	1.68E-05
A_23_P87421	PRSS23	-1.97	5.86E-07	-1.01	3.39E-04
A_23_P150789	PRSS23	-0.93	1.80E-03	-1.32	3.39E-03
A_23_P15876	ALPK2	-2.93	1.59E-05	-1.52	8.18E-03

Supplementary Table S2. (Continued)

		Cen3tel 600 spheres		Cen3tel 1000 spheres	
Probe Name	**Gene Symbol**	**Log_2FC**	**AdjPvalue**	**Log_2FC**	**AdjPvalue**
A_23_P107597	ATP8B1	-1.07	4.40E-03	-1.58	6.40E-03
A_23_P113212	TMEM45A	-1.23	6.35E-03	-1.76	9.82E-03
A_23_P214821	EDN1	-1.26	1.65E-05	-0.67	7.42E-03
A_32_P146844	0	-1.53	1.19E-05	-0.91	3.54E-03
A_24_P930337	0	-1.37	4.53E-05	-0.65	2.77E-02
A_24_P460763	0	-1.28	1.11E-04	-0.67	3.44E-02
A_23_P156970	MEST	-2.75	1.14E-03	-2.38	2.32E-02
A_24_P218151	CPA4	-0.92	5.43E-03	-1.42	6.40E-03
A_23_P162047	DKK3	-1.43	1.14E-04	-1.12	6.40E-03
A_24_P261417	DKK3	-1.28	2.72E-04	-1.02	1.13E-02
A_23_P76799	BAZ1A	-0.83	2.64E-04	-0.69	9.15E-03
A_23_P218918	FGF2	-1.06	4.50E-04	-0.73	3.17E-02
A_23_P28898	PLCB4	-2.04	8.36E-06	-0.81	1.60E-02
A_24_P32085	MOB3B	-2.52	7.69E-07	-1.24	6.03E-04
A_24_P299474	TENM2	-4.48	7.63E-06	-3.20	9.35E-04
A_23_P81392	WWC1	-1.64	1.01E-04	-0.92	2.46E-02
A_32_P181131	0	-2.71	6.87E-06	-0.83	4.26E-02
A_24_P345290	AK4	-1.91	1.75E-06	-0.75	3.96E-03
A_32_P108655	AK4	-1.36	1.69E-06	-1.08	1.11E-04
A_32_P95067	AK4	-0.98	1.75E-05	-0.63	3.46E-03
A_24_P789425	AK4	-0.68	1.51E-03	-0.81	7.09E-03
A_24_P760945	0	-1.81	1.05E-04	-1.25	1.03E-02
A_24_P882959	LOC284344	-1.62	1.03E-04	-1.24	6.62E-03
A_32_P219970	PSG5	-1.32	3.49E-04	-1.09	1.16E-02
A_23_P130948	PSG11	-0.65	9.11E-03	-1.02	9.14E-03
A_23_P350249	GLIS3	-1.67	2.53E-05	-0.68	3.52E-02
A_23_P58082	CCDC80	-2.39	1.54E-04	-2.18	3.80E-03
A_24_P240166	PHLDB2	-2.00	2.27E-06	-0.60	1.83E-02
A_23_P167256	JADE1	-1.63	9.66E-06	-0.63	2.04E-02
A_23_P19663	CTGF	-2.53	4.09E-05	-1.34	1.60E-02
A_23_P19673	SGK1	-0.73	4.19E-04	-0.91	1.91E-03
A_23_P56865	DDX18	-1.01	1.82E-04	-0.67	1.91E-02
A_24_P42603	TRIO	-1.10	2.47E-05	-0.65	6.63E-03
A_24_P255543	0	-0.96	1.65E-05	-0.65	2.42E-03
A_32_P171043	CCBE1	-3.16	1.85E-06	-1.48	1.77E-03
A_23_P140405	FOXN3	-1.32	1.64E-05	-0.74	6.08E-03
A_23_P104438	MYPN	-1.44	1.71E-05	-0.96	2.75E-03
A_24_P346807	HERC4	-0.78	2.88E-03	-0.66	4.99E-02
A_23_P46426	CYR61	-2.82	1.51E-04	-2.34	6.02E-03
A_23_P46429	CYR61	-1.91	4.46E-06	-2.14	7.51E-05
A_24_P192485	TNFRSF11B	-2.57	1.08E-04	-1.32	3.75E-02
A_23_P363344	TPM1	-2.34	1.35E-04	-1.66	1.09E-02
A_32_P89709	TPM1	-2.14	3.85E-05	-1.16	1.38E-02
A_32_P185140	0	-1.45	6.32E-05	-0.66	4.42E-02
A_23_P23996	MAT1A	-1.24	8.61E-06	-0.58	7.68E-03
A_32_P115606	PXK	-1.41	5.68E-05	-0.75	2.05E-02
A_24_P140204	PXK	-0.97	2.59E-05	-0.75	1.89E-03
A_32_P166693	HEG1	-0.77	9.46E-05	-0.85	1.02E-03
A_23_P159986	MIR503HG	-2.11	1.92E-06	-1.17	8.17E-04
A_23_P148609	PLAC1	-1.54	2.00E-05	-0.78	1.13E-02
A_24_P166663	CDK6	-1.96	2.30E-05	-1.04	9.93E-03
A_24_P227069	GPAM	-1.31	1.19E-04	-0.76	2.48E-02
A_23_P211910	PLOD2	-1.77	1.70E-05	-1.22	2.35E-03
A_24_P56317	MBNL2	-1.85	7.12E-06	-0.81	8.74E-03
A_32_P99690	NLN	-1.08	7.71E-06	-0.58	3.73E-03
A_23_P332399	GULP1	-1.66	2.61E-05	-0.69	3.19E-02
A_24_P235429	ABCA1	-0.86	8.49E-03	-0.93	4.39E-02
A_23_P122216	LOX	-2.47	4.69E-07	-1.09	5.64E-04

Supplementary Table S2. (Continued)

		Cen3tel 600 spheres		Cen3tel 1000 spheres	
Probe Name	**Gene Symbol**	**Log_2FC**	**AdjPvalue**	**Log_2FC**	**AdjPvalue**
A_24_P166407	HIST1H4B	-1.58	1.80E-06	-0.63	3.84E-03
A_23_P214487	HIST1H4C	-0.94	1.38E-04	-0.59	1.92E-02
A_24_P914479	SNX5	-1.31	5.69E-05	-0.66	2.69E-02
A_23_P137381	ID3	-0.95	3.12E-03	-2.95	1.09E-04
A_24_P686965	SH2D5	-0.93	5.53E-04	-0.72	2.21E-02
A_23_P14083	AMIGO2	-2.45	1.02E-04	-1.56	1.46E-02
A_23_P51397	ENAH	-1.31	2.58E-05	-0.84	4.56E-03
A_23_P157795	CTNNAL1	-1.23	1.99E-04	-0.76	2.65E-02
A_23_P501007	EFEMP1	-2.51	4.02E-05	-2.17	1.57E-03
A_23_P252721	DLC1	-0.76	5.58E-04	-0.66	1.31E-02
A_24_P686956	lnc-SERPINC1-1	-1.30	3.65E-05	-0.69	1.41E-02
A_32_P30905	WDFY4	-1.37	4.27E-04	-0.90	3.61E-02
A_23_P380076	ZBTB38	-0.92	8.56E-04	-0.76	2.27E-02
A_32_P105549	ANXA8L1	-2.92	2.73E-06	-1.21	4.89E-03
A_32_P44932	0	-0.68	1.23E-03	-0.62	2.05E-02
A_23_P571	SLC2A1	-1.71	9.40E-06	-0.60	3.16E-02
A_24_P385313	PTPRF	-1.69	3.54E-06	-1.22	4.42E-04
A_24_P88763	LOXL3	-0.58	6.67E-03	-0.80	1.24E-02
A_24_P921366	CALD1	-2.01	3.44E-06	-1.13	1.43E-03
A_23_P202520	ABLIM1	-1.17	2.21E-05	-0.74	4.15E-03
A_24_P548966	RAB3B	-2.51	1.29E-05	-1.04	1.96E-02
A_24_P933319	RAB3B	-1.56	4.49E-06	-0.83	2.42E-03
A_23_P138635	BNIP3	-1.64	8.54E-06	-0.89	3.85E-03
A_23_P110712	DUSP1	-1.47	1.49E-03	-1.12	4.81E-02
A_23_P147786	RIMS2	-2.11	1.29E-04	-1.57	8.46E-03
A_24_P935986	BCAT1	-1.01	4.68E-05	-0.86	1.97E-03
A_32_P117464	MB21D2	-1.86	4.95E-05	-0.95	2.18E-02
A_23_P212617	TFRC	-0.62	1.69E-02	-1.10	8.75E-03
A_24_P98975	ANKRD13A	-1.41	6.01E-05	-0.94	7.68E-03
A_23_P83579	ARNT2	-1.55	4.23E-04	-0.98	4.20E-02
A_23_P207520	COL1A1	-1.01	1.67E-04	-0.66	1.97E-02
A_23_P252306	ID1	-2.87	3.36E-05	-3.21	4.10E-04
A_23_P111995	LOXL2	-1.74	8.15E-07	-1.15	1.33E-04
A_23_P401	CENPF	-1.25	6.97E-05	-0.61	3.44E-02
A_23_P104741	KIRREL3	-2.43	1.42E-06	-0.97	3.07E-03
A_23_P7172	PGM2	-1.73	6.59E-06	-0.63	2.03E-02
A_24_P936252	0	-1.13	1.16E-05	-1.10	3.17E-04
A_23_P30254	PLK2	-2.96	2.27E-04	-1.97	2.17E-02
A_23_P360340	UACA	-1.81	3.08E-06	-0.59	1.65E-02
A_24_P785293	SNHG1	-1.02	1.36E-05	-0.61	3.81E-03
A_32_P200238	UCA1	-4.43	2.19E-05	-3.11	2.61E-03
A_23_P20864	ANGPTL2	-1.32	9.90E-05	-0.68	3.68E-02
A_23_P200001	NEXN	-0.87	8.52E-05	-0.70	4.23E-03
A_32_P167176	0	-1.47	1.29E-05	-0.90	3.40E-03
A_23_P150407	CREB3L1	-1.40	8.53E-05	-0.75	2.75E-02
A_23_P154037	AOX1	-1.45	2.42E-05	-0.66	2.17E-02
A_24_P350656	NFASC	-1.20	1.22E-05	-0.66	5.24E-03
A_23_P103561	NAV1	-1.01	1.96E-04	-0.63	2.56E-02
A_23_P208389	AXL	-1.41	3.76E-04	-1.17	1.20E-02
A_23_P56347	PSG3	-0.88	1.24E-03	-1.04	6.40E-03
A_23_P200737	RGS4	-0.85	5.57E-04	-0.99	3.33E-03
A_23_P106194	FOS	-1.38	1.68E-04	-1.80	7.21E-04
A_23_P156327	TGFBI	-3.71	8.10E-06	-2.97	5.89E-04
A_23_P169017	DEFB103B	-2.00	3.03E-05	-0.87	2.95E-02
A_23_P429998	FOSB	-2.07	1.31E-05	-1.18	4.56E-03
A_24_P37441	PDK1	-1.14	4.24E-05	-1.01	1.47E-03
A_23_P154086	BCS1L	-0.76	2.89E-04	-0.60	1.18E-02
A_23_P158593	COL5A1	-1.87	5.30E-07	-0.68	1.53E-03

Supplementary Table S2. (Continued)

		Cen3tel 600 spheres		Cen3tel 1000 spheres	
Probe Name	**Gene Symbol**	**Log_2FC**	**AdjPvalue**	**Log_2FC**	**AdjPvalue**
A_23_P210482	ADA	-0.99	3.96E-04	-0.83	1.16E-02
A_24_P298894	0	-1.13	1.47E-02	-1.74	1.53E-02
A_32_P187975	0	-2.28	9.24E-07	-0.60	1.35E-02
A_24_P45367	NIPAL3	-1.98	7.00E-06	-1.17	2.20E-03
A_23_P54055	AJUBA	-1.82	5.25E-06	-1.51	3.25E-04
A_23_P381945	KRT7	-2.64	1.81E-04	-2.94	1.60E-03
A_23_P402604	PFAS	-1.59	1.68E-06	-0.81	1.03E-03
A_23_P109345	PTTG1IP	-0.60	4.37E-03	-0.61	3.35E-02
A_23_P127948	ADM	-2.06	7.55E-05	-1.78	2.67E-03
A_23_P371824	TUFT1	-2.66	3.28E-06	-0.86	1.84E-02
A_24_P239606	GADD45B	-2.24	1.09E-04	-1.71	6.78E-03

Supplementary Table S3. List of the overrepresented biological processes (level 5 of the GO) identified using the David tool on the list of genes commonly up-regulated in cen3tel 600 and 1000 sphere cells. Processes with a *p*-value lower than 0.01 are shown. Count: number of up-regulated genes falling in each term; %: percentage of genes up-regulated in spheres respect to the total number of genes classified within that term.

	Term	**Count**	**%**	***P*-value**
1	GO:0006334~nucleosome assembly	25	5.6	4.37E-19
2	GO:0065004~protein-DNA complex assembly	25	5.6	3.43E-18
3	GO:0034728~nucleosome organization	25	5.6	5.96E-18
4	GO:0016126~sterol biosynthetic process	16	3.6	2.12E-15
5	GO:0006695~cholesterol biosynthetic process	14	3.1	1.29E-14
6	GO:0006333~chromatin assembly or disassembly	25	5.6	1.31E-14
7	GO:0016125~sterol metabolic process	20	4.5	8.73E-12
8	GO:0008202~steroid metabolic process	25	5.6	3.87E-10
9	GO:0006694~steroid biosynthetic process	17	3.8	3.95E-10
10	GO:0008285~negative regulation of cell proliferation	29	6.5	1.89E-07
11	GO:0043066~negative regulation of apoptosis	28	6.3	4.42E-07
12	GO:0043069~negative regulation of programmed cell death	28	6.3	5.81E-07
13	GO:0060548~negative regulation of cell death	28	6.3	6.16E-07
14	GO:0042981~regulation of apoptosis	45	10.0	1.46E-06
15	GO:0006916~anti-apoptosis	20	4.5	1.49E-06
16	GO:0002237~response to molecule of bacterial origin	13	2.9	1.88E-06
17	GO:0043067~regulation of programmed cell death	45	10.0	1.91E-06
18	GO:0008284~positive regulation of cell proliferation	29	6.5	2.93E-06
19	GO:0008299~isoprenoid biosynthetic process	7	1.6	7.87E-06
20	GO:0032496~response to lipopolysaccharide	11	2.5	2.61E-05
21	GO:0030324~lung development	12	2.7	4.58E-05
22	GO:0030323~respiratory tube development	12	2.7	6.04E-05
23	GO:0050729~positive regulation of inflammatory response	7	1.6	9.70E-05
24	GO:0031349~positive regulation of defense response	10	2.2	1.00E-04
25	GO:0051348~negative regulation of transferase activity	11	2.5	1.74E-04
26	GO:0007584~response to nutrient	13	2.9	2.61E-04
27	GO:0031347~regulation of defense response	13	2.9	3.17E-04
28	GO:0050778~positive regulation of immune response	13	2.9	3.60E-04
29	GO:0045137~development of primary sexual characteristics	12	2.7	4.27E-04
30	GO:0002253~activation of immune response	10	2.2	6.85E-04
31	GO:0050727~regulation of inflammatory response	9	2.0	7.21E-04
32	GO:0019220~regulation of phosphate metabolic process	26	5.8	7.67E-04
33	GO:0051174~regulation of phosphorus metabolic process	26	5.8	7.67E-04
34	GO:0006720~isoprenoid metabolic process	7	1.6	8.53E-04
35	GO:0006935~chemotaxis	13	2.9	8.73E-04
36	GO:0002526~acute inflammatory response	10	2.2	9.26E-04
37	GO:0048661~positive regulation of smooth muscle cell proliferation	6	1.3	1.07E-03

Supplementary Table S3. (Continued)

	Term	**Count**	**%**	***P*-value**
38	GO:0048660~regulation of smooth muscle cell proliferation	7	1.6	1.08E-03
39	GO:0001894~tissue homeostasis	8	1.8	1.12E-03
	Term	Count	%	*P*-value
40	GO:0032103~positive regulation of response to external stimulus	8	1.8	1.23E-03
41	GO:0031960~response to corticosteroid stimulus	9	2.0	1.51E-03
42	GO:0001568~blood vessel development	16	3.6	1.69E-03
43	GO:0048875~chemical homeostasis within a tissue	4	0.9	1.77E-03
44	GO:0043129~surfactant homeostasis	4	0.9	1.77E-03
45	GO:0048145~regulation of fibroblast proliferation	6	1.3	1.87E-03
46	GO:0010648~negative regulation of cell communication	16	3.6	1.90E-03
47	GO:0001944~vasculature development	16	3.6	2.14E-03
48	GO:0008406~gonad development	10	2.2	2.37E-03
49	GO:0019724~B cell mediated immunity	7	1.6	3.03E-03
50	GO:0002675~positive regulation of acute inflammatory response	4	0.9	3.12E-03
51	GO:0048514~blood vessel morphogenesis	14	3.1	3.20E-03
52	GO:0009966~regulation of signal transduction	37	8.3	3.59E-03
53	GO:0019362~pyridine nucleotide metabolic process	6	1.3	4.24E-03
54	GO:0001942~hair follicle development	6	1.3	4.24E-03
55	GO:0010647~positive regulation of cell communication	18	4.0	5.02E-03
56	GO:0043627~response to estrogen stimulus	9	2.0	5.63E-03
57	GO:0009887~organ morphogenesis	26	5.8	5.67E-03
58	GO:0008585~female gonad development	7	1.6	5.90E-03
59	GO:0032642~regulation of chemokine production	4	0.9	6.09E-03
60	GO:0006958~complement activation, classical pathway	5	1.1	6.13E-03
61	GO:0048754~branching morphogenesis of a tube	7	1.6	6.37E-03
62	GO:0033280~response to vitamin D	4	0.9	7.35E-03
63	GO:0045936~negative regulation of phosphate metabolic process	6	1.3	7.54E-03
64	GO:0010563~negative regulation of phosphorus metabolic process	6	1.3	7.54E-03
65	GO:0016485~protein processing	9	2.0	8.23E-03
66	GO:0046660~female sex differentiation	7	1.6	8.49E-03
67	GO:0046545~development of primary female sexual characteristics	7	1.6	8.49E-03
68	GO:0002053~positive regulation of mesenchymal cell proliferation	4	0.9	8.76E-03
69	GO:0002449~lymphocyte mediated immunity	7	1.6	9.09E-03

Supplementary Table S4. List of the overrepresented biological processes (level 5 of the GO) identified using the David tool on the list of genes commonly down-regulated in cen3tel 600 and 1000 sphere cells. Processes with a *p*-value lower than 0.01 are shown. Count: number of down-regulated genes falling in each term; %: percentage of genes down-regulated in spheres respect to the total number of genes classified within that term.

	Term	**Count**	**%**	***P*-value**
1	GO:0001568~blood vessel development	9	8.6	1.71E-04
2	GO:0001944~vasculature development	9	8.6	2.02E-04
3	GO:0010460~positive regulation of heart rate	3	2.9	1.78E-03
4	GO:0007507~heart development	7	6.7	2.57E-03
5	GO:0001525~angiogenesis	6	5.7	2.61E-03
6	GO:0009887~organ morphogenesis	11	10.5	3.18E-03
7	GO:0010810~regulation of cell-substrate adhesion	4	3.8	3.18E-03
8	GO:0045823~positive regulation of heart contraction	3	2.9	3.53E-03
9	GO:0006464~protein modification process	19	18.1	4.30E-03
10	GO:0030334~regulation of cell migration	6	5.7	4.60E-03
11	GO:0051325~interphase	5	4.8	4.78E-03
12	GO:0030336~negative regulation of cell migration	4	3.8	5.83E-03

Supplementary Table S4. (Continued)

	Term	Count	%	*P*-value
13	GO:0045785~positive regulation of cell adhesion	4	3.8	6.72E-03
14	GO:0051271~negative regulation of cell motion	4	3.8	7.69E-03
15	GO:0002027~regulation of heart rate	3	2.9	8.67E-03

Supplementary Table S5. List of the genes up-regulated in sphere cells and falling within the first 4 overrepresented terms identified by the David analysis (chromatin organization item, see Table S3). Gene expression in sphere cells is expressed as Log_2FC relative to the corresponding adherent cells. Genes with $Log_2FC > 0.58$ and adjusted *p*-value < 0.05 are reported.

		Cen3tel 600 spheres *vs* adherent cells		Cen3tel 1000 spheres *vs* adherent cells	
Probe Name	**Gene Symbol**	**Log_2FC**	**adj.P.Val**	**Log_2FC**	**adj.P.Val**
A_23_P167983	HIST1H2AC	1.17	1.40E-04	1.13	2.65E-03
A_23_P103981	HIST2H2AA4	1.37	1.06E-03	1.89	2.58E-03
A_23_P309381	HIST2H2AA4	3.02	1.44E-05	1.84	3.67E-03
A_23_P428184	HIST1H2AD	1.74	6.48E-04	1.65	9.93E-03
A_23_P59045	HIST1H2AE	0.90	4.67E-04	1.06	2.65E-03
A_23_P436281	HIST2H4B	0.61	1.53E-03	0.91	2.44E-03
A_23_P59069	HIST1H2BO	1.53	3.06E-04	1.47	5.24E-03
A_24_P68631	HIST2H2AB	0.87	2.07E-03	1.52	1.43E-03
A_24_P3783	HIST1H2BM	2.16	4.34E-06	1.37	9.51E-04
A_23_P402081	HIST1H2BN	2.76	1.36E-06	1.44	7.86E-04
A_23_P145238	HIST1H2BK	1.20	2.73E-03	1.36	1.37E-02
A_23_P8013	HIST1H2BL	1.93	2.84E-06	1.23	6.62E-04
A_23_P111041	HIST1H2BI	2.19	8.70E-06	1.22	3.59E-03
A_24_P8721	HIST2H2AC	1.09	9.42E-04	1.47	2.58E-03
A_24_P55148	HIST1H2BJ	1.41	5.33E-05	1.47	8.17E-04
A_23_P149301	HIST3H2A	1.98	2.93E-04	1.45	1.71E-02
A_23_P332992	HIST3H2BB	2.13	2.36E-04	1.21	4.40E-02
A_23_P111054	HIST1H2BB	1.56	4.64E-04	1.25	1.65E-02
A_23_P93180	HIST1H2BC	2.36	1.45E-04	1.49	1.96E-02
A_23_P7976	HIST1H1E	1.28	1.78E-03	1.59	6.66E-03
A_24_P146211	HIST1H2BD	2.27	1.19E-04	1.38	2.04E-02
A_23_P122443	HIST1H1C	1.25	4.47E-04	1.50	2.42E-03
A_23_P30776	HIST1H2BE	1.96	1.68E-05	1.33	2.44E-03
A_23_P40470	HIST1H2BE	2.74	1.92E-06	1.28	1.92E-03
A_23_P42178	HIST1H2BF	1.89	4.37E-06	1.31	6.65E-04
A_23_P167997	HIST1H2BG	2.24	4.30E-05	1.43	7.25E-03
A_23_P366216	HIST1H2BH	1.77	5.18E-05	1.48	2.43E-03
A_23_P204277	H2AFJ	1.32	1.19E-05	0.72	5.46E-03
A_24_P236003	H2AFJ	1.99	1.17E-05	0.86	1.53E-02
A_24_P324465	HIST2H3D	1.20	2.35E-05	0.68	7.68E-03
A_23_P149545	HIST2H2BE	0.65	1.60E-04	0.93	4.27E-04
A_24_P156911	HIST2H2BE	2.67	3.24E-06	1.35	2.29E-03
A_24_P174924	HIST1H3B	0.60	6.66E-03	0.89	8.18E-03
A_23_P81859	HIST1H2AH	1.02	1.53E-03	0.86	3.19E-02
A_23_P133814	HIST1H3C	1.09	7.76E-05	0.61	2.03E-02
A_24_P217834	HIST1H3D	0.74	6.26E-04	1.23	6.65E-04
A_23_P168014	HIST1H2AJ	0.85	1.52E-03	1.12	4.15E-03
A_24_P394510	HIST1H2AJ	1.40	1.71E-05	1.00	1.92E-03
A_24_P86389	HIST1H2AM	1.49	1.56E-05	1.44	4.18E-04
A_23_P42198	HIST1H3G	1.54	5.35E-05	0.91	1.23E-02

Supplementary Table S6. List of the overrepresented biological processes identified using the classification implemented by Panther within David on the list of the genes commonly up-regulated in cen3tel 600 and 1000 sphere cells. Processes with a *p*-value lower than 0.01 are shown. Count: number of up-regulated genes falling in each term; %: percentage of genes up-regulated in spheres respect to the total number of genes classified within that term.

	Term	Count	%	*P*-value
1	BP00148:Immunity and defense	75	16.7	2,19E-11
2	BP00156:Interferon-mediated immunity	15	3.3	8,40E-10
3	BP00026:Cholesterol metabolism	14	3.1	2,00E-08
4	BP00150:MHCI-mediated immunity	8	1.8	1,60E-07
5	BP00149:T-cell mediated immunity	18	4.0	7,18E-06
6	BP00295:Steroid metabolism	15	3.3	1,56E-04
7	BP00115:NF-kappaB cascade	9	2.0	6,02E-04
8	BP00107:Cytokine and chemokine mediated signaling pathway	17	3.8	6,49E-04
9	BP00019:Lipid, fatty acid and steroid metabolism	35	7.8	9,34E-04
10	BP00114:MAPKKK cascade	14	3.1	1.11E-03
11	BP00116:JNK cascade	8	1.2	1.16E-03
12	BP00273:Chromatin packaging and remodeling	13	2.9	2.89E-03
13	BP00028:Lipid and fatty acid transport	10	2.2	4.90E-03
14	BP00287:Cell motility	18	4.0	6.99E-03

Supplementary Table S7. List of the overrepresented biological processes identified using the classification implemented by Panther within David on the list of the genes commonly down-regulated in cen3tel 600 and 1000 sphere cells. Processes with a *p*-value lower than 0.01 are shown. Count: number of down-regulated genes falling in each term; %: percentage of genes down-regulated in spheres respect to the total number of genes classified within that term.

	Term	Count	%	*P*-value
1	BP00248:Mesoderm development	15	14.3	7.98E-06
2	BP00124:Cell adhesion	13	12.4	3.36E-04
3	BP00193:Developmental processes	26	24.8	8.69E-04
4	BP00223:Angiogenesis	4	3.8	4.87E-03
5	BP00285:Cell structure and motility	15	14.3	7.98E-03
6	BP00201:Skeletal development	5	4.8	8.39E-03